8. Two-dimensional Ferroelectric Models

Elliott H. Lieb*

Department of Mathematics, Massachusetts Institute of Technology, Cambridge, Massachusetts, U.S.A.

and

Fa Yueh Wu**

Department of Physics, Northeastern University, Boston, Massachusetts, U.S.A.

* Work supported by National Science Foundation grant Nos. GP–9414 and GP–26526.
** Work supported by National Science Foundation grant Nos. GP–9041 and GP–25306.

I. Introduction

A number of hydrogen-bonded crystals exhibit the phenomenon of a ferroelectric or antiferroelectric phase transition (Jona and Shirane, 1962). A typical example is potassium dihydrogen phosphate, KH_2PO_4, which undergoes a phase transition from a paraelectric state into a spontaneously polarized state at about 122°K. The structure of KH_2PO_4 is typical of these crystals, being tetragonal (West, 1930) with every phosphate group surrounded tetrahedrally by four other phosphate groups. As revealed by neutron diffraction experiments (Bacon and Pease, 1953; Peterson and Levy, 1953), the hydrogen ions are located between each pair of phosphate groups so that the crystal is a hydrogen-bonded lattice with the positions of the phosphate groups as lattice vertices. It further turns out that the equilibrium positions of the hydrogen atoms are near one or the other end of the bonds. Consequently, a "state" of the crystal is characterized by a specification of its hydrogen positions. It appears to have been first suggested by Onsager (1939) that the ferroelectric transition in KH_2PO_4 is connected with an ordering of the hydrogen atoms in the bonds. If an energy is assigned to each of the $2^4 = 16$ vertex hydrogen configurations, our problem is then simply to evaluate the partition function

$$Z = \sum_{\text{states}} e^{-\beta E}. \tag{1}$$

Here the summation is extended over all states of hydrogen distributions, $\beta = 1/kT$, and E is the energy of the crystal for a given state. A basic assumption we shall make is that E is a simple sum of energies associated with the configuration at each vertex. Ferroelectric or antiferroelectric model results from different energy assignments. For example, if the configuration with a net dipole pointing along the crystal axis is given the lowest energy, then at low enough temperatures there is a tendency for a spontaneous polarization along the crystal axis, thus resulting in a ferroelectric model. On the other hand, an antiferroelectric model results if the energy assignment favours hydrogen configurations with zero dipole moment at each vertex.

The evaluation of the partition function (1) in a closed form is in general a difficult problem for three-dimensional lattices and for arbitrary energy assignments. Very few rigorous results are known. For two-dimensional lattices, however, it is possible in some cases to carry through a rigorous analysis. It is with respect to these exact results that we shall address ourselves in this article.

The first simplification (which also applies to the three-dimensional lattices) was made by Slater (1941) in connection with the hydrogen distributions (states). Adopting hypotheses made by Bernal and Fowler (1933) and used by Pauling (1935) in his discussion of the residual entropy of ice, Slater assumed the following:

(1) There is always one and only one hydrogen atom on each bond. (We have already implicitly assumed this in our previous discussion.)

Ice Rule

(2) There are precisely two hydrogen atoms near to (and two hydrogen atoms away from) a given vertex.

The first rule is based on plausible physical and chemical assumptions and the ice rule ensures local electrical neutrality. As we shall see in later discussions, the imposition of the second condition has profound consequences for the behaviour of the system.

II. Ferroelectric Models and Related Problems

In this section we shall introduce the ferroelectric models and discuss their connection with a number of related problems. The discussion of these relations is interesting because it provides us with further insights into the problems and sometimes allows us to make use of established results in our considerations. For example, the existence of the thermodynamic limit for the most general ferroelectric model follows from the fact that the model is equivalent to an Ising problem for which the thermodynamic limit is known to exist. Only a few of the models introduced in the present section are soluble, however. Detailed discussion of the soluble cases and the solutions will be the subject matter of Sections IV through VII. Another presentation of the relationship of these models to general lattice problems can be found in Percus (1969).

A. The ice problem

We shall begin by discussing the ice problem because that forms the skeleton of the ferroelectric models. Some substances, such as ice and CO, appear to have a residual entropy even at very low temperatures. In the case of ice, the

entropy at 10°K is 0·82 ± 0·05 cal/°K-mole (Giauque and Stout, 1936). The ice crystal has a Wurtzite structure with each oxygen ion hydrogen-bonded to four nearest neighbour oxygens. If the distribution of the hydrogen ions obeys the ice rule (Section I), we can write the residual entropy, S, as

$$S = k \ln Z_0, \tag{2}$$

where Z_0 is (1) with all energies equal to zero and is the number of hydrogen configurations of the crystal consistent with the ice rule, and k is Boltzmann's constant. In an ice crystal, the oxygens are situated at the lattice vertices, and the hydrogen positions on the lattice edges can be specified by attaching arrows to the lattice edges, e.g., using → to represent —H–. Then Z_0 is the number of ways of directing the lattice edges such that there are always two arrows pointing away and two arrows pointing into each lattice point. To illustrate the allowed arrow configurations, let us consider "square" ice, which is the two-dimensional version of real ice and is defined by the same ice

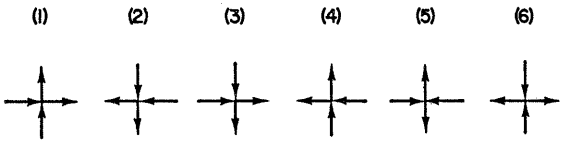

FIG. 1. The six ice rule configurations.

rule applied to a planar square lattice. The six possible states at each vertex are illustrated in Fig. 1. Note that without the ice rule there will be a total of 16 possible states at a vertex. For a large lattice of N vertices, Z_0 is of the order of e^N, and we define

$$W = \lim_{N\to\infty} {Z_0}^{1/N}. \tag{3}$$

In Section V.B we shall evaluate W exactly for square ice and obtain (Lieb, 1967a,b)

$$W_{\text{sq. ice}} = (\tfrac{4}{3})^{3/2} = 1{\cdot}5396007\ldots. \tag{4}$$

It is also possible to consider "linear" ice which is the one-dimensional version of the real ice. A picture of this one-dimensional arrangement is shown in Fig. 2. Here again the ice rule applies to all vertices. The two arrows of the two bonds on the left may be in one of four different configurations. If the two arrows are in the same direction, all other arrows of the lattice are then fixed, pointing in the same direction. If on the other hand the two

arrows are opposite, then each vertex can take two possible states. It follows that for a linear ice with free ends, $Z_0 = 2^N + 2$, or

$$W_{\text{linear ice}} = 2. \tag{5}$$

Meijering (1957) and Nagle (1966) have given numerical estimates of W for two- and three-dimensional ice. Nagle's results are

$$W_{\text{sq. ice}} = 1{\cdot}540 \pm 0{\cdot}001,$$

$$W_{\text{real ice}} = 1{\cdot}50685 \pm 0{\cdot}00015, \tag{6}$$

or $S = 0{\cdot}8154 \pm 0{\cdot}0002$ cal/°K-mole for real ice.

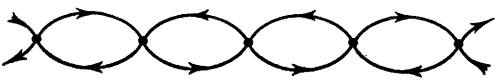

FIG. 2. A typical arrow configuration of linear ice.

Pauling (1935) made a rough estimate of W in the following way: Suppose that the lattice edges and the vertex configurations are independent. Then

$$Z_0 \cong 2^{2N}\left(\tfrac{6}{16}\right)^N = \left(\tfrac{3}{2}\right)^N, \tag{7}$$

or $W = 1{\cdot}5$. In (7), the factor $\frac{6}{16}$ comes from the fact that only 6 out of the 16 possible vertex configurations are allowed. It is remarkable that the crude estimate is so close to the accurate value (6).

Pauling's reasoning to estimate W can be immediately applied to a general "ice" lattice. Consider an arbitrary lattice L (any dimensionality) whose ith vertex is hydrogen-bonded to $2l_i$ (=even) other vertices. The edges of the lattice are directed as before and an ice configuration is defined as having precisely l_i arrows in and l_i arrows out at the ith vertex. This amounts to saying that $\binom{2l_i}{l_i}$ out of the 2^{2l_i} possible vertex configurations are allowed. Since the total number of hydrogens is $l = \sum_i l_i$, the approximate Pauling estimate for the total number of ice configurations on L is

$$Z_0 \cong 2^l \prod_i \binom{2l_i}{l_i} 2^{-2l_i} = \prod_i \binom{2l_i}{l_i} 2^{-l_i}. \tag{8}$$

It is easy to see, by extending an argument due to Onsager and Dupuis (1960), that the estimate given by (8) (and (7)) actually is a lower bound on the exact value of Z_0. Let us cover the ice lattice L *completely* by drawing non-overlapping closed polygons through *all* lattice edges. These may intersect

themselves and each other at vertices but must not overlap on edges. The resulting polygon configuration is called a pattern. In a given pattern, there are always l_i lines (i.e., parts of distinct polygons) intersecting at the ith vertex. Since there are $(2l_i)!/(l_i!2^{l_i})$ different ways that l_i lines may meet at the ith vertex (i.e., the number of pairings of $2l_i$ edges to form l_i lines), the total number of distinct patterns on L is

$$\sum_P 1 = \prod_i \frac{(2l_i)!}{l_i!2^{l_i}}, \tag{9}$$

where the summation is extended over all patterns on L. Next we define a directed pattern as a pattern in which each of the polygons is directed in either the clockwise or the counterclockwise direction. Since each polygon can be directed in two ways, we have then:

$$\text{The total number of directed patterns} \equiv T = \sum_P 2^p \tag{10}$$

where p is the number of polygons of a given pattern. Obviously, each directed pattern gives rise to a unique ice configuration. On the other hand, the number T can also be obtained by counting the number of directed patterns giving rise to the same ice configuration. For each ice configuration, we may obtain a directed pattern by matching the l_i out arrows with the l_i in. Since there are $l_i!$ ways to do this matching at the ith vertex, we have also

$$T = Z_0 \prod_i l_i! . \tag{11}$$

Combining (9), (10) and (11), we see that

$$Z_0 \prod_i l_i! = \sum_P 2^p > \sum_P 1 = \prod_i \frac{(2l_i)!}{l_i!2^{l_i}},$$

or

$$Z_0 > \prod_i \binom{2l_i}{l_i} 2^{-l_i}. \tag{12}$$

Note that this lower bound holds for a lattice of any size provided it has no free edges (i.e., edges which terminate in only one vertex). A periodic lattice is thus allowable.

A crude upper bound on W may be obtained if L has an A–B sublattice structure, i.e., it is bipartite. If we let all lattice points in A take the allowed ice configurations freely, all the possible ice configurations on L will certainly be generated. However, for some configurations, the ice rule will be violated at some vertices in B. Therefore we have generated too many configurations

and hence have the inequality

$$Z_0 < \prod_{i \in A} \binom{2l_i}{l_i}. \tag{13}$$

This bound also holds for a finite lattice with free edges. Combining (12) and (13) and for a large uniform lattice ($l_i = l$), we find

$$\binom{2l}{l} 2^{-l} < W < \binom{2l}{l}^{1/2}, \tag{14}$$

which reduces to

$$\begin{aligned} &\frac{3}{2} < W < \sqrt{6}, \qquad \text{for } l = 2 \\ &\text{and} \\ &\frac{5}{2} < W < \sqrt{20}, \qquad \text{for } l = 3. \end{aligned} \tag{15}$$

These bounds are compared with the exact values of W as follows. For linear ice ($l = 2$) we have $W = 2$ from (5). For a square lattice ($l = 2$) W is given by (4). For a planar triangular lattice ($l = 3$) Baxter (1969) has obtained the exact value (see Section VII.B)

$$W_{\Delta \text{ lattice}} = \frac{3}{2}\sqrt{3} = 2{\cdot}598 \ldots . \tag{16}$$

The Pauling lower bounds appear to provide surprisingly accurate estimates in the two- and three-dimensional cases.

B. Equivalence of the ice problem to other counting problems

Before we leave the subject of the ice problem, it is of interest to demonstrate the equivalence of the ice model with a number of other counting problems. However, it is convenient in our discussions to use an alternate description of the ice configurations which we shall now describe.

We define a bond graph as a graph pertaining to the lattice with bonds (or lines) drawn on a collection of the lattice edges. Since a lattice edge can exist in two states, bond or no bond, there exists a one-to-one correspondence between the arrow configurations on the lattice and the bond graphs on the lattice (Wu, 1967). One way to see this correspondence is to select a basic arrow configuration on a given lattice L. Then each arrow configuration on L is converted into a bond graph by comparing it with the basis and by drawing bonds on those lattice edges having arrows pointing opposite to the corresponding arrows of the basis. Conversely, each bond graph corresponds to

a unique arrow configuration. In the case of a square ice lattice L, we have the following situations:

Equivalence 1

Every vertex of the basis configuration is of type (1). Then as shown in Fig. 3, the allowed bond configuration at a vertex consists of six different kinds of

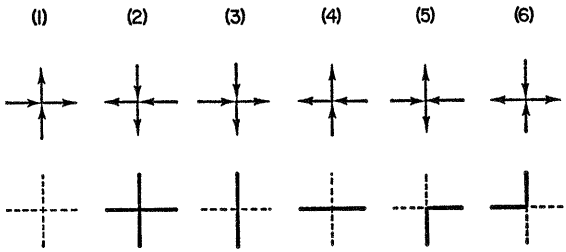

FIG. 3. Bond arrangements obtained by using vertex (1) as the basis.

bond arrangements. The number of ice configurations on L, (4), now gives the number of bond graphs that can be drawn on L using these six kinds of bond arrangements. A typical bond graph of this type is shown in Fig. 4.

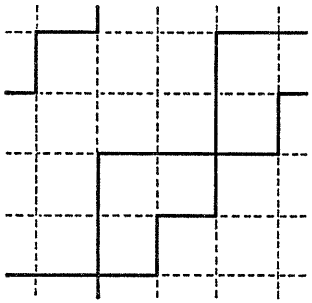

FIG. 4. A typical bond graph constructed from the bond arrangements of Fig. 3.

Equivalence 2

The basis configuration consists of configurations (5) and (6) intermixed in a sublattice construction. That is, all vertices of sublattice A are of type (5) and all vertices of sublattice B are of type (6). The allowed bond configurations on both sublattices A and B are shown in Fig. 5. Notice that the same types of vertices occur on both A and B. Therefore the number of ice configurations (4) now counts the number of polygonal configurations construc-

ted on L *without* using the straight edges. A typical bond graph of this type is given in Fig. 6.

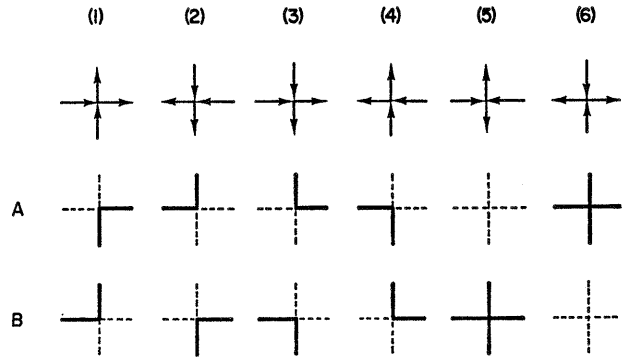

FIG. 5. Bond arrangements obtained by using the basis configurations (5) on sublattice A and (6) on sublattice B.

Equivalence 3

A third way of converting a given arrow configuration into a bond graph is to draw a bond for each arrow pointing into a vertex of sublattice A. In the case of a square lattice, the possible bond configurations are shown in Fig. 7. Again, the same types of vertices occur at both A and B. Note that it is the empty (no bond) and the crossover types of vertices which are now excluded. Therefore (4) counts the configurations of non-intersecting polygons that cover *all* lattice points. A typical bond graph of this type is shown in Fig. 8.

It is also possible to see directly that this counting is equivalent to the equivalence 2 above. If, on the horizontal (or vertical) edges, we replace bonds

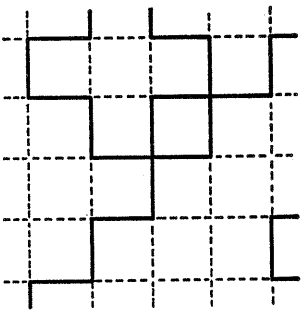

FIG. 6. A typical bond graph constructed from the bond arrangements of Fig. 5—polygons without straight edges.

by no bonds and vice versa, the vertex configurations of Fig. 5 and Fig. 7 are seen to be completely identical. Hence there is a one-to-one correspondence between these two types of configurations, and the countings are the same.

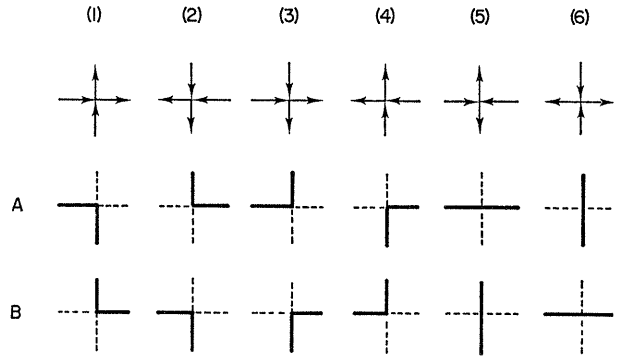

FIG. 7. Bond arrangements obtained by drawing bonds for all arrows pointing toward vertices of sublattice A.

Equivalence 4

Another equivalent counting problem [due to Rys (1963)] can be obtained by considering Fig. 9 which shows a superlattice L_s (denoted by the dotted lines) superimposed on a square ice lattice L (denoted by the solid lines). For each ice configuration on L we construct a bond graph on L_s according to the rule:

> A bond is drawn on an edge, E, of L_s if and only if the vertex of L on E has a configuration with a polarization along E, and the bond is drawn in the direction of the polarization.

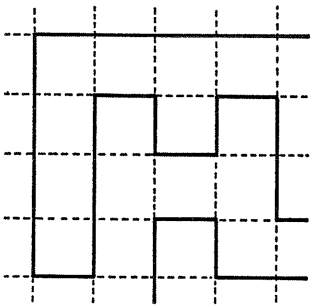

FIG. 8. A typical bond graph constructed from the bond arrangements of Fig. 7—non-intersecting polygons that cover all lattice points.

It follows that each vertex of L_s has either 0, 2 or 4 bonds but not 1 or 3 bonds. A typical example is shown in Fig. 9. As a result, we have for each ice configuration on L a polygonal configuration on L_s. Next we observe that if we reverse all the arrows on L associated with a given polygon on L_s (i.e., those arrows from which the polygon is constructed), the result is another ice

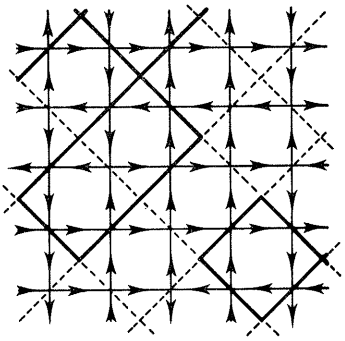

FIG. 9. A typical example of a polygonal configuration on the superlattice L_s constructed from a given ice configuration on the ice lattice L.

configuration which corresponds to the same polygonal configuration on L_s. The same effect is also observed if we reverse the four arrows on L surrounding any vertex on L_s having no bonds. Therefore, by counting the ice configurations on L, we have counted each polygon configuration on L_s 2^p times where p is the number of components of the polygon configuration. To obtain p, every polygon as well as every point of L_s not covered by a polygon is counted as one component. Therefore we arrive at

$$Z_0 = \sum_c 2^p, \tag{17}$$

where the summation is taken over all polygonal configurations on L_s, and Z_0 is the number of ice configurations on L. It must be noted that L_s contains only half as many vertices as L.

Equivalence 5

The ice model can be mapped into another counting problem involving closed polygon configurations. In a configuration of closed polygons, the number of bonds incident at each vertex is 0, 2, or 4. Let p be the number of vertices with two bonds incident in a given polygon configuration, then the number of ice configurations is equal to (Nagle, 1966)

$$Z_0 = (\tfrac{3}{2})^N \sum_c (\tfrac{1}{3})^p. \tag{18}$$

Here the summation is taken over all closed polygon configurations c that can be drawn on the ice lattice. It is verified from (18) that $(3/2)^N$ is indeed a lower bound to Z_0. The expression (18) also forms the basis of a numerical estimate of the residual entropy of real ice (Nagle, 1966). The derivation of (18) will be discussed after eqn (391).

Equivalence 6. The three-colour problem on a square map

It was pointed out to us by Lenard (the original literature reference is unknown to us) that the solution to the ice problem is also the solution to the three-colour problem on a square map. The problem posed is the following: Given a planar square lattice, in how many ways can the squares be coloured with three colours A, B and C so that adjacent squares do not have the same colour. The solution is to A colour the leftmost square in the bottom row. Then, for each ice configuration there is a unique colouring and conversely. First arrange the colours in the cyclic order A–B–C–A. Consider one of the vertices surrounding the given A colour. The squares surrounding this vertex are coloured uniquely by proceeding in a clockwise order and using the rule that an outward arrow on a bond separating two squares means that the colour of the lattice square follows that of the previous square in the order given above (conversely for an inward arrow). Because there are always two arrows out and two arrows in at a given vertex, one always returns to the starting colour A after going around a vertex. In this way one can colour the first row of the lattice, and then the other rows *ad seriatim*. It is easy to see that no ambiguity arises and that we are never prevented from adding one more colour. Finally, the starting colour may be A, B or C. Hence,

$$\text{number of three-colourings of a square map} = 3Z_0 \tag{19}$$

where Z_0 is the number of ice configurations given by (3) and (4).

The related colouring problem for a hexagonal lattice

A similar colouring problem, but one which is not quite equivalent to an ice problem, has been considered by Baxter (1970a) for a hexagonal lattice of N vertices. The problem is the following: In how many ways, Z_0, can the *edges of the lattice be coloured with three colours* so that no edges incident on a common vertex are coloured alike. Using a method similar to that for deriving the residual entropy of square ice, (4), Baxter found (see Section VII.C)

$$\lim_{N\to\infty} Z_0^{\,1/N} = \frac{2}{(1\cdot3)^{1/2}} \cdot \frac{5}{(4\cdot6)^{1/2}} \cdot \frac{8}{(7\cdot9)^{1/2}} \cdots = 1{\cdot}20872\ldots . \tag{20}$$

Since each edge can now be in one of three states, instead of the two states for the ice problem, one may use an argument (Baxter, 1970a) similar to

that of Lenard's to see that this is equivalent to counting the number of *four-colourings of the faces of the hexagonal lattice.* More precisely, one has the result

$$\text{number of four-colourings of the faces of a hexagonal lattice} = 4Z_0 \quad (21)$$

where Z_0 is given by (20).

One may arrive at yet another equivalent counting problem (Baxter, 1970a). Consider a definite edge colouring of the hexagonal lattice. If the edges of colours, say, A and B are traced out, the result is a polygon configuration. Clearly, those colourings having colours A and B interchanged along any polygon result in the same polygonal configuration. The following identity then follows as a result:

$$Z_0 = \sum_c 2^p \quad (22)$$

where the summation is taken over all polygonal configurations c on the hexagonal lattice, and p is the number of polygons of a given polygonal configuration. It is interesting to note the similarity between (22) and (17). We also mention that if the C coloured edges are regarded as dimers, then one has the result

$$\sum_c 1 = \text{the number of dimer configurations}$$

$$\sim \exp\left[\frac{N}{\pi}\int_{\pi/6}^{\pi/2} \ln(2\sin\theta)\,\mathrm{d}\theta\right]. \quad (23)$$

The last expression can be obtained by setting the activities equal to unity in the dimer generating function (359, 372) of the hexagonal lattice.

C. Ferroelectric models with the ice rule

Having introduced the ice model, we are now in a position to define the ferroelectric models. For the sake of clarity in presentation, we shall, in the present section, consider only the ferroelectric models which obey the ice rule (the *ice rule models*), and reserve the discussions of the more general models to a later section. As we shall see, the exact solution of the ice rule models can be obtained for a square lattice, while only special cases of the more general models can be solved.

The difference from the ice problem is that now we introduce energies to the vertices. Therefore, instead of computing the number of ice configurations, the problem now is to evalute the partition function (1). Ferroelectric or antiferroelectric models then result according to different energy assignments. Some energy values for a square lattice are given in Table I.

The *KDP model* is the two-dimensional version of a model proposed by Slater (1941) for the ferroelectric KH_2PO_4, whereas the *F model*, first con-

sidered by Rys (1963), is a model of two-dimensional antiferroelectrics. The *modified KDP model*, first introduced by Wu (1967, 1968), is also a model of ferroelectrics. Note that vertices 1, 2, 3 and 4 have a net polarization, while vertices 5 and 6 have no polarization. Both the modified KDP and the KDP models encourage vertices 1 or 2 or both and hence have completely polarized ground states. The F model encourages vertices 5 and 6 and has an antiferroelectric ground state. At low enough temperature, the onset of long-range order in both models leads to the occurrence of phase transitions.

TABLE I. Vertex Energies for the Ice Rule Models of Fig. 1

	e_1	e_2	e_3	e_4	e_5	e_6
ice	0	0	0	0	0	0
modified KDP	∞	0	ε	ε	ε	ε
KDP	0	0	ε_1	ε_1	ε_1	ε_1
F	ε_2	ε_2	ε_2	ε_2	0	0
direct field	$-(h+v)$	$h+v$	$-h+v$	$h-v$	0	0
staggered field	0	0	0	0	s(sublattice A) $-s$(sublattice B)	$-s$(sublattice A) s(sublattice B)

It is also possible to include an external horizontal electric field h and a vertical electric field v. Assuming each arrow represents a unit electric dipole moment, the effect of the external field can be included by adding to the vertex energies the field energies shown in Table I. The long-range order of the KDP and the modified KDP models are the polarizations and can be computed. However, the long range order for the F model is characterized by a sublattice polarization of vertices 5 and 6. Therefore, to compute this long-range order, it is necessary to apply a staggered quadrupole field which alternates from site to site. The energies of such a staggered field are also given in Table I. Unfortunately, unlike the case of inclusion of a direct field (h, v), the solution to the F model with a staggered field is known only at a particular temperature (Baxter, 1970b, see Section V. H.1).

The KDP model can be defined for lattices in all dimensions (Nagle, 1968). It has been established rigorously that a first-order phase transition occurs for the KDP model in all dimensions (Nagle, 1969 and Takahashi, 1941). The two-dimensional model was first solved by Lieb (1967d) for all temperatures T, and simultaneously by Sutherland (1967) for $T > T_0$, the transition temperature. On the other hand, the antiferroelectric model in one dimension is uninteresting because it leads to no phase trasition. Lieb (1967c) solved the two-dimensional antiferroelectric model, the F model, and showed that

it exhibits an infinite order transition. A similar antiferroelectric model, the *J model*, can also be defined in three dimensions (Nagle, 1965), but no rigorous results are known. The model with all six energy parameters arbitrary is equivalent to a ferroelectric or antiferroelectric model with an external electric field (C. P. Yang, 1967). The solution of the latter problem was obtained by Sutherland *et al.* (1967). The exact results on these models will be the subject matter of Sections IV and V.

It is of interest to mention here two generalizations of these models. We have shown that there is a 3 to 1 morphism between the ice configurations and the three-colourings of the faces of a square lattice such that no two adjacent squares are coloured alike. If we regard the three colours as three types of particles with an infinitely repulsive force between nearest neighbours of the same type, then we have a model of hard squares. It turns out that using a technique similar to that for treating the ferroelectric model, the generating function for this problem can also be evaluated in closed form (Baxter, 1970c; see also Section VII.A). The problem is different because we have to keep track of colours and not just patterns of colours. In particular, if we regard two colours as the background and the third colour as particles, the situation is very similar to the usual gas of hard squares. The model exhibits the interesting behaviour that a phase transition occurs at some intermediate value of the particle density. Another interesting extension of these models is the consideration of the F model on a triangular lattice. A result similar to the infinite order transition of a square lattice has also been obtained by Baxter (1969) (see Section VII.B).

Finally, there is the *ferrielectric model*. It is obvious that the properties of the KDP ferroelectric do not change, even with a field, if we replace the favoured vertices (1) and (2) by the vertices (3) and (4). The ferrielectric is constructed by using the KDP energy assignments except that (1) and (2) are favoured on odd numbered rows and (3) and (4) are favoured on even numbered rows. The ordered ferrielectric state will then have a vertical polarization but no net horizontal polarization. Such substances are discussed in Jona and Shirane (1962).

It is far from obvious, but nonetheless true, that in the thermodynamic limit the properties (including correlation functions) of the ferroelectric and ferrielectric are identical when $h = 0$. The reason for this is presented in Section V.H.2. When $h \neq 0$ the properties of the two models are completely different and progress in solving the ferrielectric problem for $h \neq 0$ is being made at present.

We conclude this subsection with the remark that for $\varepsilon_1 < 0$ and $h = v$ with $|h| < \frac{1}{2}|\varepsilon_1|$ the KDP model has no phase transition of any kind. Glasser (1969) has termed this case the *IKDP model* (I = inverse). The partition function can also be evaluated in this case when $h = v = 0$. (There is an

error in Glasser (1969), and the correct result will appear in Abraham *et al.* (1972) and is given in Section V.B.) Makita and Miki (1970) claimth at the choice $\exp(-\beta\varepsilon_1) = 2$ gives, using (2), the anomalous entropy of *three-dimensional* $NaH_3(SeO_3)_2$, also known as STS (sodium trihydrogen selenite). The value of W so obtained is

$$W_{\mathrm{STS}} = 2{\cdot}578\ldots. \tag{24}$$

Details of this calculation are given in Abraham *et al.* (1970, 1971).

Analogously, for the F model with $\varepsilon_2 < 0$ and h or v equal to zero, there is no phase transition. This is the *IF model.*

D. General ferroelectric models

The models described in the preceding section are the ice models satisfying the ice condition. The physical consideration which leads to the ice rule assumption is the expectation that there are always two hydrogens near to and two hydrogens away from a given lattice point. As the real physical situation is undoubtedly more complicated than this simple picture, it is important to investigate the effect of removing the ice rule restriction (Takagi, 1948). We refer to the models with the ice rule relaxed as the *general ferroelectric models.*

If no restriction at all is imposed on the positioning of the hydrogen atoms, a total of $2^4 = 16$ different kinds of vertex configurations can occur. This general model will be referred to as the *sixteen vertex problem.* The mathematical problem here is to evaluate the partition sum (1) which we now rewrite as

$$Z = \sum_{G} \prod_{i=1}^{N} \omega_{\xi(i)}. \tag{25}$$

Here the summation is extended over all possible arrow configurations, G, on the lattice, N is the total number of vertices, $\xi(i)$ indicates the type of vertex configuration at the ith lattice point, and $\omega_\xi \equiv \exp(-\beta e_\xi)$ is the weight of a vertex having energy e_ξ. The 16 different kinds of vertices for a two-dimensional square lattice are shown in Fig. 10 together with the associated bond arrangements obtained using the prescription given in Section II.B. Vertices (1) through (6) obey the ice rule. Vertices (7) and (8), having four arrows in or out, have the physical interpretation of being doubly ionized, whereas vertices (9) through (16) are singly ionized. The ice models are obtained by taking $e_\xi = \infty$ for $\xi = 7, 8, \ldots, 16$.

A less general, but important case of interest is the *eight vertex problem* for which

$$e_\xi = \infty \quad \text{or} \quad \omega_\xi = 0, \qquad \xi = 9, 10, \ldots, 16. \tag{26}$$

That is, only vertices (1) through (8) are allowed. This eight vertex problem is a first step generalization of both the ice and the Ising models. The mathematical problem is again to evaluate the partition sum (25), but the summation is taken over a more restricted set of graphs. We note from Fig. 10 that in the bond language the number of bonds incident at a vertex in the eight vertex problem is always even, so that the resulting bond graphs always form closed polygons. Thus, the partition sum Z is a generating function

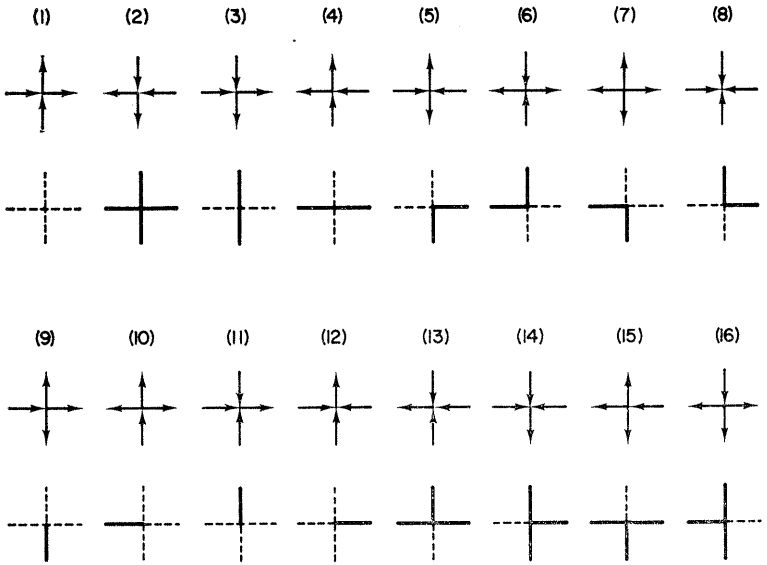

FIG. 10. The sixteen vertex configurations of the general ferroelectric model on a square lattice and the associated bond arrangements obtained by using vertex (1) as the basis.

for weighted polygons drawn on the lattice. The Ising partition function is also a generating function for such polygons, but it counts *only* the number of polygonal edges (Newell and Montroll, 1953). Since the edge weights can always be converted into vertex weights but not vice versa, the eight vertex problem is, in this sense, a generalization of the Ising problem.

One interesting aspect of the general ferroelectric models is their close relationship with the Ising model with many-body interactions. The results are summarised in the following:

(i) The eight vertex problem on a square lattice is equivalent to an Ising model with 2 and 4 body interactions and without an external magnetic field.

(ii) The sixteen vertex problem (in any dimensionality) is equivalent to an Ising model with 2, 3, and 4 body interactions and with an external magnetic field.

We now show this equivalence for the two cases separately.

1. *The eight vertex problem*

Consider a square ferroelectric lattice L. The equivalence of the eight vertex problem on L with an Ising model is established through the introduction of the dual lattice D (Fan and Wu, 1969). The dual lattice D is obtained by drawing perpendicular bisectors to all lattice edges of L, and is itself another square lattice. Let D be an Ising lattice with spins ($\sigma = \pm 1$) located at its vertices. As is well-known, there exists a two-to-one correspondence between the spin configurations of D and the polygon configurations of L (Wannier, 1945). For each spin configuration on D, we can construct a unique polygon configuration on L by drawing bonds along the edges of L separating pairs of unlike spins. In fact, the two spin configurations related by a complete spin reversal result in the same polygon configuration. Conversely, for each polygon configuration on L, we can obtain two different spin configurations on D which are related by a reversal of all spins. If the energies of these corresponding configurations are identical, we then have

$$Z = 2Z_{\text{Ising}} \tag{27}$$

where Z_{Ising} is the partition function for the Ising problem.

In order to establish (27), we introduce for the Ising lattice 2 and 4 body interactions and write the Hamiltonian as (Wu, 1971b)

$$\begin{aligned} H = & - J_0 - J_1 \Sigma^{(1)} \sigma\sigma' - J_2 \Sigma^{(1)} \sigma\sigma' \\ & - J \Sigma^{(2)} \sigma\sigma' - J' \Sigma^{(2)} \sigma\sigma' \\ & - J_4 \Sigma \sigma\sigma'\sigma''\sigma'''. \end{aligned} \tag{28}$$

Here the first two sums extend over, respectively, the first neighbour interactions in the horizontal and the vertical directions, the next two sums extend over the next nearest neighbour interactions in the diagonal directions, and the last term is the four-body interaction summed over the sets of four spins surrounding a vertex of L. The interactions surrounding a typical lattice point of L is shown in Fig. 11, where we have included only one half of the horizontal and vertical interactions. It is now easy to write down the equivalent vertex energies of L in terms of the Ising interactions. For example, the vertex (1) corresponds to having 4 identical spins ($+1$ or -1) surrounding a vertex of L. Therefore the energy e_1 is obtained from (28) as

$$e_1 = - J_0 - J_1 - J_2 - J - J' - J_4.$$

Similarly,

$$\begin{aligned} e_2 &= -J_0 + J_1 + J_2 - J - J' - J_4, \\ e_3 &= -J_0 + J_1 - J_2 + J + J' - J_4, \\ e_4 &= -J_0 - J_1 + J_2 + J + J' - J_4, \\ e_5 &= e_6 = -J_0 + J' - J + J_4, \\ e_7 &= e_8 = -J_0 - J' + J + J_4. \end{aligned} \tag{29}$$

Now the number of opposite polygonal corners (i.e., vertices (5) and (6) or (7) and (8), see Fig. 10) are equal in a given polygon configuration. Therefore, *there is no loss of generality in restricting consideration to* $e_5 = e_6$ *and* $e_7 = e_8$.

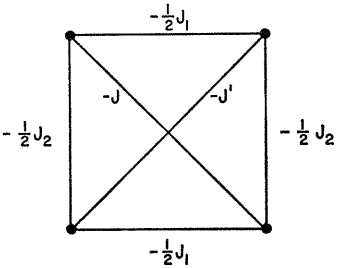

FIG. 11. The Ising interaction (28) surrounding a lattice point of the ferroelectric lattice. Only half of the horizontal and vertical interactions are associated with each lattice point. The four-body interaction is not shown.

We can then solve (29) for the Ising interactions and obtain the inverse relations

$$\begin{aligned} J_0 &= -\tfrac{1}{8}(e_1 + e_2 + e_3 + e_4 + e_5 + e_6 + e_7 + e_8), \\ J_1 &= \tfrac{1}{4}(-e_1 + e_2 + e_3 - e_4), \\ J_2 &= \tfrac{1}{4}(-e_1 + e_2 - e_3 + e_4), \\ J' &= \tfrac{1}{8}(-e_1 - e_2 + e_3 + e_4 + e_5 + e_6 - e_7 - e_8), \\ J &= \tfrac{1}{8}(-e_1 - e_2 + e_3 + e_4 - e_5 - e_6 + e_7 + e_8), \\ J_4 &= \tfrac{1}{8}(-e_1 - e_2 - e_3 - e_4 + e_5 + e_6 + e_7 + e_8). \end{aligned} \tag{30}$$

This completes the proof of equivalence of the two models. In particular for $J_4 = 0$, we have the interesting result that the next neighbour Ising model is equivalent to an eight vertex problem. On putting $e_7 = e_8 = \infty$, the resulting

ferroelectric (ice) model is soluble (Sutherland *et al.*, 1967), but the equivalent Ising model involves some infinite interactions, and this equivalence of models is not very useful in practice. On the other hand, the eight vertex problem is soluble if the corresponding Ising problem has only noncrossing two-body interactions. We find the following possibilities:

(a) $$\{e_1 + e_2, e_3 + e_4\} = \{e_5 + e_6, e_7 + e_8\}. \tag{31}$$

This ensures $J_4 = 0$ and $J = 0$ or $J' = 0$, and the ferroelectric model is equivalent to the Ising model of a triangular lattice. The condition (31) can be shown to lead to the problem of a noninteracting fermion system in the S-matrix formulation (Hurst, 1966) of the eight vertex problem, and has been termed (Fan and Wu, 1969) the *free fermion condition.*

(b) $$\begin{aligned} e_1 = e_2 = -e_3 = -e_4, \\ e_5 = e_6 = -e_7 = -e_8. \end{aligned} \tag{32}$$

This ensures $J_1 = J_2 = J_4 = 0$ (J_0 is taken to be zero), and the model is equivalent to an Ising model consisting of two superimposed square lattices. This leads to the *modified F model* considered by Wu (1969b) (see Section VI. A).

2. *The sixteen vertex problem*

The most general sixteen vertex problem is equivalent to an Ising model with 2, 3 and 4 body interactions and with an external magnetic field (Suzuki and Fisher, 1970). While this result is valid for models in all dimensions, we shall now establish it for the case of a square lattice. The extension to other lattices is straightforward.

Consider a square ferroelectric lattice L consisting of N vertices. It is convenient to consider an Ising lattice L_I whose $2N$ vertices are located at the centres of the $2N$ edges of L. This situation is shown in Fig. 12. As each spin of L_I can take on two values ± 1 and each lattice edge of L can be directed in two different ways, there clearly exists a one-to-one correspondence between the spin configurations of L_I and the arrow configurations of L. Next we assume interactions *only* among those four spins of L_I surrounding a vertex of L. It is then possible to identify the Ising interaction energies of the four spins as the corresponding vertex energies of L. For the most general ferroelectric problem the 16 energy parameters $e_1, \ldots, e_{16}$ are all different. It is therefore necessary to introduce the same number of independent parameters for the interactions among the four spins surrounding a vertex of L. This can be accomplished by including up to 4-body interactions among the spins. Relations similar to (29) and (30) can then be written down

for a unique transformation of the parameters involved. Instead of dealing with the most general case with all 16 parameters different, we shall now illustrate the procedure for the more physical situation when some vertex energies are the same. The extension to the most general case can be readily worked out.

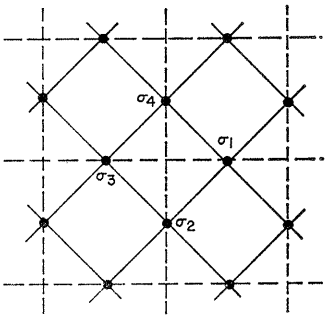

FIG. 12. The superposition of the Ising lattice L (the solid lines) and the ferroelectric lattice L (the dashed lines). The dots denote the positions of the Ising spins.

Let us consider the energy assignment for the following ferroelectric problem

$$\begin{aligned} e_1 &= E_0, \\ e_2 &= E_4, \\ e_3 &= e_4 = E_2, \\ e_5 &= e_6 = E_2', \\ e_7 &= e_8 = E_2'', \\ e_9 &= e_{10} = e_{11} = e_{12} = E_1, \\ e_{13} &= e_{14} = e_{15} = e_{16} = E_3. \end{aligned} \tag{33}$$

Here the subscripts of the E's refer to the numbers of bonds attached to the vertex in the bond language (Fig. 10). The Ising Hamiltonian for the four spins of L_I surrounding a vertex of L is now taken to be

$$\begin{aligned} H = &- J_0 - J_1(\sigma_1+\sigma_2+\sigma_3+\sigma_4) - J_2(\sigma_1\sigma_3+\sigma_2\sigma_4) - J_2'(\sigma_1\sigma_2+\sigma_3\sigma_4) \\ &- J_2''(\sigma_1\sigma_4+\sigma_2\sigma_3) - J_3(\sigma_1\sigma_2\sigma_3+\sigma_1\sigma_3\sigma_4+\sigma_2\sigma_3\sigma_4+\sigma_1\sigma_2\sigma_4) \\ &- J_4\sigma_1\sigma_2\sigma_3\sigma_4. \end{aligned} \tag{34}$$

The relative positioning of the spins σ_1, σ_2, σ_3 and σ_4 is shown in Fig. 12. For definiteness, the following rule of correspondence between the spin and the arrow (or the bond) configuartions will be used.

$$\text{spin } -1\ (+1) \text{ on } L_I \Leftrightarrow \text{a bond (no bond) on } L.$$

Using (33) and (34) we obtain

$$\begin{aligned}
E_0 &= -(J_0 + 4J_1 + 2J_2 + 2J_2' + 2J_2'' + 4J_3 + J_4),\\
E_1 &= -J_0 - 2J_1 + 2J_3 + J_4,\\
E_2 &= -J_0 - 2J_2 + 2J_2' + 2J_2'' - J_4,\\
E_2' &= -J_0 + 2J_2 - 2J_2' + 2J_2'' - J_4,\\
E_2'' &= -J_0 + 2J_2 + 2J_2' - 2J_2'' - J_4,\\
E_3 &= -J_0 + 2J_1 - 2J_3 + J_4,\\
E_4 &= -J_0 + 4J_1 - 2J_2 - 2J_2' - 2J_2'' + 4J_3 - J_4.
\end{aligned} \tag{35}$$

Solving (35) for the J's, the result is

$$\begin{aligned}
J_0 &= -\tfrac{1}{16}(E_0 + 4E_1 + 2E_2 + 2E_2' + 2E_2'' + 4E_3 + E_4),\\
J_1 &= \tfrac{1}{16}(-E_0 - 2E_1 + 2E_3 + E_4).\\
J_2 &= \tfrac{1}{16}(-E_0 - 2E_2 + 2E_2' + 2E_2'' - E_4),\\
J_2' &= \tfrac{1}{16}(-E_0 + 2E_2 - 2E_2' + 2E_2'' - E_4),\\
J_2'' &= \tfrac{1}{16}(-E_0 + 2E_2 + 2E_2' - 2E_2'' - E_4),\\
J_3 &= \tfrac{1}{16}(-E_0 + 2E_1 - 2E_3 + E_4),\\
J_4 &= \tfrac{1}{16}(-E_0 + 4E_1 - 2E_2 - 2E_2' - 2E_2'' + 4E_3 - E_4).
\end{aligned} \tag{36}$$

This completes the mapping of the two models in this special case. It is noteworthy that the matrix which transforms E's into $4J$'s is idempotent, a result which also holds in the general case when all sixteen energies are different. Suzuki and Fisher (1970) have also given the explicit transformation formulas for the case that the energies are invariant when spins are reversed:

$$e_1 = e_2, \quad e_3 = e_4, \quad e_5 = e_6, \quad e_7 = e_8, \quad e_9 = e_{13}, \quad e_{10} = e_{14},$$
$$e_{11} = e_{15}, \quad e_{12} = e_{16}.$$

The equivalent Ising model will have only two-body interactions (i.e., $J_1 = J_3 = J_4 = 0$) if we further assume that

$$E_1 = E_3,$$
$$E_0 = E_4,$$
and
$$4E_1 = E_0 + E_2 + E_2' + E_2''. \tag{37}$$

This then leads to the *general KDP* (Wu, 1970) and the *general F* (Wu, 1969a) models to be considered in Section VI.B.

Another interesting application of this equivalence of models is the finite field Ising problem for which we take

$$\begin{aligned} J_1 &= mH, \\ J_0 = J_2 = J_3 = J_4 &= 0, \\ J_2' = J_2'' &= J. \end{aligned} \tag{38}$$

From (35), we see that the Ising problem is equivalent to a sixteen vertex problem on L with energies (33) or

$$\begin{aligned} &E_0 = -4mH - 4J, \quad E_1 = -2mH, \quad E_2 = 4J, \\ &E_2' = E_2'' = 0, \qquad E_3 = 2mH, \qquad E_4 = 4mH - 4J. \end{aligned} \tag{39}$$

The corresponding vertex weights are therefore

$$\begin{aligned} &\omega_1 = 1/z^2y^2, \quad \omega_2 = y^2/z^2, \quad \omega_3 = \omega_4 = z^2, \\ &\omega_5 = \omega_6 = \omega_7 = \omega_8 = 1, \\ &\omega_9 = \omega_{10} = \omega_{11} = \omega_{12} = 1/y, \\ &\omega_{13} = \omega_{14} = \omega_{15} = \omega_{16} = y, \end{aligned} \tag{40}$$

where

$$z \equiv e^{-2\beta J}, \quad y \equiv e^{-2\beta mH}.$$

The result (40) should be compared with the following alternative formulation of the finite field Ising model as a sixteen vertex problem. In the combinatorial approach to the Ising model with zero magnetic field (Kac and Ward, 1952), the partition function is written as the generating function for polygonal configurations on the lattice (van der Waerden, 1941). This procedure of the high temperature "tanh" expansion can be easily extended to the case of a nonzero magnetic field. The only difference is that the partition function is now written as the generating function for *all* graphs. But this is

precisely the sixteen vertex problem. Following the procedure of the combinatorial approach [see, for example, Newell and Montroll (1953)], it can be shown without difficulty that the partition function of the finite field Ising model defined on L_I is

$$Z_{\text{Ising}} = (\cosh \beta J)^{4N}(\cosh \beta mH)^{2N} Z. \tag{41}$$

Here $2N$ is the total number of spins, and Z is the partition function (25) of a sixteen vertex problem also defined on L_I but with vertex weights

$$\omega_1 = 1, \quad \omega_2 = w^4, \quad \omega_3 = \omega_4 = \omega_5 = \omega_6 = \omega_7 = \omega_8 = w^2,$$

$$\omega_9 = \omega_{10} = \omega_{11} = \omega_{12} = w\tau, \quad \omega_{13} = \omega_{14} = \omega_{15} = \omega_{16} = w^3\tau, \tag{42}$$

where

$$w^2 \equiv \tanh \beta J \quad \text{and} \quad \tau \equiv \tanh \beta mH.$$

We conclude our discussion of the general ferroelectric model with the following remarks.

(a) The validity of our discussion is not restricted to the square lattice. In a three-dimensional ferroelectric crystal, each lattice vertex is hydrogen-bonded to four nearest neighbours. We can again imagine an Ising lattice superimposed on the ferroelectric crystal such that each spin occupies a hydrogen bond. The one-to-one correspondence between the hydrogen and spin configurations again holds. The Ising interactions can then be introduced and the isomorphism of the two models follows as before (see Suzuki and Fisher, 1970).

(b) If we interpret each arrow of L as carrying an electric dipole moment, then the polarizations of the ferroelectric lattice L in the horizontal and vertical directions are precisely the sublattice magnetizations of the Ising lattice L_I, as one can easily see from Fig. 12.

(c) If some vertex energies of L are infinite, then the resulting Ising lattice will have infinite interactions and the scheme of equivalence of the models is not very useful in practice.

III. The Thermodynamic Limit for the Ferroelectric Models

Logic and rigor require that we give consideration to the thermodynamic limit of the ferroelectric models. There are four types of questions. One is the usual problem of the existence of the limiting free energy per unit volume and its convexity with respect to the various intensive parameters. The second is

the relationship of the constrained ice rule models to the unconstrained sixteen vertex models. We shall show in Section III.A that for the free energy and for free edge boundary conditions it is possible to interchange the ice rule limit with the bulk limit. Thus, as far as physics in the bulk is concerned, the ice rule models, which in general are the only ones we can solve analytically, really are the limits of the more physical unconstrained models. This is not to say, however, that the critical indices of the two kinds of models are related. The third problem is to show that, *for the ice rule models*, free boundary conditions and periodic boundary conditions are identical in the bulk limit. Our interest in this last question is not entirely academic and arises from the following fact: the natural boundary condition to impose logically and physically is the free one; for it we can settle the first two questions and this we do in Section III.A. On the other hand, the boundary condition we need in the rest of this article in order to solve the problem analytically is the periodic one. In Section III.B we shall show that the thermodynamic limit exists for periodic boundary conditions but we are unable to show that it is the same as for free edge boundary conditions.

The fourth problem is the existence of the "canonical" free energy and its convexity with respect to the horizontal and vertical polarizations x and y. These concepts are defined and briefly discussed in Section III.C, but we are unable to shed much light on the problem. For the ice rule models we shall, in Sections IV and V, actually calculate a free energy which is grand canonical with respect to x and canonical with respect to y. It is not always easy to see explicitly that it is convex in y but we shall assume convexity, which surely must be true, even though we cannot prove it.

Thus, we raise more problems than we can solve and hope that in time their solution will be forthcoming. It is to be emphasized, however, that all these problems can be settled affirmatively for the eight and sixteen vertex models (provided all the vertex weights are nonzero). This is so because both of these models are equivalent (in different ways) to Ising models with finite spin interaction energies, and for the Ising model there is no difficulty in carrying through the proofs (*cf.* Ruelle, 1969).

In an attempt to be systematic we have placed the present section before the detailed analysis of the ice rule models. It is not needed in the remainder of this article and may be omitted in a first reading.

A. The thermodynamic limit for free edge boundary conditions

For the sake of concreteness we restrict ourselves to the planar square lattice although the following theorems can evidently be extended to more general lattices and even more general models as, for example, the model discussed by Baxter in Section VII.

Let L be the infinite two-dimensional square lattice.

Definition: A *domain*, Λ, is a subset of vertices of L together with the bonds of L terminating in at least one vertex of Λ. Those bonds of Λ which terminate in two vertices of Λ are called *interior* bonds and those which terminate in one vertex are called *exterior*. A vertex which is the terminus of an exterior bond is called a boundary vertex and the set of such vertices is called the *boundary* of Λ. Thus each vertex of Λ always is the terminus of four bonds of Λ. We define $V(\Lambda)$ to be the number of vertices of Λ. Finally, $\Lambda_1 \cup \Lambda_2$ has the usual meaning except for the understanding that exterior bonds may become interior bonds under the union.

Rectangular Domains: These will be denoted by (M, N) with M rows and N columns of vertices.

The partition function, $Z(\Lambda)$, is defined in (25). To specify Z more precisely we must specify what constraints, if any, we place on the arrows of the exterior bonds.

Definition: The *free partition function* (denoted by Z_F) is the sum in (25) with no restriction on the exterior bond arrows. The *periodic partition function* (denoted by Z_P) is defined for rectangular domains and is the sum in (25) with the constraint that horizontal exterior bonds on the same row have the same arrow, and similarly for vertical exterior bonds.

In both cases we define

$$z(\Lambda) = \frac{1}{V(\Lambda)} \ln Z(\Lambda). \tag{43}$$

[The free energy per vertex, $\mathscr{F}$, is defined to be $-kT\, z(\Lambda)$.]

Clearly,

$$z_F(\Lambda) \geqslant z_P(\Lambda). \tag{44}$$

In this section we shall consider only free boundary conditions and shall drop the subscript F. We shall, however, consider domains of arbitrary shape.

Now consider the sixteen vertex model which we define by the condition that ω_1 through ω_{16} are all non-zero. As shown in section II.D, this model is equivalent to an Ising model with interaction energies that involve at most four spins and that are *finite*. The only difference is in the definition of volume; for the Ising model the usual definition of the volume is $\hat{V}(\Lambda)$ = number of "spins" = number of bonds = $2NM + N + M$ for a rectangular domain. However, the use of $V(\Lambda)$ in (43) is equally appropriate. It is well known (*cf.* Ruelle, 1969) that for the Ising model under consideration the following is true:

(1) $\lim_{\Lambda\to\infty} z(\Lambda) = z$ exists for a sequence of domains tending to infinity in the sense of Van Hove (Ruelle, 1969, definition 2.1.1) and the limit is independent of shape.

(2) z, considered as a function of the 16 energies, is jointly continuous and convex and is a decreasing function of each energy.

To discuss what happens when certain particular vertex weights, $\omega_a, \omega_b \ldots$, vanish (e.g. $a, b, \ldots = \{7, \ldots, 16\}$ which would be the ice rule limit), let $\omega_j \to \omega_j e^{-\varepsilon}$ for $j = a, b, \ldots$ and denote the resulting $z(\Lambda)$ by $z(\Lambda, \varepsilon)$ and $\lim_{\Lambda\to\infty} z(\Lambda, \varepsilon)$ by $z(\varepsilon)$. By (1) above $\lim_{\varepsilon\to\infty} z(\varepsilon)$ exists (possibly it is $-\infty$) and we denote it by $z(\infty)$. Since $z(\Lambda, \infty) \leqslant z(\Lambda, \varepsilon)$ for all ε, we have, for all ε and for a sequence of domains tending to infinity in the sense of Van Hove, $\limsup_{\Lambda\to\infty} z(\Lambda, \infty) \leqslant z(\varepsilon)$ for all ε and hence

$$\limsup_{\Lambda\to\infty} z(\Lambda, \infty) \leqslant z(\infty). \tag{45}$$

To obtain an opposite bound we note that if we paste two domains, Λ_1 and Λ_2, together then

$$Z(\Lambda_1 \cup \Lambda_2, \varepsilon) \leqslant Z(\Lambda_1, \varepsilon)\, Z(\Lambda_2, \varepsilon). \tag{46}$$

This is so because any bond (spin) which was exterior in Λ_1 and Λ_2 and which becomes interior under the union has a constraint placed on it, i.e. two independent spins become one spin. For the same reason, (46) is true even if Λ_1 and Λ_2 have common interior bonds. Let $\Lambda = (M, N)$ be a rectangular domain and paste together J^2 copies of Λ (with J an integer) to form Λ^J which is a (JM, JN) domain. (46) reads

$$z(\Lambda^J, \varepsilon) \leqslant z(\Lambda, \varepsilon) \tag{47}$$

for all ε. Letting $J \to \infty$, $z(\varepsilon) \leqslant z(\Lambda, \varepsilon)$ which implies that $z(\infty) \leqslant z(\Lambda, \infty)$. Finally, letting $\Lambda \to \infty$ in the sense of Van Hove

$$\liminf_{\Lambda\to\infty} z(\Lambda, \infty) \geqslant z(\infty). \tag{48}$$

Combining (45) and (48) we arrive at the desired result for rectangular domains tending to infinity in the sense of Van Hove

$$\lim_{\Lambda\to\infty} z(\Lambda, \infty) = \lim_{\varepsilon\to\infty} z(\varepsilon) = z(\infty). \tag{49}$$

For domains of general shape the same result can be obtained by the standard trick of embedding a given domain in a larger rectangular domain. To

carry out this proof, however, we require that the sequence of domains go to infinity in the sense of Fisher (Ruelle, 1969, definition 2.1.2).

The proof leading to (49) obviously generalizes in the sense that it is not necessary to switch off all the undesired vertices simultaneously but instead they can be switched off one at a time. That is to say the six vertex (ice rule) model can be regarded as the limit of the eight vertex model and that, in turn, can be regarded as the limit of the sixteen vertex model.

We can state our conclusions as follows: let $\{\Lambda\}$ be a sequence of domains tending to infinity in the sense of Fisher (or Van Hove for rectangular domains). Let I be a subset of the integers 1 through 16 and let J be its complement. Denote by e_I the vertex energies associated with each i in I and similarly for e_J. We denote the I vertex problem by writing $e_J = \infty$. Let $z(\Lambda, e_I)$ be defined as in (43) using the free partition function. Then

(1) The limit

$$\lim_{\Lambda\to\infty} z(\Lambda, e_I, e_J = \infty) = z(e_I) \tag{50}$$

exists independent of shape. It is a convex, decreasing function of e_I.

(2) The limit $\Lambda \to \infty$ and the limit $e_J \to \infty$ can be interchanged, i.e.

$$z(e_I) = \lim_{e_J\to\infty} z(e_I, e_J). \tag{51}$$

The latter limit can be taken in any order.

B. Periodic boundary conditions

In this section we shall be concerned exclusively with periodic boundary conditions and shall omit the subscript P.

Let $\Lambda = (M, N)$ be a rectangular domain with specific configurations of arrows S(resp. S') on the left hand (resp. right hand) set of M horizontal exterior bonds. Likewise, specify configurations T and T' on the lower and upper sets of N vertical exterior bonds, and let $Z(S, S'; T, T')$ be the partition function, (25), with these imposed constraints. Then

$$Z(M, N) = \sum_S \sum_T Z(S, S; T, T). \tag{52}$$

If we define

$$\Gamma(M, N) = \max_{S,T} Z(S, S; T, T), \tag{53}$$

then

$$\Gamma(M, N) \leqslant Z(M, N) \leqslant \Gamma(M. N)2^{(M+N)}. \tag{54}$$

If we paste two such domains together to form a $(2M, N)$ rectangle then

$$Z(2M, N) \geqslant \Gamma(M, N)^2 \geqslant Z(M, N)^2 \, 2^{-2(M+N)} \tag{55}$$

since we can always impose the favoured configuration of (53) on each component of $(2M, N)$.

Now let $\Lambda_0 = (M_0, N_0)$ be an arbitrary, but henceforth fixed, rectangle and form a *standard sequence* $\Lambda_j = (2^j M_0, 2^j N_0)$ with j integral. Denoting $z(\Lambda_j)$ by z_j we have, from the trivial generalization of (55), that

$$z_{j+1} \geqslant z_j - 2^{-j}(M_0{}^{-1} + N_0{}^{-1}) \ln 2. \tag{56}$$

Hence, the sequence $\{z_j\}$ is essentially increasing and since it is bounded above it has a limit z which, of course, is a convex non-increasing function of the vertex energies since each z_j has this property.

To establish the same limit for a general, Van Hove sequence of domains $\{\Lambda\}$ we shall require that

$$e^A = \min \{\omega_2, \omega_3, \omega_4\} > 0. \tag{57}$$

Fix j and fill each Λ in the sequence with a maximal number, $k(\Lambda, j)$, of disjoint copies of Λ_j arranged in a rectangle. The remainder of Λ can be filled with vertices 2, 3 or 4. Then, in analogy with (55), one has that

$$z(\Lambda) \geqslant \alpha z_j - \alpha 2^{-j}(M_0{}^{-1} + N_0{}^{-1}) \ln 2 + A(1 - \alpha), \tag{58}$$

where $\alpha = k(\Lambda, j) 2^{2j} M_0 N_0 / V(\Lambda)$. As $\Lambda \to \infty$, $\alpha \to 1$, so that

$$\liminf_{\Lambda \to \infty} z(\Lambda) \geqslant z_j - 2^{-j}(M_0{}^{-1} + N_0{}^{-1}) \ln 2. \tag{59}$$

Hence, letting $j \to \infty$,

$$\liminf_{\Lambda \to \infty} z(\Lambda) \geqslant z. \tag{60}$$

Conversely, we can fix Λ and fill Λ_j with a maximal number, k', of copies of Λ. In the same way as we derived (59) we obtain

$$z \geqslant z(\Lambda) - (M^{-1} + N^{-1}) \ln 2 \tag{61}$$

where $\Lambda = (M, N)$. As $\Lambda \to \infty$, both M and $N \to \infty$. Combining (61) and (59) we obtain the desired result:

$$\lim_{\Lambda \to \infty} z(\Lambda) = \lim_{j \to \infty} z_j = z \tag{62}$$

for a sequence of rectangles tending to infinity in the sense of Van Hove.

In point of fact, what we shall actually calculate, as shown in (76), is the limit

$$\lim_{N\to\infty}\lim_{M\to\infty} z(M,N), \tag{63}$$

and we must demonstrate that this limit is also z. Anticipating the result of Section IV.A, which is derived using the transfer matrix, we have that

$$\lim_{M\to\infty} z(M,N) = h(N) \tag{64}$$

exists for each N. Put $M = kN$, for k an integer, and use (55) to obtain

$$z(kN,N) \geqslant z(N,N) - 2N^{-1}\ln 2. \tag{65}$$

By letting $k\to\infty$, we conclude that

$$h(N) \geqslant z(N,N) - 2N^{-1}\ln 2, \tag{66}$$

and hence that

$$\liminf_{N\to\infty} h(N) \geqslant z. \tag{67}$$

To obtain the opposite bound, consider a domain (M, kN) and use (55) to obtain

$$z(M,kN) \geqslant z(M,N) - (M^{-1}+N^{-1})\ln 2. \tag{68}$$

If we put $k = M$, then the sequence of domains (M, MN) is Van Hove, for fixed N. The limit $M\to\infty$ in (68) then gives

$$z \geqslant h(N) - N^{-1}\ln 2, \tag{69}$$

and hence

$$\limsup_{N\to\infty} h(N) \leqslant z, \tag{70}$$

which establishes that (63) does, indeed, give the correct limit z.

Unfortunately, we are unable to prove that z_P and z_F are identical. The major stumbling block seems to be the following: As we see from (55), $z_P(\Lambda)$ increases upward to its limit z_P, provided we ignore inessential "surface" terms. Contrariwise, (46) shows that $z_F(\Lambda)$ essentially decreases downward to its limit z_F. It is this disparity that stands in the way of a proof.

C. The canonical ensemble

For a given domain Λ we can, for each configuration of arrows, define the horizontal and vertical polarizations per bond, x and y, as

$$x = \frac{\text{number of right arrows} - \text{number of left arrows}}{\text{number of horizontal bonds}} \tag{71}$$

and similarly for y. Thus $-1 \leqslant x \leqslant 1$ and $-1 \leqslant y \leqslant 1$. In terms of these intensive parameters, (25) defines the grand canonical partition function. We can, however, also define the canonical partition function $Z(x, y)$ as the restricted sum over configurations with fixed values of x and y. In Sections IV, V and VII we actually use a mixed ensemble which is canonical with respect to y and grand canonical with respect to x.

The problems we pose are the following:

1. Does the canonical free energy per vertex, $\mathscr{F}(x, y) = -kTz(x, y)$, have a thermodynamic limit?

2. Is $z(x, y)$ the same for free and periodic boundary conditions?

3. Is $z(x, y)$ a concave function of (x, y) as thermodynamic stability requires?

4. Is $z(x, y)$ the same as the grand canonical z discussed in Sections III.A and III.B? That is, for all vertex energies is

$$z = \max_{(x,y)} z(x, y) \tag{72}$$

true?

We remark that an affirmative answer to 1, 2 and 4 does not imply 3. A trivial counterexample is the following: Suppose the only allowed vertices are (1) and (2) and $\omega_1 = \omega_2 = 1$. Then

$$\begin{aligned} &z(1, 1) = z(-1, -1) = 0 \\ &z(x, y) = -\infty \text{ otherwise} \\ &z = 0. \end{aligned} \tag{73}$$

Thus, in this case, all limits exist and (72) is true, but $z(x, y)$ is not concave. This example shows that a condition even stronger than (57) is required to establish 3.

IV. The Transfer Matrix and Its Diagonalization

A. The transfer matrix concept

We begin with some general remarks on the transfer matrix. It is not our intention to describe the concept in stratospheric generality or to give its history, which is a long one. The reader can find a more general treatment in Lieb (1969b) as well as in the article on the Ising model in this book.

The two-dimensional lattices we wish to consider are $N \times M$, which is to say they have N sites horizontally and M vertically. A *row* will usually mean a row of N vertical bonds, as in the case of the square lattice, but it may have a slightly different meaning as, for example, in the case of the triangular lattice (Section VI below). In any case, we can talk of the *state* of a row by

specifying the configuration of the lattice restricted to the row. For the square ice lattice the state of a row is the configuration of up or down arrows on the row of bonds. If ϕ_i is the state on the ith row then the sequence $\{\phi_1, \phi_2, \ldots, \phi_{M+1}\}$ is a partial description of the configuration of the whole lattice. As all rows are equivalent, each ϕ_i, in turn, is one of the set $\{\phi^1, \phi^2, \ldots, \phi^R\}$ where $R = 2^N$ generally and the ϕ^i are the allowed states of *any* row. We do not attempt to describe the configuration of the horizontal bonds, but instead introduce the *transfer matrix* T_{ij}, alternatively $T(\phi^i, \phi^j)$, which couples two adjacent states and is

$$T_{ij} = \Sigma \text{ (allowed configurations of horizontal bonds) } e^{-\beta E} \tag{74}$$

where E is the sum of the vertex energies formed by the two states ϕ^i and ϕ^j together with the horizontal arrows. Our convention is that ϕ^i is the state of the upper row.

It is very convenient to assume that $\phi_{M+1} = \phi_1$, i.e. that the lattice is periodic in the vertical direction, but it is not absolutely essential to do so. In the limit $M \to \infty$, the imposition of periodicity has no effect.

From the definition of the partition function (1)

$$\begin{aligned} Z &= \sum_{\phi_M} \cdots \sum_{\phi_1} T(\phi_1, \phi_M) T(\phi_M, \phi_{M-1}) \cdots T(\phi_3, \phi_2) T(\phi_2, \phi_1) \\ &= \text{Trace } (T^M) \\ &= \Sigma(\lambda_j)^M \end{aligned} \tag{75}$$

where $\{\lambda_j\}$ are the eigenvalues of T, i.e. the roots of $\det |T - \lambda I| = 0$. Since the matrix elements of T are non-negative, the Perron–Frobenius theorem (Brauer, 1964) guarantees that the λ_j of maximum modulus is positive and unique if the diagonal elements of T are positive. In our case, it will turn out that T breaks up into several diagonal blocks, in each of which the above assertion holds. Denoting the largest eigenvalue by Λ we have (even if Λ is degenerate)

$$\lim_{M \to \infty} \frac{1}{M} \ln Z = \ln (\max \lambda_j) \equiv \ln \Lambda. \tag{76}$$

To use (76) we have to solve the eigenvalue equation

$$T\Psi = \Lambda\Psi \tag{77}$$

which means finding a vector $\Psi = (\psi_1, \psi_2, \ldots, \psi_R)$ such that

$$\sum_i T_{ji} \psi_i = \Lambda \psi_j. \tag{78}$$

We remark that T need not be symmetric and, in fact, it is not for KDP. Physically, this means that turning the lattice upside down does not leave the

vertex energy assignments unchanged. However, the Perron–Frobenius theorem guarantees that the Ψ we seek is a non-negative vector and this property will be very useful in identifying Λ.

Another remark is that while periodicity in the vertical direction is not essential, periodicity in the horizontal direction is, and we shall derive T under this assumption. This entails connecting together the bonds which emanate from the right and left of each row; unless they are connected, the conservation law which we shall rely on heavily is not strict but only approximate.

B. The ice problem

It is easily inferred (Lieb, 1967b) that one consequence of the ice rule (together with the horizontal periodicity) is that $T_{ij} = 0$ unless ϕ^i and ϕ^j have the same number of down (or up) arrows. Thus, if

$$n = \text{number of down arrows in a row} \tag{79}$$

then n is a conserved quantity from row to row and T is a block diagonal matrix with one block for each value of $n = 0, 1, \ldots, N$. The order of block n is $\binom{N}{n}$. In analogy with a spin $\frac{1}{2}$ system we may define

$$S_z = \tfrac{1}{2}(N - 2n) \tag{80}$$

but a more useful quantity (in the thermodynamic limit) is

$$y = 1 - 2n/N \tag{81}$$

which is the average z component of the "spin" per vertical bond.

Instead of the notation ψ_i as in (78) it is convenient to use

$$f(x_1, x_2, \ldots, x_n) \tag{82}$$

to denote the ψ associated with the state having down arrows at the locations

$$1 \leqslant x_1 < x_2 < \ldots < x_n \leqslant N, \tag{83}$$

so that in a given n subspace (78) becomes

$$\sum_{\mathbf{Y}} T(\mathbf{X}, \mathbf{Y}) f(\mathbf{Y}) = \Lambda f(\mathbf{X}) \tag{84}$$

where $\mathbf{X}$ and $\mathbf{Y}$ refer to n-tuples as in (83). It is easily seen [see Lieb (1967b, 1969b) for elucidation] that T can be written

$$T = T_R + T_L \tag{85}$$

where

$$T_R = 1 \text{ if } x_{i-1} \leqslant y_i \leqslant x_i, \text{ all } i \tag{86a}$$

$$= 0 \text{ otherwise} \tag{86b}$$

and

$$T_L = 1 \text{ if } x_i \leqslant y_i \leqslant x_{i+1}, \text{ all } i \tag{87a}$$

$$= 0 \text{ otherwise.} \tag{87b}$$

The subscripts L(resp. R) refer to the fact that the horizontal arrows at the extremities of a row point to the left (resp. right). Clearly,

$$T_L = T_R{}^{\dagger} \tag{88}$$

where † means Hermitian conjugate.

If we combine (84–87) (always bearing in mind that we are in some definite n subspace) then

$$\Lambda f(x_1, \ldots, x_n) = \sum_{y_1=1}^{x_1} \sum_{y_2=x_1}^{x_2} \cdots \sum_{y_n=x_{n-1}}^{x_n *} f(y_1, \ldots, y_n) + \sum_{y_1=x_1}^{x_2} \cdots \sum_{y_n=x_n}^{N *} f(y_1, \ldots, y_n) \tag{89}$$

where the * means that we sum only over those $\mathbf{Y}$ consistent with (83). We emphasize, once again, that (89) is meaningful *only* when $\mathbf{X}$ and $\mathbf{Y}$ satisfy (83). The first sum is T_R and the second is T_L.

Henceforth, we shall write the first repeated summation in (89) (with the asterisk included) as Σ_R and the second as Σ_L.

C. The transfer matrix for the ice rule ferroelectric models

The transfer matrix for the ice rule ferroelectric problem (Table 1) has, in the absence of a staggered field, the same structure features as the ice problem. In particular: T has the same diagonal block structure; in each n subspace (85), (86b) and (87b) are true (although (88) may fail). The general analog of (89) is

$$\Lambda f(\mathbf{X}) = \Sigma_R D_R(\mathbf{X}, \mathbf{Y}) f(\mathbf{Y}) + \Sigma_L D_L(\mathbf{X}, \mathbf{Y}) f(\mathbf{Y}) \tag{90}$$

where the functions D_R and D_L, which are different in general, depend on the energy assignments. They are, of course, non-negative in the physical case so that the Perron–Frobenius theorem still holds. Eqn (90) is Hermitian, i.e. (88) is true, if and only if

$$D_L(\mathbf{X},\mathbf{Y}) = \bar{D}_R(\mathbf{Y}, \mathbf{X}), \tag{91}$$

where the bar means complex conjugate.

The D function, L or R, is the Boltzmann factor for the vertices "formed" by Y and X. If $n_j, j = 1, \ldots, 6$, is the number of vertices of type j so formed then

$$D = \exp\left(-\beta \sum_{j=1}^{6} n_j e_j\right). \tag{92}$$

We want to consider the general six vertex problem with $e_1, \ldots, e_6$ being arbitrary and we remark that there are only four independent energies to consider. This is so because: (a) The zero of energy can be chosen arbitrarily which merely requires multiplying Λ, or Z, by a trivial factor; (b) the conservation of n implies that $n_5 = n_6$ on every row and hence we may assume $e_5 = e_6$.

Persual of Table I shows that the most general energy assignment is a linear combination of the lines marked KDP, F and direct field, provided we allow the two ε's to be different. In other words,

$$\begin{aligned} e_1 &= \varepsilon_2 - h - v, \quad e_2 = \varepsilon_2 + h + v, \quad e_3 = \varepsilon_1 + \varepsilon_2 - h + v, \\ e_4 &= \varepsilon_1 + \varepsilon_2 + h - v, \quad e_5 = \varepsilon_1, \quad e_6 = \varepsilon_1. \end{aligned} \tag{93}$$

A ferroelectric transition occurs if the lowest energy is e_1, e_2, e_3 or e_4. Similarly an antiferroelectric transition occurs if $e_5 = e_6 < e_1, e_2, e_3, e_4$. (See further discussion of this point in Section V.F.) The model is said to be *intrinsically* ferroelectric (or antiferroelectric) if, in the absence of an external field, the transition is ferroelectric (or antiferroelectric). This can be most simply specified by defining the variable

$$\bar{\varepsilon} = \max(0, \varepsilon_1) - \varepsilon_2, \tag{94}$$

such that $\bar{\varepsilon} > 0$ (resp. $\bar{\varepsilon} < 0$) for an intrinsically ferroelectric (resp. antiferroelectric) model.

Now, with ε_1, ε_2, h and v determined, consider the three different D's we would get from each line alone, that is either the KDP row with $\varepsilon = \varepsilon_1$, the F row with $\varepsilon = \varepsilon_2$ or the direct field row with the given h and v. Call these D's, either L or R, D^{KDP}, D^F and D^E, respectively. Then from (92)

$$D = D^{KDP} D^F D^E, \tag{95}$$

where ordinary multiplication is meant. We can further write

$$D^E = D^H D^V \tag{95b}$$

where D^H and D^V are the separate contributions of the horizontal and vertical fields. We also introduce the quantities

$$\begin{aligned} K_1 &= \beta\varepsilon_1, \qquad K_2 = \beta\varepsilon_2, \\ H &= \beta h, \qquad V = \beta v. \end{aligned} \tag{96}$$

Clearly,

$$D_R{}^V(\mathbf{X}, \mathbf{Y}) = D_L{}^V(\mathbf{X}, \mathbf{Y}) = e^{NVy} \tag{97}$$

where y is defined in (81). Since D^V is independent of $\mathbf{X}$ and $\mathbf{Y}$ its effect is merely to multiply Λ by an n dependent constant.

D^H is almost as simple:

$$D_R{}^H(\mathbf{X}, \mathbf{Y}) = \exp(NH) \exp\left[2H \sum_{i=1}^{n} (y_i - x_i)\right]$$

$$D_L{}^H(\mathbf{X}, \mathbf{Y}) = \exp(-NH) \exp\left[2H \sum_{i=1}^{n} (y_i - x_i)\right]. \tag{98}$$

It is interesting to note that D^V, unlike D^H, satisfies (91) and hence is Hermitian.

To evaluate D^F we need only count the number of times some x_i = some y_j. That is

$$D_R{}^F(\mathbf{X}, \mathbf{Y}) = D_L{}^F(\mathbf{X}, \mathbf{Y})$$
$$= \exp\left[-K_2\left(N - 2n + 2\sum_{i=1}^{n}\sum_{j=1}^{n}\delta(x_i - y_j)\right)\right] \tag{99}$$

with δ being the Kronecker delta. D^F is Hermitian.

KDP is the most complicated case. With some reflection one finds

$$D_R{}^{KDP}(\mathbf{X}, \mathbf{Y}) = \exp K_1\left[-n + \sum_{i=1}^{n}(y_i - x_i) + 2\sum_{i=1}^{n-1}\delta(y_{i+1} - x_i)\right]$$

$$D_L{}^{KDP}(\mathbf{X}, \mathbf{Y}) = \exp K_1\left[-N - n + \sum_{i=1}^{n}(y_i - x_i + 2\delta(y_i - x_i))\right]. \tag{100}$$

Clearly, (91) is not satisfied for KDP. It is noteworthy that part of D^{KDP} is the same as D^H, apart from some obvious differences in parameters. The remainder of D^{KDP} is similar to, but essentially different from D^F.

Notation: If we are discussing only either F or KDP then we will denote K_1 or K_2 simply by K.

D. Relationship of two-dimensional ferroelectric models and one-dimensional spin systems (E. Barouch, *Department of Mathematics, Massachusetts Institute of Technology, Cambridge, Massachusetts, U.S.A.*).

The transfer matrix for a two-dimensional ferroelectric system can be thought of as a complicated, generally non-Hermitian operator on a quantum mechanical, one-dimensional spin system. For the general ferroelectric model considered in Section II.D, even when all vertices are allowed, the correspondence is simple. The correspondence for the models considered by Baxter

in Section VII is much more complicated and we shall not discuss those in this section.

The configurations of up or down arrows on vertical bonds are evidently isomorphic to the states of a chain of N spin $\frac{1}{2}$ particles and the transfer matrix, T, is then equivalent to some spin operator. We set ourselves two goals:

(1) Find an explicit expression for T in terms of Pauli spin operators.

(2) Find a non-trivial *linear* Hamiltonian that commutes with T.

By a linear Hamiltonian is meant one of the form

$$H = \sum_{i=1}^{N} H_i \tag{101}$$

where H_i involves *only* spin operators at sites i *and* $i+1$ (with the obvious notation that $N+1 \equiv 1$). The usual Heisenberg Hamiltonian is an example of (101). If we can accomplish goal 2 then we shall have obviously gained some additional information about the eigenvectors of T because $[H, T] = 0$ implies that the eigenvectors of T lie in the invariant subspaces of H.

The achievement of the two goals was first accomplished by McCoy and Wu (1968) for the 6 vertex problem and by Sutherland (1970), using an idea of Fan, for a special case of the 8 vertex problem. Here, we shall complete goal 1 for the 16 vertex case but shall not go beyond the 8 vertex model for goal 2.

For the ice problem (Lieb, 1967a, b)

$$T_R = 1 + \sum_{i<j} \sigma_{+i}\,\sigma_{-j} + \sum_{i<j<k<l} \sigma_{+i}\,\sigma_{-j}\,\sigma_{+k}\,\sigma_{-l} + \cdots \tag{102}$$

and $T_L = T_R{}^{\dagger}$. For the 16 vertex problem the analogue of (102) is evidently much more complicated, but even (102) is not yet in a sufficiently useful form because calculating the commutator of (101) and (102) is difficult.

To proceed, we define $T_{LR}{}^N$ to be the transfer matrix for N spins in which we insist that the leftmost horizontal arrow point left and the rightmost point right. Likewise we define $T_{RR}{}^N$, $T_{RL}{}^N$ and $T_{LL}{}^N$. We record this information in the form of a matrix

$$\mathbf{A}^N = \begin{pmatrix} T_{RR}{}^N & T_{RL}{}^N \\ T_{LR}{}^N & T_{LL}{}^N \end{pmatrix} \tag{103}$$

whose entries, it must be kept clearly in mind, are operators acting on the space of N spins. In the usual unpedantic, but imprecise, physics notation we can also think of the T^N as operators on the first N spins in a chain of more than N spins. Obviously the transfer matrix is given by

$$T_R = T_{RR}{}^N; \qquad T_L = T_{LL}{}^N; \qquad T = T_R + T_L \tag{104}$$

or, more schematically,

$$T = \text{Trace}^* \mathbf{A}^N, \tag{105}$$

where * means we take *only* the 2 × 2 trace and *not* the trace on the spin operators.

$\mathbf{A}^1$ is a matrix function of the operators on spin 1. We can, however, think of a copy of $\mathbf{A}^1$ acting on an arbitrary spin, k. This matrix we will denote by $\mathbf{A}_k$. If we wish to discuss $\mathbf{A}_k$ without specifying which spin it acts on, we shall omit the subscript k.

Clearly,

$$\mathbf{A}^{N+1} = \mathbf{A}^N \mathbf{A}_{N+1} \tag{106}$$

where matrix multiplication is meant. Hence,

$$\mathbf{A}^N = \mathbf{A}_1 \mathbf{A}_2 \ldots \mathbf{A}_N. \tag{107}$$

The next problem is to find the basic, single spin, $\mathbf{A}$. We consider the 16 vertex problem, as given in Fig. 10, with energies e_1 to e_{16} and vertex weights

$$\omega_i = \mathrm{e}^{-\beta e_i}. \tag{108}$$

$\mathbf{A}$ can be read off from Fig. 10. For instance, vertex 1 contributes only to T_{RR} and its contribution is $\frac{1}{2}\omega_1(1 + \sigma_z)$. The total result is

$$\mathbf{A} = \begin{pmatrix} T_{RR} & T_{RL} \\ T_{LR} & T_{LL} \end{pmatrix} \tag{109}$$

and

$$\begin{aligned}
T_{RR} &= \tfrac{1}{2}(\omega_1 + \omega_3) + \tfrac{1}{2}(\omega_1 - \omega_3)\sigma_z + \omega_9\sigma_+ + \omega_{11}\sigma_- \\
T_{LL} &= \tfrac{1}{2}(\omega_4 + \omega_2) + \tfrac{1}{2}(\omega_4 - \omega_2)\sigma_z + \omega_{15}\sigma_+ + \omega_{13}\sigma_- \\
T_{LR} &= \tfrac{1}{2}(\omega_{10} + \omega_{16}) + \tfrac{1}{2}(\omega_{10} - \omega_{16})\sigma_z + \omega_7\sigma_+ + \omega_6\sigma_- \\
T_{RL} &= \tfrac{1}{2}(\omega_{12} + \omega_{14}) + \tfrac{1}{2}(\omega_{12} - \omega_{14})\sigma_z + \omega_5\sigma_+ + \omega_8\sigma_-.
\end{aligned} \tag{110}$$

We now turn to goal 2. If we replace H (resp H_i) in (101) by

$$\mathscr{H} = \begin{pmatrix} H & 0 \\ 0 & H \end{pmatrix}, \tag{111}$$

$$\text{resp } \mathscr{H}_i = \begin{pmatrix} H_i & 0 \\ 0 & H_i \end{pmatrix}, \tag{112}$$

then

$$\mathbf{C} = [\mathbf{A}^N, \mathscr{H}]$$

and

$$\mathbf{C}_i = [\mathbf{A}^N, \mathscr{H}_i] \tag{113}$$

are well defined. In order to achieve $[T, H] = 0$ we could, using (105), require that $\mathbf{C} = 0$, but it turns out that this is too stringent. It is possible, however (at least for the 8 vertex case) to require that

$$\text{Trace}^* \mathbf{C} = 0 \tag{114}$$

and this is just as good. Now, note that

$$\mathbf{C}_i = (\mathbf{A}_1\mathbf{A}_2 \dots \mathbf{A}_{i-1})\mathbf{D}_i(\mathbf{A}_{i+2} \dots \mathbf{A}_N) \tag{115}$$

where

$$\mathbf{D}_i = [\mathbf{A}_i\mathbf{A}_{i+1}, \mathscr{H}_i]. \tag{116}$$

If we can choose H so that

$$\mathbf{D}_i = \mathbf{A}_i\mathbf{B}_{i+1} - \mathbf{B}_i\mathbf{A}_{i+1} \tag{117}$$

with $\mathbf{B}_i$ having the same structure as $\mathbf{A}_i$ (namely a *universal* 2×2 operator on spin i *alone*) then (114) will be true. (Taking the sum over i cancels all terms of the commutator but the boundary ones. These cancel because we take the trace*.) Another way to say this is: find $H(\sigma, \tau)$, with σ and τ being two spins, such that

$$[\mathbf{A}(\sigma)\mathbf{A}(\tau), \mathscr{H}(\sigma, \tau)] = \mathbf{A}(\sigma)\mathbf{B}(\tau) - \mathbf{B}(\sigma)\mathbf{A}(\tau) \tag{118}$$

for some $\mathbf{B}$. The problem is reduced to the consideration of two spins only, but it is complicated insofar as 2×2 matrix multiplication is understood in (118).

The procedure we use to achieve goal 2 is not hard conceptually, but extremely tedious algebraically. For the sake of continuous reading of the text, we exhibit here only the basic steps needed to draw the necessary conclusions, but eliminate most of the algebra.

The simplification obtained by the restriction to the eight vertex problem is that the transfer matrix conserves the parity of the arrows, i.e. it changes the number of up arrows by an even number as we go from row to row. We may therefore choose a parity conserving H because if H commutes with T then both the parity conserving and parity violating parts of H commute with T. There may exist a linear H that violates parity and yet commutes with T, but we shall not investigate that question here.

The most general parity conserving operator, $H = \Sigma H_i$, is

$$H_i = \frac{\Delta}{2}\sigma_{z,i}\sigma_{z,i+1} + A\sigma_{+,i}\sigma_{+,i+1} + B\sigma_{-,i}\sigma_{-,i+1} + \gamma(\sigma_{+,i}\sigma_{-,i+1} + \sigma_{-,i}\sigma_{+,i+1}) + \tfrac{1}{2}D(\sigma_{z,i} + \sigma_{z,i+1}) + C(\sigma_{+,i}\sigma_{-,i+1} - \sigma_{-,i}\sigma_{+,i+1}) \quad (119)$$

Achieving goal 2 means finding the constants of H as explicit functions of $\omega_1, \ldots, \omega_8$. Note that H is defined up to a multiplicative constant, which allows us to choose one of the constants arbitrarily. For the eight vertex case, we can set $\omega_5 = \omega_6 = \omega$ without any loss of generality because if $\omega_5 \neq \omega_6$ we can transform T by the similarity transformation $\exp\{\theta\Sigma_j\sigma_{zj}\}$ and can choose θ to make the coefficients equal, *cf.* (110). Such a transformation, when applied to H, preserves linearity. We may also assume, without loss of generality, that $\omega \neq 0$. Otherwise we would be dealing with a six vertex problem 1,2,3,4,7,8 and, as (110) shows, this may be converted into the usual six vertex model by the unitary transformation which interchanges σ_+ and σ_-.

The statement $[T, H] = 0$ is independent of N, and if true must be valid for the cases $N = 2,3,4$. It is useful to study these cases for two reasons. The first is that they allow us to determine H completely, although that would hardly be a sufficient reason for presenting them here. The second and more important reason lies in the fact that we shall deduce that an H does *not* exist for the most general eight vertex model, and that when it does exist it is essentially unique. By studying these cases we can be sure that the nonexistence of an H is not merely an artifact of Fan's method.

We compute the matrices H and T in the basis in which all σ_{zj} are diagonal, then compute the commutator and equate it to zero. For the specific cases mentioned we obtain the following results:

(i) $N = 2$

$$B\omega\omega_7 = A\omega\omega_8 \quad (120)$$

$$2D\omega\omega_7 = A(\omega_1^2 + \omega_4^2 - \omega_2^2 - \omega_3^2). \quad (121)$$

(ii) $N = 3$

$$B\omega\omega_8 = A\omega\omega_7. \quad (122)$$

If ω_7 and ω_8 are both nonzero, equations (120) and (122) tell us that we must have

$$\omega_7 = \omega_8 = \alpha; \quad A = B. \quad (123)$$

If $\omega_7 = \omega_8 = 0$ it is undoubtedly true (although we have not constructed a proof) that we must have $A = B = 0$. Otherwise T would commute with the

total z component of the spin, $S = \sum_1^N \sigma_{zj}$, and H would not. Likewise, $\omega_7 = 0$, $\omega_8 \neq 0$ implies that $A = B = 0$ and this is surely impossible because $[H, S] = 0$ and $[T, S] \neq 0$. Thus we shall assume that (123) is generally valid.

There are two more important relations in the $N = 3$ case

$$aA - 2b(D + \Delta) + 2b\gamma - (d + e)A = 0 \tag{124a}$$

$$a'A + 2b'(D - \Delta) + 2b'\gamma - (d' + e')A = 0 \tag{124b}$$

where

$$\begin{aligned} a &= \omega_1(\omega_1^2 - \omega_3^2) + \omega_4(\omega_4^2 - \omega_2^2) \\ b &= (\omega_1 + \omega_4)\omega\alpha \\ d &= \omega_2\alpha^2 + \omega_3\omega^2 \\ e &= \omega_2\omega^2 + \omega_3\alpha^2 \end{aligned} \tag{125}$$

and the $a' \ldots e'$ are obtained from $a \ldots e$ by the exchanges $\omega_1 \leftrightarrow \omega_3$, $\omega_2 \leftrightarrow \omega_4$, $\alpha \leftrightarrow \omega$.

Combining (121, 124a, 124b) we obtain

$$\left\{\left[\frac{a}{b} - \frac{a'}{b'}\right] + \left[\frac{d' + e'}{b'} - \frac{d + e}{b}\right] - 2\,\frac{\omega_1^2 + \omega_4^2 - \omega_2^2 - \omega_3^2}{\alpha\omega}\right\} A = 0. \tag{126}$$

Equation (126) has two solutions:

Case (a), $A = 0$: This is the six vertex case, and D is arbitrary since $[T, S] = 0$. We shall take $D = 0$ for the six vertex case.

Case (b), $A \neq 0$: One solution is $\omega_1 = \omega_2$ and $\omega_3 = \omega_4$. This means that there can be *no electric fields for the eight vertex case* if we want an H to exist. Another possibility is $\omega_1 = \omega_3$ and $\omega_2 = \omega_4$, but this would mean $\varepsilon_1 = 0$ and $v = 0$ which is not very interesting physically. Other solutions require a relationship among the six weights which would not be temperature independent. Assuming, henceforth, only the first possibility, (126) implies that

$$A(\omega_1^2 + \omega_3^2 - \omega^2 - \alpha^2 - 2\omega_1\omega_3) = 2(\Delta - \gamma)\alpha\omega. \tag{127}$$

(iii) $N = 4$

This case is quite elaborate, since one deals with matrices of order 16. We find the new relations:

$$\begin{aligned} &- 2\Delta(\omega_2\omega_4\omega^2 + \omega_1\omega_3\alpha^2) + (\gamma + C)(\omega_1\omega_2\alpha^2 + \omega_3\omega_4\omega^2) + 2(\gamma - C)\,\omega^2\alpha^2 \\ &+ (\gamma + C)(\omega_1\omega_2\omega^2 + \omega_3\omega_4\alpha^2) = 2A(\omega_1\omega_4\alpha\omega + \omega_2\omega_3\alpha\omega) \\ &+ (\gamma + C)(\omega^4 + \alpha^4) \end{aligned} \tag{128}$$

and another relation obtained from (128) by the exchanges $C \leftrightarrow -C$, $\omega_1 \leftrightarrow \omega_2$, $\omega_3 \leftrightarrow \omega_4$.

For case (a) we set $A = \alpha = 0$ and conclude from (128) that, up to a common factor

$$\begin{aligned} 2\Delta &= (\omega_1\omega_2 + \omega_3\omega_4 - \omega^2)(\omega_1\omega_2\omega_3\omega_4)^{-\frac{1}{2}} \\ &= e^{K_1} + e^{-K_1} - e^{2K_2 - K_1}, \end{aligned} \tag{129}$$

$$\begin{aligned} \gamma &= \tfrac{1}{2}(\omega_1\omega_3 + \omega_2\omega_4)(\omega_1\omega_2\omega_3\omega_4)^{-\frac{1}{2}} \\ &= \cosh H, \\ C &= \tfrac{1}{2}(\omega_2\omega_4 - \omega_1\omega_3)(\omega_1\omega_2\omega_3\omega_4)^{-\frac{1}{2}} \\ &= -\sinh H, \end{aligned}$$

$$A = B = D = 0. \tag{130}$$

Equations (129, 130) agree with the results of McCoy and Wu (1968). Equation (129) agrees with (138) derived in the next section.

For case (b) we set $\omega_1 = \omega_2$ and $\omega_3 = \omega_4$ and use (127) to conclude that up to a factor

$$\begin{aligned} \gamma &= \omega_1\omega_3, \\ 2\Delta &= {\omega_1}^2 + {\omega_3}^2 - \omega^2 - \alpha^2, \\ A &= B = \alpha\omega, \\ C &= D = 0. \end{aligned} \tag{131}$$

Equation (131) agrees with Sutherland (1970).

The next step is to prove that (129, 130, 131) are correct for arbitrary N (under the stated conditions) by calculating Fan's matrix $\mathbf{B}$ of (117). For six vertices, case (a) above, we find that

$$\begin{aligned} 2(\omega_1\omega_2\omega_3\omega_4)^{\frac{1}{2}}B_{RR} &= (\omega^2 - \omega_1\omega_2 - \omega_3\omega_4)(\omega_1 - \omega_3) + \omega_2\omega_4(\omega_4 - \omega_2) \\ &\quad + [\omega_2\omega_4(\omega_4 + \omega_2) + (\omega^2 - \omega_1\omega_2 - \omega_3\omega_4)(\omega_1 + \omega_3)]\sigma_z, \\ 2(\omega_1\omega_2\omega_3\omega_4)^{\frac{1}{2}}B_{LL} &= (\omega^2 - \omega_1\omega_2 - \omega_3\omega_4)(\omega_2 - \omega_4) + \omega_1\omega_3(\omega_3 - \omega_1) \\ &\quad - [\omega_1\omega_3(\omega_1 + \omega_3) + (\omega^2 - \omega_1\omega_2 - \omega_3\omega_4)(\omega_4 + \omega_2)]\sigma_z, \\ B_{RL} &= B_{LR} = 0. \end{aligned} \tag{132}$$

For eight vertices, case (b) above, it is convenient to add a constant energy to all the vertices so that $\omega_1 = {\omega_3}^{-1}$, i.e. $\gamma = 1$ in (131). Then

$$\begin{aligned} 4B_{RR} &= (\alpha^2 - \omega^2)[(\omega_1 - \omega_3) + (\omega_1 + \omega_3)\sigma_z], \\ 4B_{LL} &= (\alpha^2 - \omega^2)[(\omega_1 - \omega_3) - (\omega_1 + \omega_3)\sigma_z], \\ 2B_{RL} &= 2B_{LR}{}^{\dagger} = ({\omega_1}^2 - {\omega_3}^2)(\omega\sigma_+ - \alpha\sigma_-). \end{aligned} \tag{133}$$

The matrix **B** is, of course, only defined modulo the addition of a matrix proportional to **A**.

If we set $\omega_1 = \omega_3^{-1}$, which we can do generally, and, in addition, require that $\alpha = \omega^{-1}$, then we have the modified F model [*cf.* (404) *et. seq.*]. The Hamiltonian (131) is the so called XZ Hamiltonian. An analysis of its ground state properties (Barouch, 1971) reveals that the correlation function between two vertical arrows on the same row contains a long range component that vanishes as $(T_0 - T)^{1/2}$ for $T \cong T_0 -$.

The Hamiltonian (119) has certain symmetry properties which Sutherland (1970) exploits in order to make conjectures about the critical behaviour in the eight vertex case. See also (400).

E. Diagonalization of the ferroelectric transfer matrix

We wish to find the largest eigenfunction $f(x_1, \ldots, x_n)$ of (90) with D given by (94–100). As an introduction, consider the $n = 1$ case

$$\begin{aligned}\Lambda f(x) = \exp[V(N-2) - N(K_2 - H) + 2K_2 - K_1] \sum_{y=1}^{x} \exp[(2H + K_1)(y-x) \\ - 2K_2\delta(y-x)]f(y) \\ + \exp[V(N-2) - N(K_1 + K_2 + H) + 2K_2 - K_1] \sum_{y=x}^{N} \exp[(2H + K_1)(y-x) \\ + (2K_1 - 2K_2)\delta(y-x)]f(y). \quad (134)\end{aligned}$$

We try

$$f(x) = e^{ikx}. \quad (135)$$

The sums in (134) are simple geometric series. Each term in (134) produces one term proportional to (135). We call these proportionality constants Λ_R and Λ_L, respectively. Thus,

$$\begin{aligned}\Lambda &= \Lambda_R + \Lambda_L \\ \Lambda_R &= \exp[V(N-2) - N(K_2 - H)]\lambda_R(k; K_1, K_2, H) \\ \Lambda_L &= \exp[V(N-2) - N(K_1 + K_2 + H)]\lambda_L(k; K_1, K_2, H), \quad (136) \\ \lambda_R(k; K_1, K_2, H) &= \frac{2\Delta - \exp(K_1) - \exp(ik + 2H)}{1 - \exp(ik + K_1 + 2H)}\end{aligned}$$

$$\lambda_L(k; K_1, K_2, H) = \frac{2\Delta - \exp(-K_1) - \exp(-ik - 2H)}{1 - \exp(-ik - K_1 - 2H)} \quad (137)$$

and

$$2\Delta = e^{K_1} + e^{-K_1} - e^{2K_2 - K_1}. \quad (138)$$

In addition to these terms proportional to $f(x)$, each sum in (134) produces a constant term and these cancel when k is such that

$$e^{ikN} = 1. \tag{139}$$

Equation (139) could also have been surmised from translation invariance.

The largest eigenvalue must occur for $k = 0$, the nodeless eigenvector, but it is not easy to see this from (136)–(138). The Perron–Frobenius theorem is thus useful even for $n = 1$.

The remarkable fact is that the $n = 1$ solution can be generalized. We make the so called Bethe *ansatz* as follows:

(1) Choose n numbers $\{k\} = \{k_1, k_2, \ldots, k_n\}$ which are distinct modulo 2π;

(2) Denote permutations of n objects by

$$P = \begin{pmatrix} 1, & 2, & \ldots, & n \\ P1, & P2, & \ldots, & Pn \end{pmatrix};$$

(3) Let $\mathfrak{A}(P)$ be a complex valued function defined on the permutations.

(4) Define

$$f(x_1, \ldots, x_n) = \sum_P \mathfrak{A}(P) \exp\left[i \sum_{j=1}^{n} k_{Pj} x_j\right]. \tag{140}$$

The sum is on the $n!$ permutations. Note that (140) is defined only as indicated in (83).

When (140) is inserted into (89) one term proportional to f comes from each sum as before. That is

$$\Lambda = \Lambda_R + \Lambda_L$$

$$\Lambda_R = \exp\left[N(Vy - K_2 + H)\right] \prod_{j=1}^{n} \lambda_R(k_j; K_1, K_2, H)$$

$$\Lambda_L = \exp\left[N(Vy - K_1 - K_2 - H)\right] \prod_{j=1}^{n} \lambda_L(k_j; K_1, K_2, H) \tag{141}$$

and $y = 1 - 2n/N$.

Next, there are unwanted terms that come from the fact that we have Σ^* instead of Σ, i.e. terms that come from such forbidden points as $y_1 = y_2 = x_1$ in Σ_R. For an arbitrary choice of $\{k\}$ these cancel in each sum separately if $\mathfrak{A}(\cdot)$ is chosen correctly as follows: Let P and Q be two permutations which differ only in the jth and $(j+1)$th position, i.e.

$$\{k_{P1}, \ldots, k_{Pn}\} = \{\ldots, p, q, \ldots\}$$

$$\{k_{Q1}, \ldots, k_{Qn}\} = \{\ldots, q, p, \ldots\}$$

where $k_{Pj} = p = k_{Q(j+1)}$ and $k_{P(j+1)} = q = k_{Qj}$. Then, for every such pair, we require that

$$\mathfrak{A}(P) = \mathfrak{A}(Q)B(p, q). \tag{142}$$

where

$$B(p, q) = -\frac{1 + \exp[4H + i(p + q)] - 2\Delta \exp(2H + ip)}{1 + \exp[4H + i(p + q)] - 2\Delta \exp(2H + iq)}$$

$$= B(q, p)^{-1}. \tag{143}$$

If n is large, (142) obviously represents far more equations than the $n!$ unknowns $\mathfrak{A}(\cdot)$. They can all be satisfied, nevertheless, by defining

$$B(p, q) \equiv -\exp[-i\theta(p, q)] \tag{144}$$

with $\theta(p, q) = -\theta(q, p)$ and then setting

$$\mathfrak{A}(P) = (-)^P \exp\left[-\frac{i}{2}\sum_{i<j}\theta(k_{Pi}, k_{Pj})\right], \tag{145}$$

where $(-)^P$ is the signature of P.

Finally, each of the sums in (89) have unwanted terms associated with the fact that Σ_R has a beginning, $y_1 = 1$, and Σ_L has an end, $y_n = N$. These terms cancel each other if, for every pair of permutations, P and Q, of the form

$$P = \begin{pmatrix} 1, & 2, & \ldots, & n \\ P1, & P2, & \ldots, & Pn \end{pmatrix},$$

$$Q = \begin{pmatrix} 1, & 2, & \ldots, & n-1, & n \\ P2, & P3, & \ldots, & Pn, & P1 \end{pmatrix}$$

$$\mathfrak{A}(P) = \mathfrak{A}(Q)\exp(ik_{P1}N). \tag{146}$$

Using (143)–(145), this is accomplished if

$$\exp(ik_jN) = \prod_{\substack{i=1 \\ \neq j}}^{n} B(k_j, k_i), \quad j = 1, \ldots, n. \tag{147}$$

Again, (146) could have been surmised by translation invariance.

Conclusion: *Any set* $\{k\}$ *of* n *numbers distinct modulo* 2π *satisfying* (147) *will, when inserted into* (141), *yield an eigenvalue of the transfer matrix.* It is important that the k's be distinct, otherwise (145) implies that $f(\mathbf{X})$ vanishes

identically. (Strictly speaking, one has to check that $f(\mathbf{X})$ does not vanish identically even when the k's are distinct.)

The reader is invited to verify the above statements for $n = 2$ where the algebra is elementary. To prove that the pattern holds for arbitrary n is not easy. At the present time we can only offer an unilluminating inductive proof (*cf.* Lieb, 1967b, where a proof, the generalization of which is trivial, is given for the ice case). The conclusion we have reached is the same as for the Heisenberg model, the only difference being in the dependence of Λ on $\{k\}$. In view of the proof in Section IV.D that the transfer matrix commutes with the Heisenberg Hamiltonian it would appear that the unwanted terms must, *a fortiori*, cancel and no proof is required. This would indeed be so if each term in (140) were linearly independent. That they are not for large n follows from the remark that there are $n!$ plane waves in (140) whereas we are in a space of dimension only $\binom{N}{n}$. Consequently, we can not even be sure that $f(\mathbf{X})$ is non-zero even when $\{k\}$ is distinct modulo 2π. To elucidate this question we consider the $\Delta = 0$ case which, while not particularly important physically, is the only case for which (147) can be solved in simple form.

Henceforth we shall adopt the notation

$$\begin{aligned} z(y) &= \lim_{N\to\infty} N^{-1} \ln \Lambda(y) - Vy \\ &= \lim_{N\to\infty} N^{-1} \ln \left[\max_{R,L} (\Lambda_R, \Lambda_L)\right] - Vy \end{aligned} \tag{148}$$

where Λ is, of course, the largest eigenvalue as in (76), so that the free energy per vertex, $\mathscr{F}$, is given by

$$-\beta\mathscr{F} \equiv \lim_{\substack{M\to\infty \\ N\to\infty}} \frac{1}{MN} \ln Z = \max_{-1\leqslant y\leqslant 1} [z(y) + Vy]. \tag{149}$$

Since $z(y)$ is symmetric and concave in y, for $H = 0$, then

$$-\beta\mathscr{F} = z(0) \quad \text{for } V = 0, H = 0. \tag{150}$$

$\Delta = 0$ *Case*: Here $B(p, q) = -1$ so that $e^{ik_jN} = 1$ for all j (take n odd for convenience). Also, $\mathfrak{A}(P) = (-)^P$ so that $f(\mathbf{X})$ is a determinantal function. We conjecture, and will verify, that as in the $n = 1$ case we want the k's to be as small as possible. Hence

$$k_j = (2j - n - 1)\pi/N. \qquad \Delta = 0 \tag{151}$$

$f(\mathbf{X})$ is essentially a Vandermonde determinant in this case and hence

$$f(\mathbf{X}) = \prod_{i<j} \sin \frac{\pi(x_j - x_i)}{N} \qquad \Delta = 0 \tag{152}$$

which is certainly a positive function in the region defined by (83). Hence the Bethe *ansatz* leads to the largest eigenvalue.

The condition $\Delta = 0$ means that

$$e^{2K_2} = e^{2K_1} + 1 \tag{153}$$

so that $K_2 > \max(K_1, 0) \geqslant 0$. Hence we should think of this system as basically antiferroelectric (more on this in Section V). We also note that $\lambda_R = -\lambda_L$, a condition that is not true in general. As the two products in (141) are identical, except for a minus sign when n is odd, $\Lambda_{\max}$ is determined from (141) by the sign of $K_1 + 2H$. The reader can puzzle out for himself what happens in the limit $K_1 + 2H = 0$.

Using (148) and (141) one can see that while Λ_R and Λ_L are of opposite sign, the larger one is always positive. It is then easy to pass to the thermodynamic limit:

$$z(y) = -K_2 + \max(H, -K_1 - H) + \frac{1}{4\pi}\int_{-Q}^{Q} dk \ln\left[\frac{\cosh(K_1 - 2H) + \cos k}{\cosh(K_1 + 2H) - \cos k}\right]$$

$$\Delta = 0 \tag{154}$$

with $Q = \frac{1}{2}\pi(1 - y)$. This expression appears to be non-analytic at $K_1 + 2H = 0$. However, when $K_1 + 2H = 0$ the integrand has a singularity and it is not hard to follow the contours and prove that: *$z(y)$ is real analytic in K_1, H and y for $-1 < y < 1$.* In other words, the two expressions in (154) are analytic continuations of each other. At $y = \pm 1$, $z(y)$ ceases to be analytic when $K_1 + 2H = 0$. This property, that Λ_L and Λ_R appear to be quite different but really define one analytic function, is one that we shall meet again in Section V in connection with the passage from the KDP model ($K_1 > 0$) to the IKDP model ($K_1 < 0$).

It is easy to verify explicity that $z(y)$ is concave in y; this is a general thermodynamic requirement. It is clear from (93) that $\mathscr{F}$ is symmetric under $(H, V) \to (-H, -V)$ (and in H and V separately if $K_1 = 0$). The concavity implies that (149) has a unique solution given by

$$\sin\frac{\pi}{2}y = \cosh K_1 \cosh 2H \tanh 2V + \sinh K_1 \sinh 2H. \qquad \Delta = 0 \tag{155}$$

Note that if $K_1 \neq 0$, a horizontal field alone can produce a vertical polarization. For sufficiently large (H, V) the maximizing y can "stick" at ± 1.

A simple calculation yields $y = +1$ for

$$e^{K_1} \geqslant \frac{\cosh(V-H)}{\sinh(V+H)} \text{ or } e^{K_1} \leqslant \frac{\sinh(V-H)}{\cosh(V+H)} \tag{156a}$$

while $y = -1$ for $\Delta = 0$

$$e^{K_1} \geqslant \frac{\cosh(H-V)}{\sinh(H+V)} \text{ or } e^{K_1} \leqslant \frac{\sinh(H-V)}{\cosh(H+V)}. \tag{156b}$$

These equations (to be discussed further in Section V, eqn. (355a, b)) define curves in the (H, V) plane along which *a phase transition (as a function of field) to the completely ordered ferroelectric state takes place.* This occurs despite the fact that the system is intrinsically an antiferroelectric.

The $\Delta = 0$ case, and only this case, can also be solved by a completely different technique—the Pfaffian method. This was first noticed by Wu (*cf.* Lieb, 1967c) but Baxter (1970b) showed how one could also solve the problem in a staggered quadrupole field, s, as given on the last line of Table I. His result for $K_1 = 0$ (to which we shall return in Section V.H.1) is

$$-\beta\mathscr{F} = \frac{1}{8\pi^2}\int_{-\pi}^{\pi}\int d\theta\, d\phi \ln[2\cosh 2\beta s - 2\cos(\theta + i2H)\cos(\phi + i2V)], \quad \Delta = 0. \tag{157}$$

Baxter's calculation can presumably be generalized to $K_1 \neq 0$. The dependence of $\mathscr{F}$ on s is very interesting and, generally speaking, *the behaviour in a staggered field for arbitrary Δ is the outstanding unsolved problem for the ferroelectrics.*

We also note that for the F model $K_1 = H = 0$, $K_2 = \frac{1}{2}\ln 2$ and

$$\begin{aligned} z(0) &= -\tfrac{1}{2}\ln 2 - \frac{1}{\pi}\int_0^{\pi/2} \ln\tan(\tfrac{1}{2}k)\, dk \\ &= -\tfrac{1}{2}\ln 2 + \frac{2}{\pi}G \\ &= 0{\cdot}2365482\ldots, \qquad \Delta = 0 \end{aligned} \tag{158}$$

where G is Catalan's constant (Gradshteyn and Ryzhik, 1965; p. 529).

Our detour through the $\Delta = 0$ case was intended to convince the reader of the correctness of the Bethe *ansatz* and to illustrate the general features of the calculation we are about to undertake for arbitrary Δ. In the remainder of this section we shall carry the calculation as far as the analog of (154) and in Section V shall discuss the physical consequences of it. When $H \neq 0$ the

function θ is not real for real (p, q) so that $\{k\}$ is complex. The papers of C. P. Yang (1967) and Sutherland, Yang and Yang (1967) explore this question, but since the details of their calculation have not yet appeared we shall *restrict ourselves to* $H = 0$ *in this section.* In Section V we shall mention some of their conclusions.

The calculation is complicated by the fact that the range of Δ is naturally divided into three parts: $\Delta < -1$, $-1 < \Delta < 1$, and $\Delta \geqslant 1$. The point $\Delta = -1$ requires special treatment, too. The range $\Delta \geqslant 1$, however, can be handled by a simple argument as will be seen presently. To avoid having to write each equation three times we have arranged the formulas in Table II and will refer to a line in the Table as (Table II. ·). The equation we are trying to solve, (147), is the same as for the Heisenberg model and what we present here is borrowed from Yang and Yang (1966a, b, c).

We write Δ as in (Table II.1) and consider (p, q) in the range (Table II.2). Then θ, defined in (145), is

$$\theta(p, q) = 2 \tan^{-1} \left[\frac{\Delta \sin [(p-q)/2]}{\cos [(p+q)/2] - \Delta \cos [(p-q)/2]} \right], H = 0. \tag{159}$$

In (Table II.3), θ is a uniquely defined, continuous, antisymmetric function of (p, q). For the largest eigenvalue we look for a solution to (147) of the form

$$Nk_j = (2j - n - 1)\pi - \sum_{i=1}^{n} \theta(k_j, k_i). \tag{160}$$

Yang and Yang prove that a unique solution to (160) exists, with $\{k\}$ in (Table II.2), *provided* $2n \leqslant N$ (or $y \geqslant 0$). This solution has the property that if k is in $\{k\}$ so is $-k$. A problem that has not been discussed so far is what happens when $2n > N$? (Recall that for $\Delta = 0$ there was no difficulty). Henceforth, we shall *restrict our attention to* $y \geqslant 0$ because $V \geqslant 0$ implies that (149) is maximized for $y \geqslant 0$, since $z(y)$ is symmetric. We can then rely on symmetry in V to infer the free energy for $V < 0$. Yang and Yang also prove that this solution for $\{k\}$ leads to a positive eigenvector (except possibly for finitely many Δ). It is important to note that $\{k\}$ depends only on Δ and not on K_1 and K_2 separately.

What happens for $\Delta \geqslant 1$? Here $\{k\}$ becomes complex, in general, but notice that (Table II. 2) tells us that all $k_j = 0$ when $\Delta = 1$. This is consistent with (147) and (143) since $B(0, 0) = +1$ for $\Delta = 1$, (Set $\Delta = 1$ and expand in p and q). In other words,

$$f(\mathbf{X}) = 1 \quad \text{for } \Delta = 1. \tag{161}$$

TABLE II

	$\Delta < -1$	$\Delta = -1$	$-1 < \Delta < 1$
1. $\Delta =$	$-\cosh\lambda,\ \lambda > 0$	-1	$-\cos\mu,\ 0 > \mu > \pi$
2. Range of k	$(-\pi, \pi)$	$(-\pi, \pi)$	$(\mu - \pi, \pi - \mu)$
3. Range of θ	$(-2\pi, 2\pi)$	$(-\pi, \pi)$	$(-\lvert\pi - 2\mu\rvert, \lvert\pi - 2\mu\rvert)$
4. $e^{ip} =$	$\dfrac{e^{\lambda} - e^{-i\alpha}}{e^{\lambda - i\alpha} - 1}$	$\dfrac{1 + 2i\alpha}{1 - 2i\alpha}$	$\dfrac{e^{i\mu} - e^{\alpha}}{e^{i\mu + \alpha} - 1}$
5. Range of α	$(-\pi, \pi)$	$(-\infty, \infty)$	$(-\infty, \infty)$
6. $y = 1$	$Q = 0,\ b = 0$	$Q = 0,\ b = 0$	$Q = 0,\ b = 0$
7. $y = 0$	$Q = \pi,\ b = \pi$	$Q = \pi,\ b = \infty$	$Q = \pi - \mu,\ b = \infty$
8. $\cos p =$	$\dfrac{1 + \Delta\cos\alpha}{\Delta + \cos\alpha}$	$\dfrac{1 - 4\alpha^2}{1 + 4\alpha^2}$	$\dfrac{1 + \Delta\cosh\alpha}{\Delta + \cosh\alpha}$
9. $\xi(\alpha) = \dfrac{dp}{d\alpha} =$	$\dfrac{\sinh\lambda}{\cosh\lambda - \cos\alpha}$	$\dfrac{4}{1 + 4\alpha^2}$	$\dfrac{\sin\mu}{\cosh\alpha - \cos\mu}$
10. $\tilde{\theta}(\alpha, \beta) \equiv \theta(p, q) =$	$2\tan^{-1}\left[(\coth\lambda)\tan\dfrac{\beta - \alpha}{2}\right],\ 2\tan^{-1}(\beta - \alpha)$		$2\tan^{-1}\left[(\cot\mu)\tanh\dfrac{\beta - \alpha}{2}\right].$
11. $2\pi K(\alpha - \beta) \equiv \dfrac{\partial\tilde{\theta}(\alpha, \beta)}{\partial\beta} =$	$\dfrac{\sinh 2\lambda}{\cosh 2\lambda - \cos(\alpha - \beta)}$	$\dfrac{2}{1 + (\alpha - \beta)^2}$	$\dfrac{\sin 2\mu}{\cosh(\alpha - \beta) - \cos 2\mu}$
12. Fourier Series and Transforms			
$\hat{h}(n) =$	$\displaystyle\int_{-\pi}^{\pi} h(\alpha)\, e^{in\alpha}\, d\alpha,\ n$ integral		
$h(\alpha) =$	$(2\pi)^{-1}\displaystyle\sum_{-\infty}^{\infty}\hat{h}(n)\, e^{-in\alpha}$		

	$\Delta < -1$	$\Delta = -1$	$-1 < \Delta < 1$
$\hat{h}(\gamma) \equiv$			$\int_{-\infty}^{\infty} h(\alpha)\, e^{i\gamma\alpha}\, d\alpha$
$h(\alpha) =$			$(2\pi)^{-1} \int_{-\infty}^{\infty} \hat{h}(\gamma)\, e^{-i\gamma\alpha}\, d\gamma$
13. $\hat{K}(n) =$	$\exp(-2\lambda\lvert n\rvert)^a$		
$\hat{K}(\gamma) =$		$\exp(-\lvert\gamma\rvert)^b$	$\sinh[(\pi - 2\mu)\gamma]/\sinh \pi\gamma^c$
14. $\hat{R}_0(n) =$	$\dfrac{\pi}{\cosh n\lambda}$		
$\hat{R}_0(\gamma) =$		$\left(\dfrac{\pi}{\cosh \frac{1}{2}\gamma}\right)^a$	$\left(\dfrac{\pi}{\cosh \mu\gamma}\right)^d$
15. $R_0(\alpha) =$	$\frac{1}{2} \sum_{n=-\infty}^{\infty} e^{in\alpha} \operatorname{sech} n\lambda$	$\dfrac{\pi}{\cosh \pi\alpha}$	$\dfrac{\pi}{2\mu \cosh(\pi\alpha/2\mu)}$
16. $C(\alpha) =$	$\ln\left[\dfrac{\cosh(2\lambda - \theta_0) - \cos\alpha}{\cosh\theta_0 - \cos\alpha}\right]$	$\ln\left[\dfrac{\alpha^2 + (1-\alpha_0)^2}{\alpha^2 + \alpha_0{}^2}\right]$	$\ln\left[\dfrac{\cosh\alpha - \cos(2\mu - \phi_0)}{\cosh\alpha - \cos\phi_0}\right]$
17. $\hat{C}(n) =$	$\dfrac{4\pi}{n} e^{-\lambda\lvert n\rvert} \sinh n(\lambda - \theta_0)^e$		
	$4\pi(\lambda - \theta_0),\ n = 0$		
$\hat{C}(\gamma) =$		$\dfrac{4\pi}{\gamma} e^{-\frac{1}{2}\lvert\gamma\rvert} \sinh\gamma(\frac{1}{2} - \alpha_0)^f$	$\dfrac{4\pi \sinh[(\pi - \mu)\gamma] \sinh[(\mu - \phi_0)\gamma]^g}{\gamma \sinh \pi\gamma}$

[a] Gradshteyn and Ryzhik, 1965, p. 366.
[b] Gradshteyn and Ryzhik, 1965, p. 406.
[c] Gradshteyn and Ryzhik, 1965, p. 505.
[d] Gradshteyn and Ryzhik, 1965, p. 503.
[e] Gradshteyn and Ryzhik, 1964, p. 593.
[f] Oberhettinger, 1966, p. 16.
[g] Oberhettinger, 1966, p. 41.

Then $\lambda_R = \lambda_L = 1$ and

$$z(y) = -K_2 + \max(0, -K_1) \quad \text{independent of } y. \tag{162}$$

It is easy to see under what circumstances $\Delta = 1$ can be realized. Since

$$\frac{\partial \Delta}{\partial K_1} = e^{K_1} - \Delta = \tfrac{1}{2}e^{-K_1}(e^{2K_1} + e^{2K_2} - 1) \tag{163a}$$

and $\Delta = 1$ means that

$$e^{K_1} = 1 \pm e^{K_2}, \tag{163b}$$

one sees that $K_1 > 0$ implies $K_1 > K_2$ (vertices 1 and 2 preferred) and $\partial\Delta/\partial K_1 > 0$. Similarly, $K_1 < 0$ implies $K_2 < 0$ (vertices 3 and 4 preferred) and $\partial\Delta/\partial K_1 \leqslant 0$ for $\Delta \geqslant 1$. In either case, the model is intrinsically ferroelectric. These facts are shown in Fig. 13. Now note that: (i) eqn (1) implies

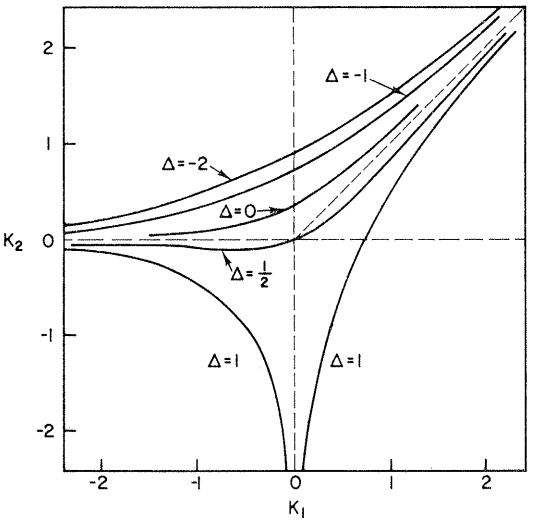

FIG. 13. Constant Δ plot in the (K_1, K_2) plane. The three curves $\Delta = \pm 1$ are symmetric with respect to the line $K_1 = K_2$.

that $z(y)$ is convex and non-increasing in (K_1, K_2) and thus is also convex and non-increasing in the limit $N \to \infty$; (ii) If we subtract ε_1 from all energies $e_1, \ldots, e_6$ then $z(y) \to z'(y) \equiv z(y) + K_1$ and $z'(y)$ is convex in (K_1, K_2), non-increasing in K_2 and non-decreasing in K_1; (iii) In the thermodynamic limit the right side of (162) is a lower bound to $z(y)$ for all Δ because it can be achieved, for $K_1 > 0$, by a single configuration composed of a spiral band

of type 1 vertices and a spiral band of type 2 vertices in the relative proportions $(1+y):(1-y)$. The two bands are separated by spiral columns of type 5 and 6 vertices, but these contribute nothing in the thermodynamic limit. For $K_1 < 0$ one uses bands of vertices 3 and 4. Thus, if we fix K_2 and use (i) and (iii) for positive K_1 and (ii) and (iii) for negative K_1 we conclude:

Equation (162) *is true for all* $\Delta \geqslant 1$ *and all* y. Thus, the system is completely "frozen" into vertex 1 or 4 when $\Delta \geqslant 1$ and there is no need to solve eqn (147) in this case. Nagle (1969), using an idea of Takahashi (1941), gave a rigorous proof of this "freezing" when $K_2 = 0$, but presumably his proof can be generalized. He also found an exact formula for the latent heat, to which we shall return in Section V.

Returning to (160) for $\Delta < 1$, we now make a crucial assumption: As n, $N \to \infty$ with y fixed (non-negative) the n numbers $\{k\}$ lie in some interval $(-Q, Q)$, in (Table II.2), and fill it densely, without gaps, so that one may introduce a positive, integrable density function $\rho(q)$ in this limit. More precisely, for each (k, p) in (Table II. 2) with $p > k$

$$\lim_{\substack{N\to\infty \\ n/N=\frac{1}{2}(1-y)}} N^{-1}\{\text{number of } k\text{'s in } (k,p)\} = \int_k^p \rho(q)\,\mathrm{d}q, \tag{164}$$

$$\int_{-Q}^{Q} \rho(q)\,\mathrm{d}q = \tfrac{1}{2}(1-y), \tag{165}$$

and

$$\rho(q) > 0 \quad \text{for} \quad -Q < q < Q. \tag{166}$$

Yang and Yang (1966b) claim to have a proof of these assertions, but it has not yet appeared. One easily deduces that (160) is equivalent to

$$1 = 2\pi\rho(p) - \int_{-Q}^{Q} \frac{\partial\theta(p,q)}{\partial p}\,\rho(q)\,\mathrm{d}q, \tag{167}$$

but it is essential to understand that this is true if and only if p is in $(-Q, Q)$. We expect this equation to have a unique solution, that the solution is positive and, in view of the Yang–Yang proof that for every k in $\{k\}$ there is also a $-k$, that the solution is symmetric. We also expect that as Q increases from 0 to $\pi - \mu$, y decreases monotonically from 1 to 0. All these facts are proved by Yang and Yang.

Section V will be devoted to the solution of (167). We conclude here with a formula for the free energy (148–150), in terms of $p(q)$. Our only problem is to decide which of Λ_L or Λ_R is larger. We compute

$$\begin{aligned} &|1 - \mathrm{e}^{ik+K_1}|^2\{|\lambda_R(k; K_1, K_2, 0)|^2 - |\mathrm{e}^{-K_1}\lambda_L(k; K_1, K_2, 0)|^2\} \\ &\quad = 4\sinh K_1[-2\Delta + \cosh K_1 + \cos k]. \end{aligned} \tag{168}$$

If $K_1 > 0$ the right side is positive since $\Delta < 1$ and since $\cos k \geqslant \Delta$ when $|k| \leqslant \pi - \mu$ (or $|k| \leqslant \pi$ for $\Delta < -1$). Furthermore, $N \geqslant n$ so that

$$\begin{aligned} |\Lambda_R| &> |\Lambda_L| \qquad \text{for } K_1 > 0 \\ |\Lambda_R| &< |\Lambda_L| \qquad \text{for } K_1 < 0 \\ |\Lambda_R| &= |\Lambda_L| \qquad \text{for } K_1 = 0. \end{aligned} \tag{169}$$

The second inequality follows from an obvious symmetry in K_1.

Our conclusion, then, for $\Delta < 1$ and $H = 0$ is:

$$z(y) = -K_2 + \max(0, -K_1) + \tfrac{1}{2}\int_{-Q}^{Q} \rho(q) \times \ln\left[\frac{(2\Delta - \eta)^2 + 1 - 2(2\Delta - \eta)\cos q}{1 + \eta^2 - 2\eta \cos q}\right] dq \tag{170}$$

where

$$\eta \equiv e^{|K_1|} \tag{171}$$

and $2\Delta = \eta + \eta^{-1} + e^{2K_2 - K_1}$. Various special cases are obtained as follows:

Ice $K_1 = K_2 = 0$, $\Delta = \frac{1}{2}$. (172a)

F model $K_1 = 0$, $K_2 \equiv K \geqslant 0$, $\Delta = 1 - \frac{1}{2}e^{2K}$. (172b)

KDP model $K_1 \equiv K \geqslant 0$, $K_2 = 0$,

or $K_1 = K_2 \equiv K \leqslant 0$, $\Delta = \frac{1}{2}e^{|K|}$. (172c)

IKDP model $K_1 \equiv K \leqslant 0$, $K_2 = 0$,

or $K_1 = K_2 \equiv K \geqslant 0$, $\Delta = \frac{1}{2}e^{-|K|}$. (172d)

IF model $K_1 = 0$, $K_2 \equiv K \leqslant 0$, $\Delta = 1 - \frac{1}{2}e^{2K}$. (172e)

We emphasize that $\rho(q)$ and Q depend on Δ and y through (165, 167).

V. Ice Rule Ferroelectric Models on a Square Lattice

A. Transformation of the integral equation

We now face the task of solving the integral equation (167) subject to the constraint (165). The free energy is then obtained by using (149), (150) and (170). It is unfortunate that the kernel of (167) is not a difference kernel, otherwise we could think in terms of Fourier transforms. However, it is possible to transform the kernel to a difference kernel by introducing an appropriate change of variable [originally due to Hulthén (1938) and to

Walker (1959)], and the solution can then be obtained in closed form in some cases. We now list these transformations in (Table II.4). The range b of the new variable α increases as y decreases as shown in (Table II.6, 7), and attains the maximum value (Table II.5) at $y = 0$ (Yang and Yang, 1966b). We write

$$R(\alpha)\mathrm{d}\alpha \equiv 2\pi\rho(p)\mathrm{d}p. \tag{173}$$

Then the integral equation (167) and the constraint (165) become, respectively,

$$R(\alpha) = \xi(\alpha) - \int_{-b}^{b} K(\alpha - \beta)\, R(\beta)\mathrm{d}\beta \tag{174a}$$

$$\pi(1 - y) = \int_{-b}^{b} R(\alpha)\mathrm{d}\alpha, \tag{174b}$$

with $\xi(\alpha)$ and $K(\alpha - \beta)$ defined in (Table II.9) and (Table II.11). We note that now we have a difference kernel in the integral equation (174a). Therefore we can solve (174a) by a Fourier series ($\Delta < -1$) or Fourier transform ($-1 \leqslant \Delta < 1$) when $y = 0$. Our general convention in this regard is shown in (Table II.12). Furthermore, if one introduces (173) and the parameters ϕ_0, θ_0 and α_0 defined by (Sutherland *et al.*, 1967)

$$\mathrm{e}^{i\phi_0} = (1 + \eta\mathrm{e}^{i\mu})/(\mathrm{e}^{i\mu} + \eta), \qquad 0 \leqslant \phi_0 \leqslant \mu, \qquad |\Delta| < 1, \tag{175}$$

$$\mathrm{e}^{\theta_0} = (1 + \eta\mathrm{e}^{\lambda})/(\mathrm{e}^{\lambda} + \eta), \qquad 0 \leqslant \theta_0 \leqslant \lambda, \qquad \Delta < -1, \tag{176}$$

$$\alpha_0 = (\eta - 1)/2(\eta + 1), \qquad 0 \leqslant \alpha_0 \leqslant \tfrac{1}{2}, \qquad \Delta = -1, \tag{177}$$

where $\eta \equiv \mathrm{e}^{|K_1|}$, it is readily seen that (170) reduces to

$$z(y) = -K_2 + \max(0, -K_1) + \frac{1}{4\pi}\int_{-b}^{b} R(\alpha)\, C(\alpha)\mathrm{d}\alpha \tag{178}$$

with $C(\alpha)$ given by (Table II.16). Later on we shall need the Fourier series (for $\Delta < -1$) and the Fourier transform (for $-1 \leqslant \Delta < 1$) of $C(\alpha)$. These results are listed in (Table II.17). Using (172), one obtains the following values for ϕ_0, θ_0 and α_0 and the ranges of μ and λ:

Ice $\qquad \Delta = \tfrac{1}{2}, \quad \phi_0 = 0, \quad \mu = \tfrac{2}{3}\pi.$ (179a)

F Model $\qquad -1 < \Delta \leqslant \tfrac{1}{2}, \quad \phi_0 = 0, \quad 0 < \mu \leqslant \tfrac{2}{3}\pi$

$$-\infty < \Delta < -1, \quad \theta_0 = 0, \quad \infty > \lambda > 0$$

$$\Delta = -1, \quad \alpha_0 = 0. \tag{179b}$$

KDP model $\frac{1}{2} \leqslant \Delta \leqslant 1, \quad \phi_0 = 3\mu - 2\pi, \quad \frac{2}{3}\pi \leqslant \mu \leqslant \pi.$ (179c)

IKDP model $0 \leqslant \Delta \leqslant \frac{1}{2}, \quad \phi_0 = 2\pi - 3\mu, \quad \frac{1}{2}\pi \leqslant \mu \leqslant \frac{2}{3}\pi.$ (179d)

IF model $\frac{1}{2} \leqslant \Delta \leqslant 1, \quad \phi_0 = 3\mu - 2\pi, \quad \frac{2}{3}\pi \leqslant \mu \leqslant \pi.$ (179e)

In all models, infinite temperature corresponds to $\mu = \frac{2}{3}\pi$, i.e. $\Delta = \frac{1}{2}$. For the F model, μ decreases monotonically as the temperature is lowered until $\mu = 0$ at T_0 or $\Delta = -1$. Then we pass to the $\Delta < -1$ region and λ increases monotonically to infinity at zero temperature. For KDP, μ increases monotonically until $\mu = \pi$ at T_0 or $\Delta = 1$. For $T < T_0$ we are in the $\Delta > 1$ region analyzed in Section IV.E. For IKDP, μ decreases monotonically with temperature and $\mu = \frac{1}{2}\pi$ at $T = 0$. The F and KDP models have the same transition temperature, T_0:

$$\varepsilon/kT_0 = K_0 = \ln 2. \tag{180}$$

In the next section we are going to solve (173, 174) when $y = 0$ for $\Delta < 1$. We shall find that this solution, $R_0(\alpha)$, is not analytic in Δ at $\Delta = -1$. This feature is, however, peculiar to the $y = 0$ case and otherwise we can state the following:

THEOREM: *$R(\alpha)$, considered as a function of Δ and y, is real analytic in Δ and y for $1 \geqslant y > 0$ and $\Delta < 1$.* (See Yang and Yang, 1966b, p. 331.)

COROLLARY: *$z(y)$ is real analytic in the temperature and in y provided $0 < y \leqslant 1$ and $\Delta \leqslant 1$.*

B. Solution in the case $y = 0$. (Douglas B. Abraham, *Department of Mathematics, Massachusetts Institute of Technology, Cambridge, Massachusetts, U.S.A.*)

1. *Closed Form Expressions for the Free Energy*

When $y = 0$, the variable α attains its maximum range (Table II.7) and we can solve (174a) by a Fourier series or Fourier transform. Here use is made of the important fact that $K(\alpha - \beta)$ is 2π-periodic for $\Delta < -1$. Relevant transforms are given in (Table II.13, 14). The solution $R_0(\alpha)$ at $y = 0$ is given in (Table II.15). [The subscript zero denotes $y = 0$.]

Before we proceed to substitute $R_0(\alpha)$ into (178) to obtain $z(0)$, we remark that the expression for $R_0(\alpha)$ for $\Delta < -1$,

$$R_0(\alpha) = \tfrac{1}{2} \sum_{n=-\infty}^{\infty} e^{in\alpha} \operatorname{sech} n\lambda, \quad \Delta < -1 \tag{181}$$

can be identified as a Jacobian elliptic function. We follow the notation of

Milne-Thomson (1964) on the elliptic functions. First we define the nome $q = e^{-\lambda}$ and obtain (use eqn (16.23.3) of Milne-Thomson, 1964)

$$R_0(\alpha) = \tfrac{1}{2} + 2\sum_{n=1}^{\infty} \frac{q^n}{1+q^{2n}} \cos n\alpha$$

$$= \frac{\mathbf{K}}{\pi} \operatorname{dn}\left(\frac{\alpha \mathbf{K}}{\pi}\middle| m\right), \quad \Delta < -1. \tag{182}$$

Here dn is one of the Jacobian elliptic functions whose parameter m is defined by

$$\lambda = \pi \mathbf{K}'/\mathbf{K} \tag{183}$$

and

$$\mathbf{K} = \int_0^{\pi/2} d\theta (1 - m \sin^2\theta)^{-\frac{1}{2}}, \tag{184a}$$

$$\mathbf{K}' = \int_0^{\pi/2} d\theta [1 - (1-m)\sin^2\theta]^{-\frac{1}{2}}. \tag{184b}$$

An equivalent expression which exhibits $R_0(\alpha)$ for $\Delta < -1$ in a power series in λ^{-1} can be obtained by introducing Jacobi's imaginary transformation [eqn (16.20.3) of Milne-Thomson, 1964]

$$\operatorname{dn}(u \mid m) = \operatorname{dc}(-iu \mid 1-m). \tag{185}$$

Thus, upon using the Fourier expansion of the elliptic function dc given by eqn (16.23.7) of Milne-Thomson (1964), we find

$$R_0(\alpha) = \frac{\pi}{2\lambda} \operatorname{sech}\left[\frac{\pi\alpha}{2\lambda}\right] + \frac{2\pi}{\lambda} \sum_{n=0}^{\infty} (-1)^n \frac{\exp[-(2n+1)\pi^2/\lambda]}{1 - \exp[-(2n+1)\pi^2/\lambda]} \times$$

$$\cosh\left[(2n+1)\frac{\pi\alpha}{2\lambda}\right], \quad |\operatorname{Re}(\alpha)| < 2\pi. \tag{186a}$$

The obvious advantage of (186a) is that it is very rapidly convergent for small λ whereas (181) is not. Another formula of similar type is

$$R_0(\alpha) = \frac{\pi}{2\lambda} \sum_{n=-\infty}^{\infty} \operatorname{sech}\left(\frac{\pi}{2\lambda}(\alpha + 2\pi n)\right) \tag{186b}$$

which may be derived as follows: From the known properties of $\operatorname{dn}(\cdot)$, $R_0(\alpha)$ is a doubly periodic meromorphic function with periods 2π and $4i\lambda$. In the fundamental parallelogram there are poles at $i\lambda$ and $3i\lambda$ with residues $-i$ and i respectively. The sum in (186b) converges absolutely and uniformly

in any compact subset of the α plane that contains none of the above poles and is a doubly periodic function with these same properties. The difference between the two sides of (186b) must therefore be an entire doubly periodic function which can only be a constant. To show this constant is zero we consider $R_0(\alpha) - (\pi/2\lambda)$ sech $[\pi\alpha/2\lambda]$, which is holomorphic in a neighbourhood of $\alpha = i\lambda$, then set $\alpha = i\lambda$ and note that (186a) and (186b) are both identically zero. (186b) converges even faster than (186a) for $|\operatorname{Re}(\alpha)| > \pi$ and, moreover, does not have such a restricted domain of convergence. (186b) was also discovered by Yang and Yang [1966b, eqn (B5)] by a different method and it is incredible that the expansion (186b) of the dn function does not seem to appear commonly in the elliptic function handbooks.

We have made this little detour because: (a) As $\lambda = 0$ is the critical point, it is desirable to have a well behaved series for $R_0(\alpha)$ for small λ; (b) there is undoubtedly a deep connection between elliptic functions and the ice problem which we only glimpse by this example. Here is a topic for further research.*

We now return to (178) for an explicit expression of $z(0)$ which, according to (150), is proportional to the free energy for zero external field. Substituting (Table II.7) and (Table II.15) into (178), one finds

$$z(0) = -K_2 + \max(0, -K_1) + \tfrac{1}{4}\int_{-\infty}^{\infty} \frac{d\alpha}{\cosh \pi\alpha} \times \ln\left[\frac{\cosh 2\mu\alpha - \cos(2\mu - \phi_0)}{\cosh 2\mu\alpha - \cos\phi_0}\right], \quad -1 < \Delta < 1 \tag{187a}$$

$$= -K_2 + \max(0, -K_1) + \tfrac{1}{2}[\lambda - \theta_0] + \sum_{n=1}^{\infty} \frac{e^{-\lambda n}\sinh n(\lambda - \theta_0)}{n\cosh n\lambda}, \quad \Delta < -1 \tag{187b}$$

$$= -K_2 + \max(0, -K_1) + \ln\frac{\Gamma(\frac{5}{4} - \frac{1}{2}\alpha_0)\,\Gamma(\frac{1}{4} + \frac{1}{2}\alpha_0)}{\Gamma(\frac{3}{4} - \frac{1}{2}\alpha_0)\,\Gamma(\frac{3}{4} + \frac{1}{2}\alpha_0)}, \quad \Delta = -1. \tag{187c}$$

Here, use has been made of (Table II.17) and the definite integral (Gradshteyn and Ryzhik, 1965, p. 581)

$$\int_0^{\infty} \frac{\ln(a^2 + b^2 x^2)}{\cosh \pi x}\, dx = 2\ln\frac{2\Gamma(\frac{3}{4} + \frac{1}{2}|a/b|)}{\Gamma(\frac{1}{4} + \frac{1}{2}|a/b|)} + \ln(\tfrac{1}{2}|b|) \tag{187d}$$

* *Added in proof.* See Baxter (1971b, 1972) for more recent results in this connection.

in deriving (187b, c). Formula (187b) was obtained from Table (II.14, 17) using Parseval's theorem. We also recall from (162) and discussions given there that

$$z(0) = -K_2 + \max(0, -K_1), \quad \Delta \geqslant 1. \tag{188}$$

2. *Summary of Main Results*

Since $-z(0)/\beta$ is the free energy for $h = v = 0$ (see (150)), we are now in a position to study the thermodynamic properties of the ice rule models in the absence of an external field. The remainder of this section is devoted to this analysis while the analytic properties of $z(0)$ in the complex T-plane will be given in the next section. For the reader's convenience, we first summarize below the main results on the thermodynamics. *Readers who are not interested in the details of the analysis may omit the portion of this section beginning with* (199).

Evaluation of Integrals in Special Cases

The integral in (187a) may be evaluated in terms of elementary functions for the ice, KDP and IKDP cases. The results are:

(i) *Ice Problem*

We have $K_1 = K_2 = 0$, $\Delta = \frac{1}{2}$, $\mu = \frac{2}{3}\pi$ and $\phi_0 = 0$. Hence

$$z(0) = \tfrac{1}{4}\int_{-\infty}^{\infty} \frac{d\alpha}{\cosh \pi\alpha} \ln\left[\frac{\cosh(4\pi\alpha/3) + \frac{1}{2}}{\cosh(4\pi\alpha/3) - 1}\right]$$

$$= \tfrac{3}{2}\ln\tfrac{4}{3}. \tag{189}$$

The integral in (189) was first evaluated by Lieb (1967b) and can also be obtained by setting $\Delta = \frac{1}{2}$ in (192) below. On combining (150) and (3) we obtain for square ice

$$W_{\text{sq. ice}} = (\tfrac{4}{3})^{3/2} = 1{\cdot}5396007\ldots, \tag{190}$$

the result quoted in (4).

(ii) *KDP model*

We have $K_1 \equiv K \geqslant 0$, $K_2 = 0$, or $K_1 = K_2 \equiv K \leqslant 0$, $\frac{1}{2} \leqslant \Delta \leqslant 1$, $\phi_0 = 3\mu - 2\pi$ and $\frac{2}{3}\pi \leqslant \mu \leqslant \pi$. Hence

$$z(0) = 2\max(0, -K) + \tfrac{1}{4}\int_{-\infty}^{\infty} \frac{d\alpha}{\cosh \pi\alpha} \ln\left[\frac{\cosh 2\mu\alpha - \cos\mu}{\cosh 2\mu\alpha - \cos 3\mu}\right],$$

$$\tfrac{1}{2} \leqslant \Delta \leqslant 1. \tag{191a}$$

Also from the discussion in Section IV.E we know that

$$z(0) = 0, \quad \Delta > 1. \tag{191b}$$

The integral (191a) can be evaluated (Glasser, 1969) by applying Parseval's theorem to the Fourier transforms (Table II.14, 17).
The result is:

$$z(0) = \ln\left[\frac{2\mu}{\pi \sin \mu} \cot\left(\frac{\pi^2}{2\mu}\right)\right] + 2 \max(0, -K), \; \tfrac{1}{2} \leqslant \Delta \leqslant 1. \tag{192}$$

(iii) *IKDP model*
We have $K_1 \equiv K \leqslant 0$, $K_2 = 0$ or $K_1 = K_2 \equiv K \geqslant 0$, $0 < \Delta \leqslant \frac{1}{2}$, $\phi_0 = 2\pi - 3\mu$ and $\frac{1}{2}\pi < \mu \leqslant \frac{2}{3}\pi$. Hence

$$z(0) = -K + \tfrac{1}{4}\int_{-\infty}^{\infty} \frac{d\alpha}{\cosh \pi\alpha} \ln\left[\frac{\cosh 2\mu\alpha - \cos 5\mu}{\cosh 2\mu\alpha - \cos 3\mu}\right], \quad 0 < \Delta \leqslant \tfrac{1}{2}. \tag{193}$$

The integral in (193) can also be evaluated in exactly the same way as for KDP (Abraham *et al.*, 1970a, b and 1971). The result is also given essentially by the expression (192), namely,

$$z(0) = \ln\left[\frac{2\mu}{\pi \sin \mu} \cot\left(\frac{\pi^2}{2\mu}\right)\right] - 2 \max(0, K), \quad 0 < \Delta \leqslant \tfrac{1}{2}. \tag{194}$$

Thus we see explicitly that the free energies for KDP and IKDP are analytic continuations of each other despite the different expressions (191a) and (193). It is natural that this should be so, otherwise there would be a singularity at infinite temperature ($K = 0$).

Conjecture: In general, even when $K_2 \neq 0$ and $y \neq 0$, $z(y)$ given by (178) is real analytic in K_1 at $K_1 = 0$ (except when $K_1 = 0$ corresponds to the critical point $\Delta = -1$ and at the same time $y = 0$).

Nature of the Phase Transitions

The nature of the phase transition in the absence of a field is now briefly summarized. We see from (187a–d) that, for a given assignment of ε_1 and ε_2, a phase transition occurs at those values of T for which $\Delta = \pm 1$. It is clear from (138) or Fig. 13 that in every case *only one* transition is realized. In fact the $\Delta = 1$ (or $\Delta = -1$) transition is always associated with the intrinsically ferroelectric (or antiferroelectric) model defined by $\bar{\varepsilon} > 0$ (or $\bar{\varepsilon} < 0$). (See eqn (94).) If we write $u_1 \equiv \omega_1 = \omega_2$, $u_2 \equiv \omega_3 = \omega_4$, $u_3 \equiv \omega_5 = \omega_6$ where ω_ξ are the vertex weights, the condition $\Delta = \pm 1$ for determining the transition temperature T_0 is always equivalent to the expression

$$u_1 + u_2 + u_3 = 2 \max\{u_1, u_2, u_3\}, \quad T = T_0. \tag{195a}$$

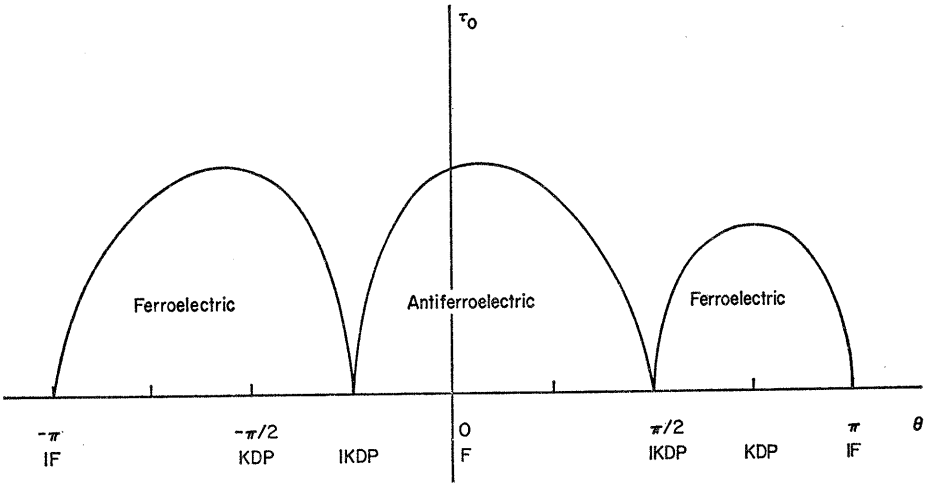

FIG. 14. Plot of scaled transition temperature τ_0 against the angle θ in the $(\varepsilon_1, \varepsilon_2)$ plane; $\theta = -\tan^{-1}(\varepsilon_1/\varepsilon_2)$, and a constant value of $(\varepsilon_1{}^2 + \varepsilon_2{}^2)^{1/2}$ is assumed with $\tau_0 = kT_0/(\varepsilon_1{}^2 + \varepsilon_2{}^2)^{1/2}$. This plot is obtained from Fig. 13.

We plot T_0 in Fig. 14 as a function of orientation $\theta = \tan^{-1}(\varepsilon_1/\varepsilon_2)$ in the $(\varepsilon_1, \varepsilon_2)$ plane. The two regions $\bar{\varepsilon} \gtrless 0$ of the $(\varepsilon_1, \varepsilon_2)$ plane are shown once again in Fig. 15 with various special cases indicated. The critical behaviour turns out to be quite different in the two regions:

(i). $\bar{\varepsilon} < 0$.

This is the intrinsically antiferroelectric case (region II of Fig. 15) because vertices (5) and (6) are favoured. The transition occurs at $\Delta = -1$. As we

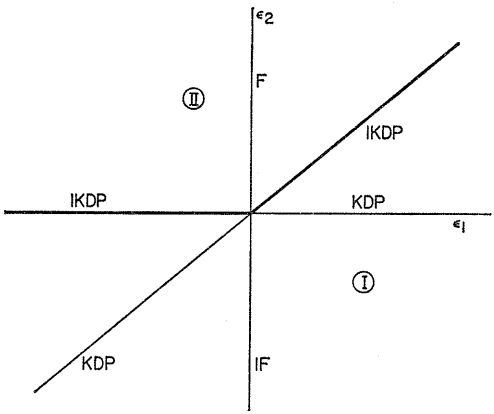

FIG. 15. The $(\varepsilon_1, \varepsilon_2)$ plane is decomposed into two regions separated by a heavy line, which display different critical behaviour.

shall see below, the transition is of infinite order. This means that all derivatives of the free energy with respect to temperature are bounded and agree on both sides of the transition temperature, but that the free energy is not real analytic at T_0. The free energy has an asymptotic expansion which is the same above and below T_0 and is given by (272). For the F model ($K_1 = 0$, $K_2 = K$) this expansion reduces to (Lieb, 1967c)

$$z(0) \cong -K + 2\ln\left[\frac{\Gamma(\frac{1}{4})}{2\Gamma(\frac{3}{4})}\right] + \sum_{n=1}^{\infty} \frac{(-1)^n}{2n(2n)!} B_{2n}(1 - E_{2n})\,\mu^{2n}, \qquad (195b)$$

where B_n and E_n are the Bernoulli and Euler numbers. By direct differentiation of (195b), we find the internal energy, U, and the specific heat, C, for the F model at T_0:

$$\begin{aligned} U &= \tfrac{1}{3}\varepsilon, \\ C &= k(\ln 2)^2\,\tfrac{288}{45}. \end{aligned} \qquad \text{(F model)} \qquad (196)$$

(ii). $\bar{\varepsilon} > 0$, $\varepsilon_1 \neq 0$

This is the intrinsically ferroelectric case because one of the polarized vertices (1)–(4) is favoured. The transition occurs at $\Delta = 1$ in region I of Fig. 14, and is of first order. The free energy is a constant for $T \leqslant T_0$ as given by (188). By direct differentiation of (187a), we may compute the internal energy U and the specific heat C. In particular, we find the latent heat L and the singular behaviour of C as follows:

$$\begin{aligned} L &= \lim_{T \to T_0+} U = \tfrac{1}{2}\left[\bar{\varepsilon} + (|\varepsilon_1| - \bar{\varepsilon})\frac{1}{\eta_0}\right], \\ C &\cong \frac{k}{\pi}(\eta_0 - 1)^{\frac{1}{2}}(L/K\,T_0)^{3/2}(1 - T_0/T)^{-1/2}, \quad T \cong T_0+, \end{aligned} \qquad (197)$$

where

$$\eta_0 = \exp(|\varepsilon_1|/k\,T_0).$$

(iii). $\bar{\varepsilon} > 0$, $\varepsilon_1 = 0$, $\varepsilon_2 < 0$

This is the IF model for which a ferroelectric transition occurs at absolute zero. The free energy has an essential singularity at $T = 0$, since

$$\Delta = 1 - \tfrac{1}{2}\exp(-|\varepsilon_2|/kT). \qquad (198)$$

Nevertheless, all the derivatives of the free energy with respect to T on the real positive T-axis *vanish* as $T \to 0+$.

(iv). $\varepsilon_1 = \varepsilon_2 > 0$ or $\varepsilon_2 = 0$, $\varepsilon_1 < 0$

From Fig. 15, this is the IKDP model. The free energy has an essential singularity at $T = 0$, but all temperature derivatives *vanish* as $T \to 0+$. There is no ordered state.

To conclude our summary on the thermodynamic properties, in Figs. 16–18 we plot the internal energy U and specific heat C for some typical cases. In Fig. 16 U and C are shown for the F model. In Fig. 17 we plot U

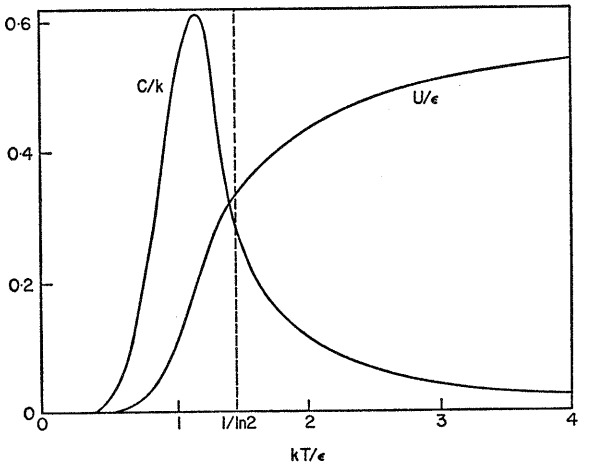

FIG. 16. Energy and specific heat per vertex, U and C, of the F model ($\varepsilon_1 = 0$, $\varepsilon_2 = \varepsilon > 0$) in zero field. The transition temperature is $T_0 = \varepsilon/(k\ln 2)$.

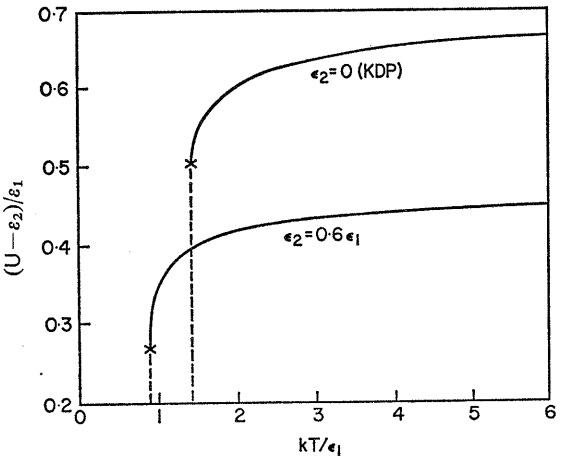

FIG. 17. Energy per vertex, U, of the intrinsically ferroelectric models.

for two ferroelectric cases, $\varepsilon_1 > 0$, $\varepsilon_2 = 0$ (KDP) and $\varepsilon_2 = 0{\cdot}6\,\varepsilon_1 > 0$. The specific heats in these two cases are shown in Fig. 18.

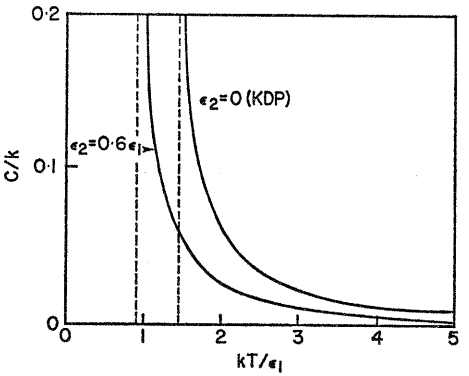

FIG. 18. Specific heat per vertex, C, of the intrinsically ferroelectric models.

3. *Analytic Properties of the Function* $\phi(\mu)$

Consider the integral in (187a):

$$\phi(\mu) = \tfrac{1}{4}\int_{-\infty}^{\infty} \frac{dx}{\cosh(\pi x)} \ln\left[\frac{\cosh 2\mu x - \cos(2\mu - \phi_0)}{\cosh 2\mu x - \cos\phi_0}\right] \tag{199}$$

where $\phi_0(\mu)$ is defined by (175)

$$e^{i\phi_0(\mu)} = \frac{1 + \eta e^{i\mu}}{\eta + e^{i\mu}} \tag{200}$$

as a function of the complex variable μ which we write as

$$\mu = \mu_1 + i\mu_2. \tag{201}$$

In the range $-1 < \Delta < 1$, which corresponds to $0 < \mu_1 < \pi$, (187a) gives

$$z(0) = -K_2 + \max(0, -K_1) + \Phi(\mu). \tag{202}$$

Clearly there is a *single independent* variable in the physical problem; obvious choices for this are μ or T. Thus η depends on T, or indirectly on μ. Several remarks are relevant in this connection.

(1) For the F and IF cases, the problem is much more simple since $\eta \equiv 1$ for all T; thus $\phi_0(\mu) \equiv 0$. Theorem 1 below discusses the analytic properties in the μ plane for this case.

(2) For the KDP and IKDP cases, the function $\Phi(\mu)$ can be evaluated in terms of elementary functions (Glasser, 1969).

(3) The physical properties of the model are evidently all obtained by considering a small neighbourhood of the real positive temperature axis or the equivalent region of the μ-plane. Theorem 2, below, is the analogue of Theorem 1, below, when η is regarded as an *independent* real positive variable. This result is then generalized to allow η to be in a small sector about the real positive $(\eta - 1)$ axis.

THEOREM 1. *Consider the case* $\phi_0 \equiv 0$ *or* $\eta \equiv 1$:

(1) $\Phi(\mu)$ *can be analytically continued to the entire* μ*-plane, except the line* $\mu_2 = 0$, $\mu_1 \leqslant 0$, *which is a natural boundary.*

(2) $$\Phi(\bar{\mu}) = \overline{\Phi(\mu)}. \tag{203}$$

(3) *For real* $\lambda > 0$,

$$\tfrac{1}{2}[\Phi(i\lambda) + \Phi(-i\lambda)] = \frac{\lambda}{2} + \sum_{n=1}^{\infty} n^{-1}\, \mathrm{e}^{-n\lambda} \tanh(n\lambda). \tag{204}$$

This should be compared with eqn (187b).

(4) *For all* μ *except points on the real axis,*

$$\Phi(\mu) - \Phi(-\mu) = \sum_{n=0}^{\infty} \frac{(-1)^n}{2n+1} \cot\left(\frac{\pi^2(2n+1)}{2\mu}\right) - i\pi. \tag{205}$$

Proof. The integrand in (199) with $\phi_0 \equiv 0$ has simple poles at

$$x_0(n) = (n + \tfrac{1}{2})i, \quad n = 0, \quad \pm 1, \ldots \tag{206}$$

and logarithmic branch points at

$$x_1^{\pm}(n) = \pm i + \frac{n\pi i}{\mu} \tag{207a}$$

$$x_2(n) = \frac{n\pi i}{\mu}, \quad n = 0, \pm 1, \ldots . \tag{207b}$$

As μ moves away from the real axis, the branch points move in the x-plane. Evidently $\Phi(\mu)$ may be analytically continued to the entire μ-plane, except the negative real μ-axis; in that case, the contour of integration is pinched by the branch points against the singularities $x_0(n)$, for *all* rational values of μ.

Since $\Phi(\mu)$ is real analytic and real on the line segment ($\mu_2 = 0$, $0 < \mu_1 < \pi$), the Schwarz reflection principle gives (203), the second part of Theorem 1.

In order to derive (204) and (205), and prove that ($\mu_2 = 0$, $\mu_1 \leqslant 0$) is a natural boundary, $\Phi(\mu)$ may be rewritten, using the Parseval formula, as

$$\Phi(\mu) = \tfrac{1}{2}\int_{-\infty}^{\infty} \frac{\mathrm{d}x}{x} \frac{\sinh \mu x \sinh (\pi - \mu)x}{\cosh \mu x \sinh \pi x} \tag{208}$$

provided $0 < \mu_1 < \pi$. (This result may be extended to other strips, but this will not be needed here.)

In this case, the integrand has simple poles at

$$p_1(n) = (n + \tfrac{1}{2})\pi i/\mu, \quad n = 0, \quad \pm 1, \ldots \tag{209}$$

$$p_0(n) = ni, \quad n = \pm 1, \quad \pm 2, \ldots . \tag{210}$$

As μ rotates, the poles $p_1(n)$ rotate synchronously and impinge upon the real axis when $\mu = i\lambda$. An elementary, but tedious, calculation shows that

$$\Phi(i\lambda) = \frac{\lambda}{2} + \sum_{n=1}^{\infty} n^{-1} \mathrm{e}^{-n\lambda} \tanh (n\lambda) + i \sum_{n=0}^{\infty} \frac{(-1)^n \exp[-\pi^2 (n + \frac{1}{2})/\lambda]}{(n + \frac{1}{2}) \sinh (\pi^2 (n + \frac{1}{2})/\lambda)}. \tag{211}$$

Using (2) of Theorem 1, one readily obtains (204) from (211) and, using Section 1.442 of Gradshteyn and Ryzhik (1965), the result

$$\Phi(i\lambda) - \Phi(-i\lambda) = -i\pi + 4i \sum_{n=0}^{\infty} \frac{(-1)^n}{2n + 1} \coth \left(\frac{\pi^2 (n + \frac{1}{2})}{\lambda} \right). \tag{212}$$

According to the identity theorem for analytic functions, the analytic continuation of $\Phi(\mu)$, whenever it exists, must satisfy the equation

$$\Phi(\mu) - \Phi(-\mu) = -i\pi + 2 \sum_{n=0}^{\infty} \frac{(-1)^n}{2n + 1} \cot \left(\frac{\pi^2 (2n+1)}{2\mu} \right). \tag{213}$$

The series above represents an analytic function in the finite μ-plane except for the line $\mu_2 = 0$, upon which there are simple poles at the points μ_0, given by

$$\mu_0 = \pi(2r + 1)/2s \tag{214}$$

where r and s are any integers. In order to prove that the real axis is a natural boundary, we have to consider the approach to $\mu_2 = 0$ along a line

$$\mu = \pi(2r + 1)/2s + i\,\mu_2. \tag{215}$$

This gives

$$\Phi(\mu) - \Phi(-\mu) = \frac{4\mu(-1)^r}{\mu_2\,\pi(2r+1)^2} \sum_{n=0}^{\infty} \frac{(-1)^n}{(2n+1)^2} + G(\mu_2, \mu_0) \qquad (216)$$

where $G(\mu_2, \mu_0)$ can be bounded. The sum of the series is the Catalan constant, which is non-zero. The intercepts of the lines given by (215) with the real axis form a dense set of points in $\mathbb{R}$. Thus the line $\{\mu_2 = 0, -\infty < \mu_1 \leqslant 0\}$ is a natural boundary. This completes the proof of Theorem 1. The physical interpretation will be described later.

When $\eta > 1$, intuition suggests that a similar theorem should hold. Singularities of $\Phi(\mu)$ arise again because motion of the branch points at

$$x_2{}^{\pm}(n) = \pm i(1 - \phi_0/2\mu) + n\pi i/\mu \qquad (217a)$$

and

$$x_2{}^{\pm}(n) = \pm i\,\phi_0/2\mu + n\,\pi i/\mu, \quad n = 0, \quad \pm 1, \ldots \qquad (217b)$$

as μ varies, causes the contour of integration to pinch the stationary poles at

$$x_0(n) = (n + \tfrac{1}{2})i, \quad n = 0, \quad \pm 1, \ldots . \qquad (218)$$

It is clear that the motion of the branch points has an epicyclic character (see Fig. 19) which arises from the dependence of ϕ_0 on μ. It should also be noted that singular behaviour of $\Phi(\mu)$ is given by the branch points of $\phi_0(\mu)$ at

$$\mu = i|\,K_1\,| + (2n+1)\pi, \quad n = 0, \quad \pm 1 \ldots \qquad (219)$$

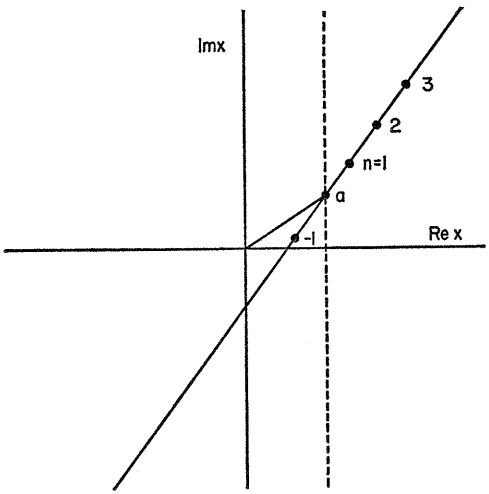

FIG. 19. Motion of the branch points in the complex plane of the integration variable x. The set $x_2{}^{+}(n)$ is shown. The point a) is $\phi_0(\mu)/2\mu$. The line of branch points makes an angle ($-$ arg μ) with the vertical direction.

The nature of the mapping $\phi_0(\mu)$ may be obtained conveniently by considering lines parallel to the axes in the μ-plane. In this way, $\phi_0(\mu)$ can be investigated on a family of polygonal arcs, along which the possibility of pinching may be examined. If $w = e^{i\phi_0}$ and $z = e^{i\mu}$, (200) becomes

$$w = \frac{1 + \eta z}{\eta + z} \tag{220}$$

which is a bilinear transformation. The line $L_1 = \{\mu = \mu_1 + i\mu_2 : 0 \leqslant \mu_1 \leqslant 2\pi\}$ corresponds to a circle $|z| = e^{-\mu_2}$, whereas $L_2 = \{\mu = \mu_1 + i\mu_2 : -\infty < \mu_2 < \infty\}$ corresponds to a half line from the origin of argument μ_1 in the z-plane.

The line L_1 maps into

$$\left| \frac{w - \eta^{-1}}{w - \eta} \right| = \eta^{-1} e^{-\mu_2} \tag{221}$$

which is a circle of Apollonius with inverse points η and η^{-1}, centre w_1, and radius ρ_1 given by

$$w_1 = \frac{\eta^{-1} - k^2\eta}{1 - k^2}, \tag{222}$$

$$\rho_1 = \frac{k(\eta - \eta^{-1})}{|1 - k^2|}, \tag{223}$$

with $k = \eta^{-1} e^{-\mu_2}$.

The mapping of the line L_2, extended to infinity on both sides of the origin, may be obtained by using the theorem that any bilinear transformation maps circles into circles (a line is regarded as a degenerate circle) inverse points into inverse points and complementary domains into complementary domains. Consider the inverse points

$$z_\pm = \pm i e^{i\mu_1}. \tag{224}$$

The associated inverse points in the w-plane are given by

$$w_+ = -i e^{-i\mu_1} (1 + i\eta e^{i\mu_1})/(1 - i\eta e^{-i\mu_1}) \tag{225}$$

and

$$w_+ w_- = 1. \tag{226}$$

Thus

$$w_\pm = e^{\pm i\theta}, \tag{227}$$

where θ is a real angle. The equation of the circle is

$$\left| \frac{w - w_+}{w - w_-} \right| = \eta^{-1}. \tag{228}$$

The centre w_2 and radius ρ_2 are given by

$$w_2 = \cos\theta + i\left(\frac{\eta^2 + 1}{\eta^2 - 1}\right)\sin\theta \tag{229}$$

and

$$\rho_2 = 2\eta\cos\theta/(\eta^2 - 1). \tag{230}$$

Evidently the centre lies on the line through w_+ and w_-, as expected on geometrical grounds. Typical circles are shown in Fig. 20.

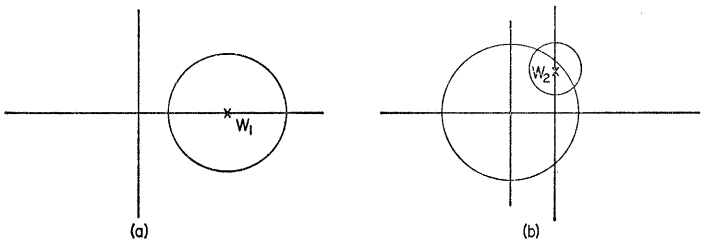

FIG. 20. Typical circles of Apollonius:
(a) $|(w - \eta^{-1})/(w - \eta)| = \eta^{-1}\,e^{-\mu_2}$. The point w_1 is the centre.
(b) $|(w - w_+)/(w - w_-)| = \eta^{-1}$. The point w_2 is the centre.

Using the above results, the reader may convince himself, if he so desires, that there is a region of the μ-plane defined by $-\theta \leqslant \arg\mu \leqslant \theta$, with $\theta > \pi/2$, for which the motion of the branch points does not cause the contour of integration to pinch against the poles $x_0(\mu)$ of (218). Thus $\Phi(\mu)$ may be analytically continued to this sector. With more delicacy, the argument may be extended further into the domain $-\pi < \arg\mu < \pi$, but this will not be needed here. As with the F model, the quantity $\Phi(i\lambda) - \phi(-i\lambda)$ will be calculated, but its analytic continuation will not be required.

First, since $\Phi(\mu)$ is real analytic on $0 < \mu_1 < \pi$, by the Schwarz reflection principle

$$\Phi(\bar{\mu}) = \overline{\Phi(\mu)} \tag{231}$$

in the domain of analyticity. Using the Persaval transform of $\Phi(\mu)$, one obtains

$$\Phi(\mu) = \tfrac{1}{2}\int_{-\infty}^{\infty} \frac{dx}{x}\left[\frac{\sinh(\pi - \mu)x \sinh(\mu - \phi_0)x}{\cosh\mu x \sinh\pi x}\right] \tag{232}$$

for $0 < \mu_1 < \pi$. By employing the same argument as for the F case (only the residues at the poles are changed), one may obtain the result for $\lambda > 0$:

$$\Phi(i\lambda) = \frac{\lambda - \theta_0}{2} + \sum_{n=1}^{\infty} \frac{e^{-n\lambda}}{n} \frac{\sinh(\lambda - \theta_0)n}{\cosh(n\lambda)}$$

$$+ i \sum_{n=0}^{\infty} \frac{(-1)^n}{(n + \frac{1}{2})} \frac{\cos[(\pi\theta_0/\lambda)(n + \frac{1}{2})]}{\sinh[(\pi^2/\lambda)(n + \frac{1}{2})]} \exp[-\frac{\pi^2}{\lambda}(n + \tfrac{1}{2})] \quad (233)$$

where θ_0 is given by (176). Equation (233) then gives

$$\tfrac{1}{2}[\Phi(i\lambda) + \Phi(-i\lambda)] = \frac{\lambda - \theta_0}{2} + \sum_{n=1}^{\infty} \frac{e^{-n\lambda}}{n} \frac{\sinh(\lambda - \theta_0)n}{\cosh(n\lambda)} \quad (234)$$

and

$$\tfrac{1}{2}[\Phi(i\lambda) - \Phi(-i\lambda)] = i \sum_{n=0}^{\infty} \frac{(-1)^n}{(n + \frac{1}{2})} \frac{\cos[(\pi\theta_0/\lambda)(n + \frac{1}{2})] \exp[-(\pi^2/\lambda)(n + \frac{1}{2})]}{\sinh[(\pi^2/\lambda)(n + \frac{1}{2})]}. \quad (235)$$

Once again, the identity theorem requires that wherever $\Phi(\mu)$ is analytic, it must obey the equation

$$\Phi(\mu) - \Phi(-\mu) =$$

$$-i\pi + 4 \sum_{n=0}^{\infty} \frac{(-1)^n}{2n + 1} \cos\left(\frac{\pi\phi_0}{2\mu}(2n + 1)\right) \cot\left(\frac{\pi^2(2n + 1)}{2\mu}\right). \quad (236)$$

This series represents an analytic function; the occurrence of the function $\phi_0(\mu)$ complicates convergence questions. The singularities include branch points arising from those of $\phi_0(\mu)$, and a dense set of poles on the real axis at

$$\mu = \pi(2r + 1)/2s, \quad (237)$$

as was found for the F case above. In this case the residue is

$$R[\mu = (2r + 1)/2s] = \frac{4\mu}{\pi} \frac{(-1)^r}{(2r + 1)^2} \sum_{n=0}^{\infty} \frac{(-1)^n}{(2n + 1)^2} \cos[s\pi\phi_0(\mu)(2n + 1)]. \quad (238)$$

The sum of this series vanishes only if

$$s\phi_0(\mu)(2n + 1) = k + \tfrac{1}{2}. \quad (239)$$

If this relationship is not satisfied, then $[\Phi(\mu) - \Phi(-\mu)]$ has a natural boundary on $\mu_2 = 0$. The argument may be extended to include complex

values of η in a sector about the positive real axis in the $(\eta - 1)$ plane. In this case, the previous argument shows that the singularities of $\Phi(\mu)$ spread out over a sector about the negative real μ-axis.

The results may be summarised in a theorem, the statement of which could undoubtedly be strengthened by more detailed analysis of the series in (236):

THEOREM 2: *If the variable η satisfies $\eta > 1$, then for all such values*

(1) *$\Phi(\mu)$ may be analytically continued to a sector S of the μ-plane given by*

$$-(\tfrac{1}{2}\pi + \delta) \leqslant \arg \mu \leqslant (\tfrac{1}{2}\pi + \delta), \quad \delta > 0. \tag{240a}$$

There are singularities at the branch points of $\phi_0(\mu)$ given by

$$\mu_n = \pm i|K_1| + (2n + 1)\pi, \quad n = 0, \quad \pm 1, \ldots . \tag{240b}$$

(2) $$\Phi(\bar{\mu}) = \overline{\Phi(\mu)} . \tag{241}$$

(3) *For $\lambda > 0$*

$$\tfrac{1}{2}[\Phi(i\lambda) + \Phi(-i\lambda)] = \frac{\lambda - \theta_0}{2} + \sum_{n=1}^{\infty} \frac{e^{-n\lambda}}{n} \frac{\sinh(\lambda - \theta_0)n}{\cosh n\lambda}. \tag{242}$$

(4) *Whenever the series converges, we have*

$$\Phi(\mu) - \Phi(-\mu) = -i\pi + 4 \sum_{n=0}^{\infty} \frac{(-1)^n}{2n + 1} \cos\left(\frac{\pi\phi_0(2n + 1)}{2\mu}\right) \times \cot\left(\frac{\pi^2(2n + 1)}{2\mu}\right). \tag{243}$$

The series has a natural boundary unless (237) *and* (239) *are satisfied.*

This theorem allows one to consider those cases when $\Delta = -1$ is attained for real positive T; η then satisfies the condition of the theorem.

The function $\Phi(\mu)$ may be evaluated in closed form for the particular functional relationship $\eta(\mu)$ which obtains for KDP and IKDP. Equation (232) may be rewritten as

$$\Phi(\mu) = J_1(\mu) + J_2(\mu) \tag{244}$$

where

$$J_1(\mu) = \tfrac{1}{2}\int_0^{\infty} \frac{dx}{x} [\operatorname{sech} \mu x](e^{-\phi_0 x} - e^{-(2\mu - \phi_0)x})$$

$$= \ln\left(\frac{\Gamma(1 + \frac{1}{4}s)\,\Gamma(\frac{1}{2} - \frac{1}{4}s)}{\Gamma(1 - \frac{1}{4}s)\,\Gamma(\frac{1}{2} + \frac{1}{4}s)}\right) \tag{245}$$

with

$$s = 1 - \phi_0/\mu. \tag{246}$$

The integral $J_2(\mu)$ is given by

$$J_2(\mu) = \int_0^\infty \frac{dx}{x} \frac{e^{-\pi x}}{\cosh(\mu x)\sinh(\pi x)} \sinh(\phi_0 x)\sinh(\mu - \phi_0)x. \tag{247}$$

The evaluation of this integral is given below for KDP and IKDP.

(1) KDP: $\phi_0 = 3\mu - 2\pi$, $\frac{2}{3}\pi \leqslant \mu_1 \leqslant \pi$ for $T \geqslant 0$ and $s = 2\pi/\mu - 2$.

A simple manipulation gives

$$J_2(\mu) = 2\int_0^\infty \frac{dx}{x} e^{-\pi x} \sinh(3\mu - \pi)x \left[\frac{\cosh \pi x \cosh 2\mu x}{\cosh \mu x} - \frac{\cosh 2\pi x \sinh \mu x}{\sinh \pi x}\right]. \tag{248}$$

Each integral may be evaluated in terms of Γ functions by reference to a table of Laplace transforms given by Glasser (1969). Use of the reflection formula

$$\Gamma(z)\Gamma(1 - z) = \pi \operatorname{cosec} \pi z \tag{249}$$

then gives the remarkably simple result

$$\Phi(\mu) = \ln\left[\frac{2\mu}{\pi \sin \mu} \cot\left(\frac{\pi^2}{2\mu}\right)\right]. \tag{250}$$

(2) IKDP: $\phi_0 = 2\pi - 3\mu$, $\frac{1}{2}\pi \leqslant \mu \leqslant \frac{2}{3}\pi$ for $T \geqslant 0$ and $s = 4 - 2\pi/\mu$. In this case

$$J_2(\mu) = 2\int_0^\infty \frac{dx}{x} e^{-\pi x} \sinh(2\pi - 3\mu)x \left[\frac{\sinh 4\mu x \cosh \pi x}{\cosh \mu x} - \frac{\cosh 4\mu x \cosh \pi x}{\sinh \pi x}\right]. \tag{251}$$

This integral may be evaluated in the same way as for KDP, giving

$$\Phi(\mu) = \ln\left[\frac{2\mu}{\pi \sin \mu} \cot\left(\frac{\pi^2}{2\mu}\right)\right] \tag{252}$$

which, surprisingly enough, is the analytic continuation of the KDP result.

4. *Origin of the Phase Transition*

Critical behaviour arises firstly because of the singularities of the function $\Phi(\mu)$ on the segment of the real axis given by $0 \leqslant \mu_1 \leqslant \pi$. It was shown in the previous subsection that the low-temperature behaviour is given by $(\Phi(i\lambda) + \Phi(-i\lambda))/2$, with $\lambda > 0$. In Theorem 2 it was shown that the only physically relevant singularity is at $\mu = 0$, which corresponds to $\Delta = -1$. The second source of critical behaviour is the dependence of μ on Δ; $\mu(\Delta)$ has branch points at $\Delta = \pm 1$. It is important to decide what values of Δ can be realised on the real temperature axis for a given assignment of vertex energies. This is summarised in the following theorem:

THEOREM 3. *If the temperature T is real and positive, then $\eta \geqslant 1$ and*

(1) *For no values of ε_1 and ε_2 can both $\Delta = +1$ and $\Delta = -1$ be realised.*

(2) *If $\varepsilon_2 > \max(0, \varepsilon_1)$, then $-\infty < \Delta < \frac{1}{2}$ for real T, whereas if $\varepsilon_2 < \max(0, \varepsilon_1)$, $\frac{1}{2} < \Delta < \infty$. If $\varepsilon_2 = \max(0, \varepsilon_1)$, then $0 \leqslant \Delta < \frac{1}{2}$; there is no singular behaviour in this case.*

The theorem can be proved along the lines of (162) *et seq.* The $(\varepsilon_1, \varepsilon_2)$ plane is divided as shown in Fig. 15, and the temperature T_0 at which $\Delta = \pm 1$ is realised is plotted as a function of angle in the $(\varepsilon_1, \varepsilon_2)$ plane in Fig. 14.

In the following the critical behaviour at $\Delta = -1$ and $\Delta = 1$ will be obtained.

(i) *Asymptotic Behaviour of $\Phi(\mu)$ near $\mu = 0$: $\Delta = -1$ transition*

From (234), the low temperature free energy near the transition temperature may be obtained from the series

$$\tfrac{1}{2}(\Phi(i\lambda) + \Phi(-i\lambda)) = -\tfrac{1}{2}\lambda t + \lambda \sum_{n=0}^{\infty} F(n\lambda, t) \tag{253}$$

where the parameter t is defined by

$$t = 1 - \theta_0/\lambda$$

and

$$F(x, t) = \frac{e^{-x}}{x} \frac{\sinh(tx)}{\cosh x}. \tag{254}$$

An asymptotic expansion in powers of λ may be obtained by the Euler–

Maclaurin summation formula (see, e.g. Haynsworth and Goldberg, 1964, p. 806), which is

$$\sum_{n=0}^{M} F(n\lambda, t) = \frac{1}{\lambda}\int_0^{M\lambda} F(x,t)\mathrm{d}x + \tfrac{1}{2}(F(0,t) + F(M\lambda,t))$$

$$+ \sum_{n=1}^{N-1} \frac{1}{(2n)!}(F^{(2n-1)}(M\lambda) - F^{(2n-1)}(0))B_{2n}\lambda^{2n-1}$$

$$+ \frac{\lambda^{2N}}{(2N)!}B_{2N}\sum_{n=0}^{M-1} F^{(2N)}(n\lambda + \theta\lambda), \quad 0 < \theta < 1. \tag{255}$$

In order to evaluate the derivatives $F^{(2n-1)}(0,t)$ we relate $F(x,t)$ to the generating function for the Euler polynomials $E_n(x)$ (Haynsworth and Goldberg, 1964; p. 804):

$$\frac{\mathrm{e}^{(2\lambda-1)x}}{\cosh x} = \sum_{n=0}^{\infty} E_n(\lambda)\frac{(2x)^n}{n!}, \quad |x| < \pi/2. \tag{256}$$

Thus one obtains

$$F(x,t) = \frac{1}{2x}\sum_{n=0}^{\infty}\frac{(2x)^n}{n!}\left[E_n\left(\frac{t}{2}\right) - E_n\left(-\frac{t}{2}\right)\right], \quad |x| < \pi/2, \tag{257}$$

from which

$$F^{(2n-1)}(0,t) = \frac{2^{2n-1}}{2n}\left[E_{2n}\left(\frac{t}{2}\right) - E_{2n}\left(\frac{-t}{2}\right)\right]. \tag{258}$$

The integral in the first term is approximated exponentially well by

$$\int_0^{\infty} F(x,t)\mathrm{d}x = \ln\left(\frac{\Gamma(1+\frac{1}{4}t)\,\Gamma(\frac{1}{2}-\frac{1}{4}t)}{\Gamma(1-\frac{1}{4}t)\,\Gamma(\frac{1}{2}+\frac{1}{4}t)}\right). \tag{259}$$

This result is obtained by reference to a table of Laplace transforms (Glasser, 1969). Thus

$$\tfrac{1}{2}(\Phi(i\lambda) + \Phi(-i\lambda)) = \ln\left(\frac{\Gamma(1+\frac{1}{4}t)\,\Gamma(\frac{1}{2}-\frac{1}{4}t)}{\Gamma(1-\frac{1}{4}t)\,\Gamma(\frac{1}{2}+\frac{1}{4}t)}\right)$$

$$+ \sum_{n=1}^{N-1}\frac{2^{2n}}{2n}\left[E_{2n}(-\tfrac{1}{2}t) - E_{2n}(\tfrac{1}{2}t)\right]\frac{B_{2n}}{2n!}\lambda^{2n} + 0(\lambda^{2N}). \tag{260}$$

This series has zero radius of convergence, as expected since $(\Phi(\mu) + \Phi(-\mu))$ has a natural boundary on the negative real μ-axis. Never-

theless, it defines a C^∞ function both in λ at $\lambda = 0$, and in η near η_0 at $\lambda = 0$; the differential coefficients are obtained by term differentiation of (260).

The asymptotic expansion of $\Phi(\mu)$ in a suitable neighbourhood of $\mu = 0$ will now be considered, along the lines of Yang and Yang (1966b). First, let a region S be defined by the prescription.

$$|\mu| \leqslant r, \quad -\delta \leqslant \arg \mu \leqslant \delta$$

with

$$\delta = \tfrac{1}{2}\pi + \varepsilon, \quad \varepsilon > 0.$$

From Theorem 2, the path of integration in the x-plane can be deformed to the line L which is the set of points $x: x = t\,\mathrm{e}^{-i\varepsilon/2}$, $-\infty < t < \infty$. There are no singularities in the x-plane in a neighbourhood of this line.

The function $G(\mu, x)$ defined by

$$G(\mu, x) = \frac{\sinh(\pi - \mu)x \sinh(\mu - \phi_0)x}{\cosh \mu x} \tag{261}$$

which occurs in the integrand of $\Phi(\mu)$ in (232) has the following properties:

(1) For all $x \in L$, $G(\mu, x)$ is analytic in μ for $\mu \in S$. Thus the mean value theorem gives

$$G(\mu, x) = \sum_{j=0}^{n} c_j(x)\, \mu^j + g_n(x)\, \mu^{n+1} \tag{262}$$

where

$$g_n(x) \leqslant M_n \tag{263}$$

for all $x \in L$.

(2) The functions $g_n(x)$ and $c_j(x)$ are even, and

$$g_n(0) = c_j(0) = 0. \tag{264}$$

It follows that

$$\Phi(\mu) = \sum_{j=0}^{n} \mathrm{d}_j\, \mu^j + 0(\mu^{n+1}) \tag{265}$$

where

$$\mathrm{d}_j = \tfrac{1}{2} \int_{-\infty}^{\infty} \frac{c_j(x)\,\mathrm{d}x}{x \sinh \pi x}. \tag{266}$$

The d_j must grow sufficiently fast to make the radius of convergence of (265) zero. The function $\Phi(\mu)$ is C^∞ with respect to $|\mu|$ along any radial line in S at $\mu = 0$. The differential coefficients with respect to μ and η at the point $(\mu = 0, \eta = \eta_0)$ are evidently obtained by term by term differentiation of the asymptotic series.

The coefficients d_j are readily obtained by using (244). The second term of this equation may be written as

$$J_2(\mu) = \int_0^\infty \frac{dy}{y} \left[\exp\left(\frac{2\pi y}{\mu}\right) - 1\right]^{-1} \frac{\cosh(1-s)y - \cosh(1+s)y}{\cosh y}. \tag{267}$$

By using the generating function (256) and the relation (Haynsworth and Goldberg, 1964)

$$E_n(1-x) = (-1)^n E_n(x) \tag{268}$$

one obtains

$$J_2(\mu) = \int_0^\infty \frac{dy}{y} \left[\exp\left(\frac{2\pi y}{\mu}\right) - 1\right]^{-1} \sum_{n=1}^\infty \frac{1}{(2n)!} y^{2n} [E_{2n}(\tfrac{1}{2}s) - E_{2n}(-\tfrac{1}{2}s)]. \tag{269}$$

Finally, the standard integral

$$\int_0^\infty \frac{dy}{y} \left[\exp\left(\frac{2\pi y}{\mu}\right) - 1\right]^{-1} y^{2n} = 2^{2n} \frac{(-1)^{n+1}}{4n} \mu^{2n} B_{2n} \tag{270}$$

gives the result

$$J_2(\mu) = \sum_{n=1}^\infty \frac{2^{2n}}{(2n)!} [E_{2n}(-\tfrac{1}{2}s) - E_{2n}(\tfrac{1}{2}s)] B_{2n}\left[\frac{(i\mu)^{2n}}{4n}\right]. \tag{271}$$

Thus $\Phi(\mu)$ has the asymptotic expansion

$$\Phi(\mu) = \ln\left[\frac{\Gamma(1+\frac{1}{4}s)\,\Gamma(\frac{1}{2}-\frac{1}{4}s)}{\Gamma(1-\frac{1}{4}s)\,\Gamma(\frac{1}{2}+\frac{1}{4}s)}\right] + \sum_{n=1}^\infty \frac{2^{2n}}{(2n)!} [E_{2n}(-\tfrac{1}{2}s) - E_{2n}(\tfrac{1}{2}s)] \times B_{2n}\left[\frac{(i\mu)^{2n}}{4n}\right] \tag{272}$$

valid for $|\mu| < \frac{1}{2}\pi$. Evidently $\Phi(\mu)$ may be written

$$\Phi(\mu) = \Theta(\mu^2). \tag{273}$$

Using the preceding general remarks about the asymptotic series, it is clear

that $\Phi(\mu)$ belongs to the class C^∞ under differentiation with respect to μ^2 at $\mu = 0$ along any radius through $\mu = 0$ in the sector $-\delta < \arg \mu < \delta$, $\delta = \pi/2 + \varepsilon$, $\varepsilon > 0$. Further, by the implicit function theorem, μ^2 is an analytic function of Δ in a neighbourhood of $\Delta = -1$. Thus one concludes that even though $\Phi(\mu)$ is not analytic at $\mu = 0$, which corresponds to the critical point, nevertheless all temperature derivatives of $z(0)$ exist at $T = T_0$, and are continuous and bounded there. This concludes the proof of the assertion that the F type models in region II of Fig. 15 have phase transitions of infinite order. This is associated with antiferroelectric ordering in which the unpolarised vertices 5 and 6 are favoured in the low-temperature region.

(ii) $\Delta = 1$ *Transition*

In a neighbourhood of $\mu = \pi$, $\Phi(\mu)$ has the Taylor expansion (provided $\eta > 1$)

$$\Phi(\mu) = \frac{(\pi - \mu)^2}{\mu(\eta - 1)} \int_0^\infty \mathrm{d}x \operatorname{sech}\left(\frac{\pi x}{2\mu}\right)(1 + \cosh x)^{-1} + 0(\pi - \mu)^4$$

$$= \frac{(\pi - \mu)^2}{4(\eta - 1)}\left\{1 + \frac{2(\pi - \mu)}{3\pi} + 0(\pi - \mu)^2\right\}. \tag{274}$$

The function $\Phi(\mu)$ depends on β through $\mu(\Delta)$ and through η. Thus

$$\frac{\mathrm{d}\Phi}{\mathrm{d}\beta} = \left(\frac{\partial \mu}{\partial \beta}\right)_\eta \frac{\mathrm{d}\Phi}{\mathrm{d}\mu} + \frac{\partial \eta}{\partial \beta}\frac{\mathrm{d}\Phi}{\mathrm{d}\eta} \tag{275}$$

where

$$\frac{\partial \mu}{\partial \beta} = \frac{1}{\sin \mu}\frac{\mathrm{d}\Delta}{\mathrm{d}\beta}. \tag{276}$$

The last expression is evidently singular at $\mu = \pi$. Nevertheless, the internal energy U_0 at β_0 is finite whereas the specific heat diverges; in particular

$$U_0 = \left.\frac{\mathrm{d}\Delta}{\mathrm{d}\beta}\right|_{\beta_0 -} \left[\frac{1}{2(\eta_0 - 1)}\right] \equiv L \tag{277}$$

and the singular part of the specific heat is

$$C \cong \frac{k}{\pi}(\eta_0 - 1)^{1/2}\,(L/kT_0)^{3/2}\,(1 - T_0/T)^{-1/2}. \tag{278}$$

In Section IV.E it was shown that if an energy $\varepsilon_2 - \max(0, -\varepsilon_1)$ is added to each vertex, then

$$z(0) \equiv 0 \text{ for } T \leqslant T_0.$$

Thus the phase transition at $\Delta = 1$, which occurs in region I of Fig. 15, is of first order, and has a ferroelectric character, provided $\eta \neq 1$. The IF case, for which $\varepsilon_1 = 0$, $\varepsilon_2 < 0$, is special since $\eta = 1$ for all T, and (274) no longer holds. Instead, we have the Taylor expansion

$$\Phi(\mu) = \frac{\pi - \mu}{2}\left[1 + (\pi - \mu)\left(\tfrac{1}{2} - \frac{1}{\pi}\right) + 0(\pi - \mu)^2\right] \tag{279}$$

valid for $|\pi - \mu| < \pi$.

Use of (275) and (276) gives

$$U(\beta) = |\varepsilon_2| \exp(-\beta|\varepsilon_2|)\{1 + 0[\exp(-\beta|\varepsilon_2|)]\}. \tag{280}$$

Thus U and all its derivatives with respect to T along the real positive T axis vanish as $T \to 0$, even though $z(0)$ has an essential singularity in the T plane at $T = 0$ coming from the function

$$\Delta(T) = 1 - \tfrac{1}{2}\exp(-|\varepsilon_2|/kT). \tag{281}$$

C. Analytic properties of the free energy in the complex T-plane (Douglas B. Abraham, *Department of Mathematics, Massachusetts Institute of Technology, Cambridge, Massachusetts, U.S.A.*)

In the previous section it was shown that the behaviour of the free energy when $y = 0$ is related to the analytic properties of the function $\Phi(\mu)$ in the complex μ-plane. It is important to recall that $\Phi(\mu)$ also contains temperature dependence through the parameter η. Analytic structure of the free energy in the complex T-plane arises for the following reasons:

(1) Singularity of Φ in the μ and η-planes.

(2) The mapping $\Delta = -\cos\mu$. (282)

(3) The mapping (138)

$$2\Delta = \exp(\beta\varepsilon_1) + \exp(-\beta\varepsilon_1) - \exp[(2\varepsilon_2 - \varepsilon_1)\beta]. \tag{283}$$

This third mapping is elementary for KDP, IKDP, F and IF; further, it is easy to locate the singularities of $\Phi(\mu)$ in these cases. The Riemann surface may then be constructed by considering carefully the way the μ-plane maps onto the Δ Riemann surface. This mapping is shown in Fig. 21. First, the temperature Riemann surfaces will be obtained for KDP and F. This will be followed by a short discussion of the general case, which shows that KDP and F are typical of regions I and II in Fig. 15, at least in a neighbourhood of the real positive temperature axis. (Further details may be found in Abraham *et al.* (1972).)

1. *F model*

From Theorem 1 of Section V.B, it is clear that the only singularity of $\Phi(\mu)$ in the finite μ-plane is a natural boundary on the negative real μ-axis (see Fig. 22). On the Δ Riemann surface, this corresponds to a natural boundary on the segment of the real Δ axis from -1 to 1, but only for the sheets Δ_{-n}, $n = 1, 2, \ldots$. The low temperature free energy is (except for an additional term of $-K_2 + \max(0, -K_1)$) given by the mean value of $\Phi(\mu)$ across the cut on $-1 \geqslant \Delta \geqslant -\infty$.

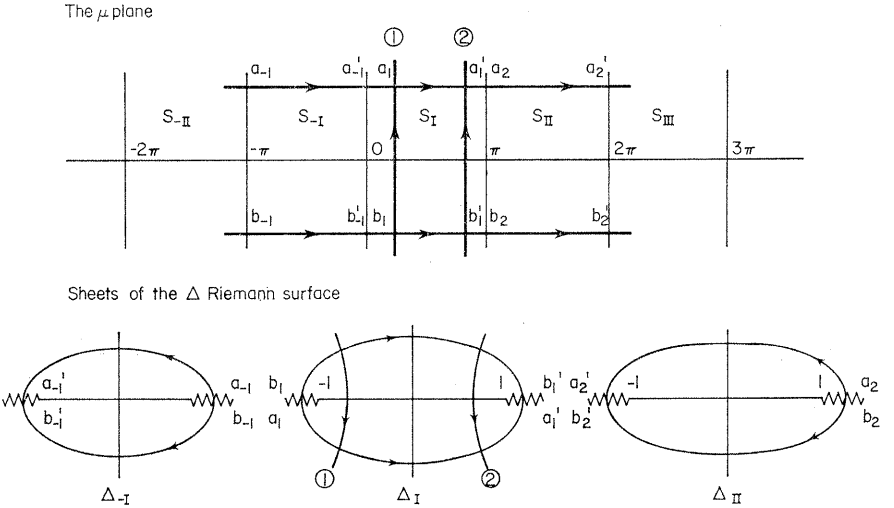

FIG. 21. The mapping $\Delta = -\cos\mu$. The loci on the Δ sheets corresponding to lines in the μ-plane are shown.

The mapping onto the β-plane is easy, since in the F case

$$\varepsilon_1 = 0 \text{ and } \varepsilon_2 \equiv \varepsilon$$

and

$$\Delta = 1 - \tfrac{1}{2}\exp(2\varepsilon\beta) \tag{284}$$

from (283). The β-Riemann surface has the same singularity structure as the Δ surface, except that the fundamental strip

$$0 \leqslant \operatorname{Im}\beta \leqslant \pi i/\varepsilon \tag{285}$$

is repeated periodically throughout each sheet. The cuts $(\pm 1, \pm\infty)$ become $(-\infty + \pi i/2\varepsilon, \infty + \pi i/2\varepsilon)$ and $(\ln 2)/\varepsilon < \beta < \infty$. The natural boundaries on Δ_{-n}, $n = 1, 2, \ldots$ map into $(-\infty, (\ln 2)/\varepsilon)$ on β_{-n}. The Riemann structure

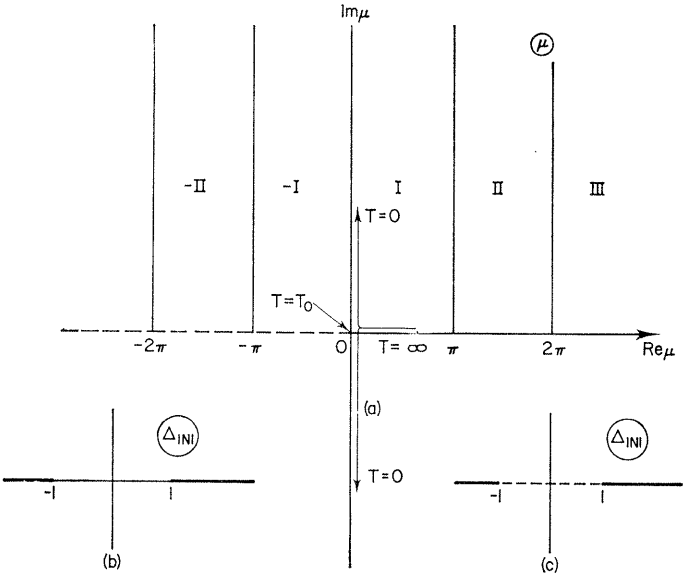

FIG. 22. (a) Analytic structure of the F model in the μ-plane. The dashed line denotes a natural boundary. Physical values of the temperature are plotted. For the low temperature region, the mean value $(\Phi(i\lambda) + \Phi(-i\lambda))/2$ should be taken. (b) and (c) show physical and unphysical sheets of the Δ Riemann surface. Again, a dotted line indicates a natural boundary.

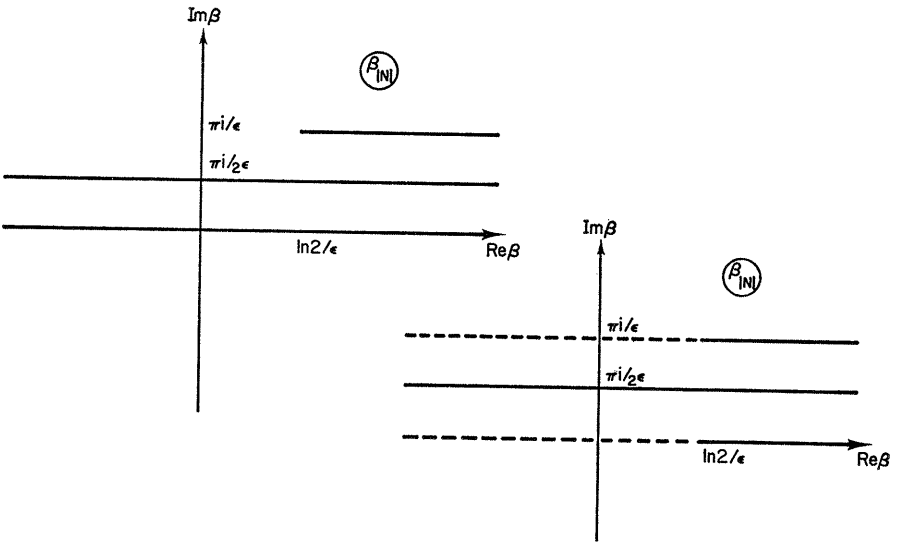

FIG. 23. The β-Riemann surface for free energy of the F model. The heavy lines denote branch cuts; the dashed lines denote natural boundaries.

in β is shown in Fig. 23. A simple invertive transformation then gives the T-structure of Fig. 24. The free energy for $T < T_0$ is evaluated by taking the mean across the cut from 0 to T_0. Thus it is perhaps slightly surprising that the phase transition at T_0 is of infinite order.

2. *KDP Case*

From (250), the high temperature behaviour for KDP is given by

$$\Phi(\mu) = \ln\left[\frac{2\mu}{\pi}\operatorname{cosec}\mu\cot\left(\frac{\pi^2}{2\mu}\right)\right]. \tag{286}$$

This function has logarithmic branch points at

$$\mu_1(n) = n\pi, \quad \mu_2(n) = \pi/n, \quad n = \pm 2, \pm 3, \ldots .$$

The plane may have cuts $\pm\pi(1/2\,|\,n\,|,\ 1/2(|\,n\,|+1))$ and cuts from $\mu = n\pi$ to ∞ parallel to the imaginary axis. The line $\mu = n\pi$ clearly corresponds to the two edges of the positive (negative) cut if n is odd (even). The small branch cuts between the points $\mu = \mu_2(n)$ map onto Δ_1 and Δ_{-1} only.

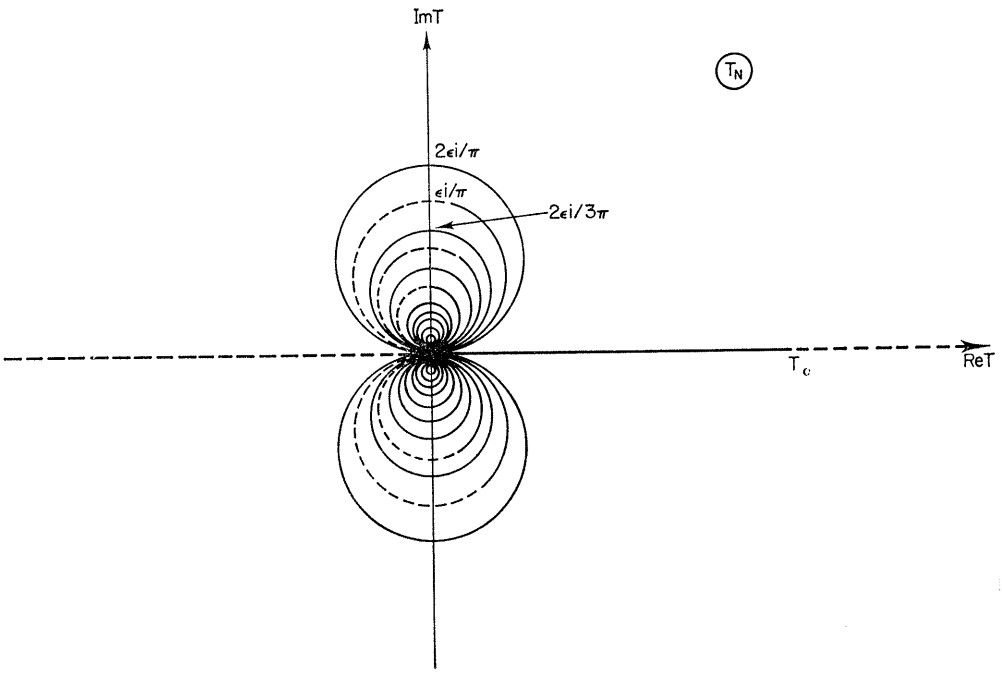

FIG. 24. The temperature Riemann structure for the free energy of the F model. The dashed lines, which denote natural boundaries, are absent for $N = I, II, \ldots$. The heavy lines are branch cuts.

The mapping onto the β-Riemann structure is given by

$$\Delta = \tfrac{1}{2}\exp(\beta\varepsilon), \quad \varepsilon_2 = 0, \quad \varepsilon_1 = \varepsilon. \tag{287}$$

which is periodic in β with period $2\pi i/\varepsilon$. The sheets β_{I} and β_{II} are shown in Fig. 25. β_{II} does not have the small branch cuts, as was shown above. The cuts $(\pm 1, \pm\infty)$ in Δ map into $((\ln 2)/\varepsilon, \infty)$ and $((i\pi + \ln 2)/\varepsilon, \infty + i\pi/\varepsilon)$. The behaviour on the principal sheet of the T-structure is indicated in Fig. 26. There is a branch cut on $(0, T_0)$. Below T_0, the KDP system is described by the different function $\Phi \equiv 0$.

3. *The General Case—F Transitions*

In region II of Fig. 15, the value $\Delta = -1$ occurs once in a suitably small neighbourhood of the real positive T-axis, and $\Delta = +1$ does not occur therein. This follows from theorem 3 of Section V.B, and the analyticity properties of $\Delta(T)$. By the same arguments as were used in the pure F case, there is a Riemann surface in T. Considering points near the real axis in the first sheet, T_{I}, there is a branch cut from 0 to T_0. The low-temperature free energy is again obtained from the mean of Φ across the cut. On $T_{-\mathrm{I}}$, there are singularities in the strip $-1 \leqslant \mathrm{Re}(\Delta) \leqslant 1$ which are not necessarily confined to the real Δ axis, but which become a natural boundary as $T \to T_0^-$.

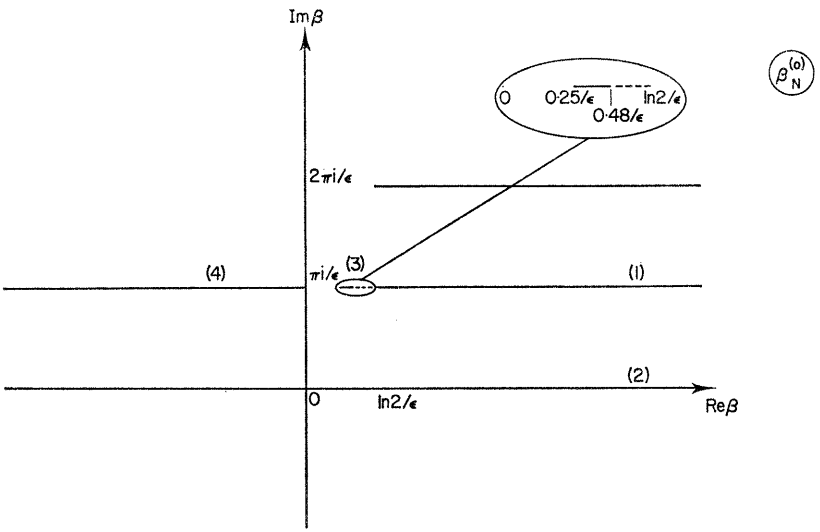

FIG. 25. Riemann structure for the high temperature behaviour of the KDP model in the inverse temperature plane. The structure is periodic with period $2\pi i/\varepsilon$. For $\beta_{\mathrm{I}}^{(0)}$, cuts (1) and (2) are of second order and (3) and (4) are of infinite order. For $\beta_{\mathrm{II}}^{(0)}$ cuts (3) and (4) are absent, but (1) and (2) are of infinite order.

4. *The General Case—KDP Transitions*

The extension of the preceding remarks on the general F model to region I of Fig. 15 is obvious. On the first sheet of the T-Riemann surface, sufficiently near the real positive T-axis, the only analytic feature will be a branch cut from 0 to T_0 which arises from the mapping $\mu \to \Delta$.

Thus one may conclude that the structure of the Riemann surface in T given by KDP and F is typical of the general behaviour (in a neighbourhood of the real positive T-axis of the first sheet).

D. Behaviour of $z(y)$ at $y \cong 1-$ and $y \cong 0+$

For a complete description of the thermodynamic properties of the ice rule models we need to know $z(y)$ for $0 \leqslant y \leqslant 1$ [*cf.* (149)]. Now $z(y)$ given by (178) depends on the solution of the integral equation (174a). Unfortunately, (174a) cannot be solved in closed form for arbitrary y, except in the zero temperature limit or when $\Delta = 0$. Nevertheless, all physically interesting information can be extracted by examining the behaviour of $z(y)$ near $y = 0$ and $y = 1$. It is our purpose in the present section to study this behaviour.

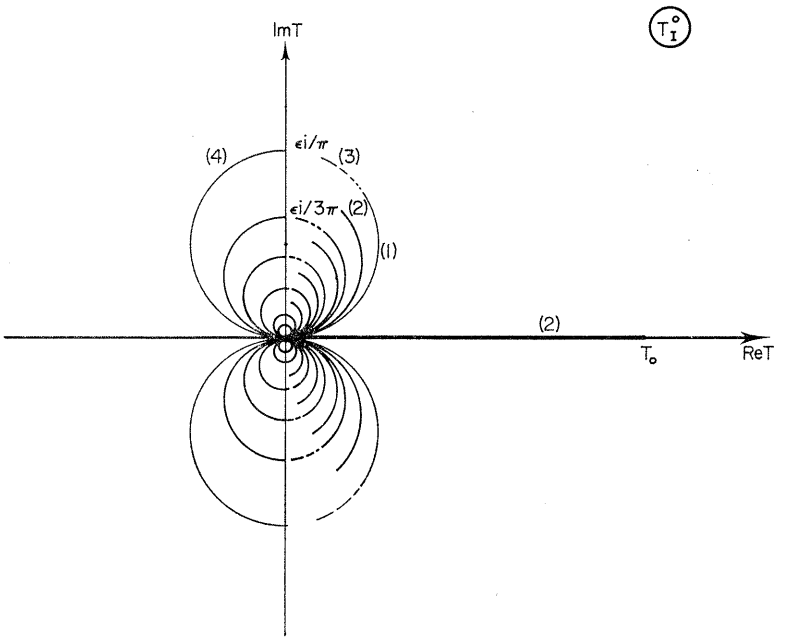

FIG. 26. Riemann structure for the high temperature free energy of the KDP model in the complex temperature plane. The numbers correspond to those in Fig. 25. The physical sheet is shown.

First, a closed expression can be obtained for $z(y)$ in the zero temperature limit. It is convenient at this point to recall the definition (94)

$$\bar{\varepsilon} \equiv \max(0, \varepsilon_1) - \varepsilon_2 = \tfrac{1}{2}(\varepsilon_1 + |\varepsilon_1|) - \varepsilon_2 \tag{288}$$

such that $\bar{\varepsilon} > 0$ (or $\bar{\varepsilon} < 0$) for an intrinsically ferroelectric (or antiferroelectric) model. One then sees from (138) that

$$\begin{aligned} \lim_{T\to 0} \Delta &= +\infty, \quad \bar{\varepsilon} > 0, \quad \varepsilon_1 \neq 0 \\ &= 1, \qquad \bar{\varepsilon} > 0, \quad \varepsilon_1 = 0 \text{ (IF model)} \\ &= -\infty, \quad \bar{\varepsilon} < 0. \end{aligned} \tag{289}$$

It is also to be noted that $\bar{\varepsilon} = 0$ implies the IKDP model (see Fig. 15) for which

$$\lim_{T\to 0} \Delta = 0, \quad \bar{\varepsilon} = 0. \tag{290}$$

For $\bar{\varepsilon} > 0$, the intrinsically ferroelectric model, we have, from (162) and (289), the result

$$\lim_{T\to 0} \beta^{-1} z(y) = -\varepsilon_2 + \max(0, -\varepsilon_1), \quad \bar{\varepsilon} > 0. \tag{291}$$

For $\bar{\varepsilon} < 0$ one can deduce from (178), (174b) and the limiting expression

$$\lim_{T\to 0} \beta^{-1} C(\alpha) = -4\bar{\varepsilon}, \tag{292}$$

that

$$\lim_{T\to 0} \beta^{-1} z(y) = -\varepsilon_1 + |y|\,\bar{\varepsilon}, \quad (\bar{\varepsilon} < 0, \varepsilon_1 \neq 0). \tag{293}$$

Thus $\beta^{-1} z(y)$ has a cusp at $y = 0$ with an initial slope $\bar{\varepsilon}$. As we shall see presently, the cusp actually exists for all $\Delta < -1$.

We now proceed to investigate generally the behaviour of $z(y)$ near $y = 1$ and $y = 0$. We shall regard $R(\alpha)$ as defined for all α in (Table II.5) (even $|\alpha| > b$) by means of the right hand side of (174a). The following formulas prove to be useful. First, by directly differentiating (178) with respect to y, we obtain

$$z'(y) = \frac{1}{4\pi}\int_{-b}^{b} \dot{R}(\alpha)\, C(\alpha)\mathrm{d}\alpha + \frac{1}{2\pi} R(b)\, C(b) \frac{\mathrm{d}b}{\mathrm{d}y}, \tag{294a}$$

$$\begin{aligned} z''(y) = \frac{1}{4\pi}\int_{-b}^{b} \ddot{R}(\alpha)\, C(\alpha)\mathrm{d}\alpha + \frac{1}{2\pi} \dot{R}(b)\, C(b) \frac{\mathrm{d}b}{\mathrm{d}y} \\ + \frac{1}{2\pi} \frac{\mathrm{d}}{\mathrm{d}y}\left[R(b)\, C(b) \frac{\mathrm{d}b}{\mathrm{d}y}\right], \end{aligned} \tag{294b}$$

etc. where we have used the fact that the functions R and C are even in α. In (294), $\dot{R}$ and $\ddot{R}$ are the partial derivatives of $R(\alpha)$ with respect to y, and are given by differentiating (174a) and (174b), namely,

$$\dot{R}(\alpha) = -\int_{-b}^{b} K(\alpha - \beta)\,\dot{R}(\beta)\mathrm{d}\beta - [K(\alpha - b) + K(\alpha + b)]\,R(b)\frac{\mathrm{d}b}{\mathrm{d}y}, \quad (295a)$$

$$-\pi = \int_{-b}^{b} \dot{R}(\alpha)\mathrm{d}\alpha + 2R(b)\frac{\mathrm{d}b}{\mathrm{d}y}, \text{ etc.} \quad (295b)$$

1. *Expansion at* $y = 1$

Since $y = 1$ implies $b = 0$ (Table II.6), (295) is simple to solve yielding at $y = 1$,

$$\begin{aligned} R(\alpha) &= \xi(\alpha) \\ \dot{R}(\alpha) &= \pi K(\alpha), \\ \ddot{R}(\alpha) &= 0, \\ \dddot{R}(\alpha) &= \pi^3 K''(\alpha)/4\xi^2(\alpha), \text{ etc.} \end{aligned} \quad (296)$$

Note that $K'(\alpha)$, $C'(\alpha)$ refer, of course, to derivatives with respect to α. Using these results and the relation $C'(0) = 0$, one obtains from (294) (assuming that the quantities below are finite)

$$\begin{aligned} z'(1) &= -\tfrac{1}{4}C(0), \\ z''(1) &= 0, \\ z'''(1) &= -\pi^2 C''(0)/16\xi^2(0), \text{ etc.} \end{aligned} \quad (297)$$

It is then easy to verify that we have, for all $\Delta < 1$ and $\varepsilon_1 \neq 0$,

$$z'(1) = -\tfrac{1}{2}\ln\left(\frac{\eta + 1 - 2\Delta}{\eta - 1}\right) < 0,$$

$$z'''(1) = \frac{\pi^2(\eta^2 + 1 - 2\eta\Delta)(\eta - \Delta)}{4(\eta^2 + 1 - 2\Delta)^2\,(\eta - 1)^2} > 0. \quad (298)$$

Furthermore,

$$b = [-\pi/2\xi\,(0)]\,y + 0(y^2). \quad (299)$$

The expansion of $z(y)$ at $y = 1$ now reads

$$z(y) = -K_2 + \max\,(0, -K_1) + z'(1)(y - 1) + \tfrac{1}{6}z'''(1)(y - 1)^3 + 0(y - 1)^4. \quad (300)$$

We note that the slope of $z(y)$ at $y = 1$ is negative finite for $\varepsilon_1 \neq 0$.

For the pure F (and IF) model ($\varepsilon_1 = 0$), (297, 298, 299) are nonsense since $C(0)$ is infinite. To get an asymptotic expansion we have to treat the integral of $C(\alpha)$ more carefully. For small b

$$\frac{1}{4\pi}\int_{-b}^{b} R(\alpha)\, C(\alpha)\mathrm{d}\alpha \approx R(0)\frac{b}{\pi}\left\{1 + \ln\frac{2}{b} + \tfrac{1}{2}\ln|1 - \Delta^2|\right\}. \tag{301}$$

Using (Table II.9) and (299) we obtain finally

$$z(y) = -K_2 + \frac{1-y}{2}\left\{1 + \ln\frac{4(1-\Delta)}{\pi(1-y)}\right\} + o(1-y). \tag{302}$$

Thus, $z(y)$ for the pure F model, and for this model only, has an infinite slope at $y = 1$. This infinite slope is exhibited in Fig. 29 below.

The function $z(y)$ near $y = 1$ is miraculously analytic in Δ for $\Delta < 1$ despite what one might have thought from the different routes leading to (300) and (302). This is consistent with the theorem quoted at the end of Section V.A.

Remark: One other case for which $z(y)$ has infinite slope at $|y| = 1$ is that of infinite temperature. This can be seen from (298) by noting that $\Delta \to \frac{1}{2}$ and $\eta \to 1$.

2. *Expansion at* $y = 0$

(i) $\Delta < -1$

When $y = 0$ and $\Delta < -1$, we have $b = \pi$ (Table II.7) and both $\xi(\alpha)$ and $K(\alpha)$ are 2π-periodic. Therefore (295) can be solved by Fourier series. One finds after some manipulation.

$$z'(0) = -\tfrac{1}{4}(1 + \hat{K}_0)C(\pi) + \frac{1}{8\pi}(1 + \hat{K}_0)\sum_{n=-\infty}^{\infty}\frac{(-1)^n\hat{C}_n}{1 + \hat{K}_n^{-1}},$$

$$z''(0) = 0,$$

$$z'''(0) = -\frac{\pi^2(1 + \hat{K}_0)^3}{16R_0^2(\pi)}\left[C''(\pi) + \sum_{n=-\infty}^{\infty}\frac{(-1)^n n^2\hat{C}_n}{2\pi(1 + \hat{K}_n^{-1})}\right], \tag{303}$$

etc.

$$z(y) - z(0) = z'(0)y + \tfrac{1}{6}z'''(0)y^3 + 0(y^4) \tag{304}$$

where $\hat{K}_n$ and $\hat{C}_n$ are the Fourier coefficients of $K(\alpha)$ and $C(\alpha)$ given in (Table II. 13, 17),

$$R_0(\pi) = \tfrac{1}{2}\sum_{n=-\infty}^{\infty}(-1)^n \operatorname{sech} n\lambda, \qquad \text{(Table II.15)}$$

and we have explicitly used the result $C'(\pi) = 0$. Also,

$$\pi - b = [\pi/R_0(\pi)]y + 0(y^2). \tag{305}$$

The initial slope of $z(y)$ at $y = 0$ is seen to be non-zero and is given by

$$z'(0) = -\Xi(\lambda - \theta_0), \tag{306}$$

where

$$\Xi(\phi) \equiv \ln \frac{\cosh \frac{1}{2}(\lambda + \phi)}{\cosh \frac{1}{2}(\lambda - \phi)} - \tfrac{1}{2}\phi - \sum_{n=1}^{\infty} \frac{(-1)^n \mathrm{e}^{-2n\lambda} \sinh n\phi}{n \cosh n\lambda}, \quad |\phi| < 3\lambda. \tag{307a}$$

An alternate expression of $\Xi(\phi)$ is (Sutherland, *et al.* 1967)

$$\Xi(\phi) = \tfrac{1}{2}\phi + \sum_{n=1}^{\infty} \frac{(-1)^n \sinh n\phi}{n \cosh n\lambda}, |\phi| < \lambda \text{ only.} \tag{307b}$$

The identity of (307a, b) can be established by introducing the relation

$$\ln (2 \cosh x) = x - \sum_{n=1}^{\infty} \frac{(-1)^n}{n} \mathrm{e}^{-2nx}, \quad x > 0.$$

The expression (307a) converges faster and in a larger domain, however, and is more suitable for numerical computations.

It can also be shown that the Ξ function is related to the Jacobian elliptic function nd:

$$\Xi(\phi) = \cosh^{-1}\left[\mathrm{nd}\left(\frac{1}{\pi}\mathbf{K}\phi \,\middle|\, 1 - m\right)\right], \tag{307c}$$

where the nome $q = \mathrm{e}^{-\lambda}$ of nd is related to the parameter $1 - m$ through (183, 184a, b). The expression (307c) can be obtained by combining (16.23.6) with (16.24.6) of Milne-Thomson (1964) and introducing some elementary identities between the elliptic functions. The function $\mathrm{nd}[(1/\pi)\,\mathbf{K}\phi \mid 1 - m]$, as a function of ϕ, has periods 2λ and $4\pi i$ with poles at $\lambda + \pi i$ and $\lambda + 3\pi i$ in the fundamental rectangle. The zeros are at πi and $3\pi i$, but more importantly for small ϕ the function behaves as $1 + \frac{1}{2}(1 - m)(\mathbf{K}\phi/\pi)^2$. Since $\cosh^{-1}(x)$ has a square root branch point at $x = 1$, $\Xi(\phi)$ is analytic at $\phi = 0$ but is odd in ϕ. Using this and other elementary properties of the nd function it can be shown that

$$\Xi(\phi) = -\Xi(-\phi); \quad \Xi(\lambda - \phi) = \Xi(\lambda + \phi); \quad \Xi(\phi + 4\lambda) = \Xi(\phi).$$

Combining (306) and (307c), we find

$$z'(0) = -\cosh^{-1}[\mathrm{nd}\,(u \mid 1 - m)] < 0, \tag{308a}$$

where

$$u \equiv \frac{1}{\pi}\mathbf{K}(\lambda - \theta_0) = \mathbf{K}'\left(1 - \frac{\theta_0}{\lambda}\right) < \mathbf{K}'.$$

Similarly we find from (303), (182) and (307c) that

$$z'''(0) = \left[\frac{\pi}{R_0(\pi)}\right]^2 \Xi''(\lambda - \theta_0)$$

$$= -\pi^2 m(1-m)^{-\frac{1}{2}} \operatorname{nd}^2(u \mid 1-m) \operatorname{sn}(u \mid 1-m) < 0. \tag{308b}$$

The last inequality follows from the fact that $\operatorname{sn}(u \mid 1-m) > 0$ for $u < 2\mathbf{K}'$.

For the F model ($\varepsilon_1 = 0$) we have $\theta_0 = 0, u = \mathbf{K}'$. Hence, explicitly,

$$z'(0) = -\cosh^{-1}(m^{-\frac{1}{2}}), \tag{308c}$$

$$z'''(0) = -\pi^2(1-m)^{-\frac{1}{2}}, \text{ F model.} \tag{308d}$$

We shall need these formulas in Section V.E.

Since $\Delta \leqslant -1$ only for $\bar{\varepsilon} < 0$ and low temperature, we conclude that the intrinsically antiferroelectric model is characterized by the appearance of a cusp in $z(y)$ at $y = 0$ for $\Delta < -1$. It is easy to verify from (306) that the cusp disappears, i.e., $z'(0) \to 0$, as $\Delta \to -1$. In fact, as we shall see from (321), $z'(0)$ vanishes identically for $\Delta = -1$. These situations are exhibited in Figs. 28 and 29 below.

(ii) $-1 < \Delta < 1$

When $y = 0$ and $-1 < \Delta < 1$, we have $b = \infty$ (Table II.7). We must undertake a perturbative study of the integral equation (174a). Since our discussions follow closely that of Yang and Yang (1966b), we shall only point out the differences and use their results without repeating the detailed analysis.

The physical quantity of interest in the case of the Heisenberg chain (Yang and Yang, 1966b) is the ground state energy

$$f(y) = -\frac{\Delta}{4} - \frac{\sin\mu}{2\pi}\int_{-b}^{b} \xi(\alpha) R(\alpha) \mathrm{d}\alpha, \quad -1 < \Delta < 1 \tag{309}$$

which can also be written (see (24c) of Yang and Yang, 1966b) as

$$f(y) - f(0) = \int_{-\infty}^{\infty} \frac{\sin\mu}{2\pi} R_0(\alpha) B(\alpha) R(\alpha) \mathrm{d}\alpha \tag{310}$$

and

$$B(\alpha) = 1 \quad |\alpha| > b \tag{311}$$

$$= 0 \quad |\alpha| < b.$$

For our case, we can derive an analogous formula which is outlined schematically as follows:

$$R = \xi - K(1 - B)R \Leftrightarrow R = (1 + K)^{-1}\xi + K(1 + K)^{-1}BR \Leftrightarrow$$

$$R = R_0 + BR - (1 + K)^{-1}BR. \tag{312}$$

$$z(y) - z(0) = \frac{1}{4\pi}\int C[(1 - B)R - R_0] = -\frac{1}{4\pi}\int C(1 + K)^{-1}BR$$

$$= \int_{-\infty}^{\infty} D(\alpha)B(\alpha)R(\alpha)\mathrm{d}\alpha, \tag{313}$$

where

$$D(\alpha) = -\frac{1}{8\pi^2}\int_{-\infty}^{\infty}\frac{\hat{C}(\gamma)}{1 + \hat{K}(\gamma)}\,\mathrm{e}^{i\alpha\gamma}\,\mathrm{d}\alpha$$

$$= -\frac{1}{2\pi}\int_0^{\infty}\cos(\alpha\gamma)\sinh[(\mu - \phi_0)\gamma]\,\mathrm{sech}(\mu\gamma)\frac{\mathrm{d}\gamma}{\gamma}$$

$$= -\frac{1}{4\pi}\ln\left[\frac{\cosh(\pi\alpha/2\mu) + \cos(\pi\phi_0/2\mu)}{\cosh(\pi\alpha/2\mu) - \cos(\pi\phi_0/2\mu)}\right]$$

$$= -\pi^{-1}\cos(\pi\phi_0/2\mu)[\mathrm{e}^{-\pi\alpha/2\mu} + O(\mathrm{e}^{-3\pi\alpha/2\mu})]. \tag{314}$$

The integral in (314) can be found in Gradshteyn and Ryzhik (1965, p. 513) and the asymptotic expansion is obvious. The analogous formula pertinent to (310) is

$$\frac{\sin\mu}{2\pi}R_0(\alpha) = \frac{\sin\mu}{2\mu}[\mathrm{e}^{-\pi\alpha/2\mu} + O(\mathrm{e}^{-3\pi\alpha/2\mu})]. \tag{315}$$

Since the dependence of $R(\alpha)$ and b on y is independent of the model, we can compare (315) and (310) with (314) and (313) to obtain the leading order in the expansion of $z(y)$:

$$z(y) - z(0) \cong [-2\mu\cos(\pi\phi_0/2\mu)/\pi\sin\mu][f(y) - f(0)]$$

or

$$z(y) - z(0) = \frac{\mu - \pi}{4}\cos(\pi\phi_0/2\mu)y^2 + o(y^2). \tag{316}$$

The latter formula is taken from Yang and Yang (1966b) and is based on a

complicated solution of a Wiener–Hopf equation which we shall not reproduce here.* Another formula of interest is the dependence of b on y:

$$\exp(-\pi b/2\mu) = (\text{constant})y + o(y), \tag{317}$$

where "constant" depends on μ but not on y. This completes the derivation of the expansion of $z(y)$ near $y = 0$ for $-1 < \Delta < 1$. We note, in particular, that the slope of $z(y)$ at $y = 0$ is zero. This fact is exhibited in Figs. 27–29 below.

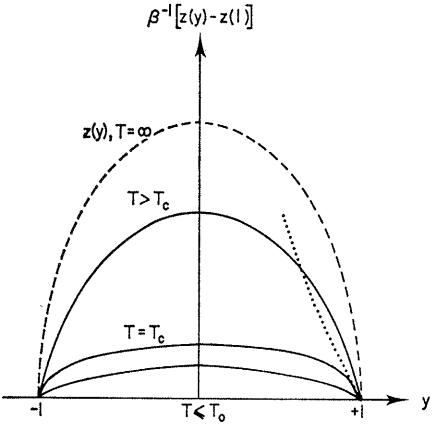

FIG. 27. Schematic plot of $\beta^{-1}z(y)$ for the intrinsically ferroelectric model with $\bar{\varepsilon} > 0$. The dotted curve is the locus of all points with a given slope and the dashed curve denotes $z(y)$ at $T = \infty$.

(iii) $\Delta = -1$

When $y = 0$ and $\Delta = -1$, we again have $b = \infty$ (Table II.7) and it is again necessary to perform a perturbative study of the integral equation. The discussion is similar to that of the case $-1 < \Delta < 1$. Here we give only the key formulae.

In the case of the Heisenberg chain the factor $(2\pi)^{-1}\sin\mu$ is replaced by $(4\pi)^{-1}$ and we have

$$\frac{1}{4\pi}R_0(\alpha) = \tfrac{1}{2}[e^{-\pi\alpha} + O(e^{-3\pi\alpha})]. \tag{318}$$

Yang and Yang (1966b) give the result

$$f(y) - f(0) = \frac{\pi^2}{8}y^2[1 + O(y^2/\ln y)]. \tag{319}$$

* Eqn (16) of Lieb, 1967d is wrong by a factor of 2.

For the ferroelectrics $(4\pi)^{-1} R_0(\alpha)$ is replaced by (compare with (314))

$$D(\alpha) = -\frac{1}{4\pi}\int_{-\infty}^{\infty} \frac{\sinh\gamma(\frac{1}{2}-\alpha_0)}{\gamma\cosh\frac{1}{2}\gamma} e^{i\alpha\gamma} d\gamma$$

$$= -\frac{1}{4\pi}\ln\left[\frac{\cosh\alpha\pi + \cos(\alpha_0\pi)}{\cosh\alpha\pi - \cos(\alpha_0\pi)}\right]$$

$$= -\frac{1}{\pi}\cos(\alpha_0\pi)\,[e^{-\pi\alpha} + O(e^{-3\pi\alpha})]. \tag{320}$$

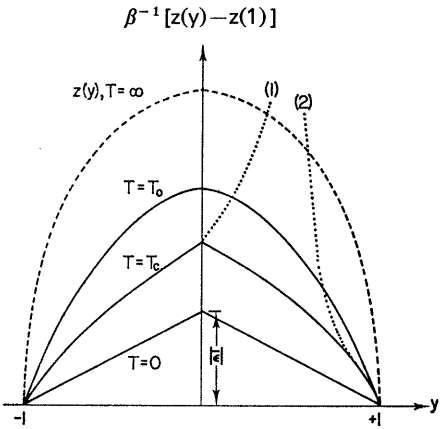

FIG. 28. Schematic plot of $\beta^{-1}z(y)$ for the intrinsically antiferroelectric model with $\bar{\varepsilon} < 0$ but $\varepsilon_1 \neq 0$. The slope of $z(y)$ at $y = +1$ is finite at all temperatures. The dotted curves (1) and (2) are, respectively, the loci of all points with some fixed slope whose magnitude is smaller and greater than $|\bar{\varepsilon}|$. The dashed curve denotes $z(y)$ at $T = \infty$.

It follows then that

$$z(y) - z(0) = -\frac{\pi}{4}\cos(\alpha_0\pi)y^2\,[1 + 0(y^2/\ln y)], \quad \Delta = -1. \tag{321}$$

It is easily seen from the result

$$\left.\frac{d\phi_0}{d\mu}\right|_{\mu=\phi_0=0} = 2\alpha_0 \tag{322}$$

that the coefficient of y^2 in (321) agrees with that in (316) by taking the limit $\Delta \downarrow -1$.

The dependence of b on y is

$$\exp(-\pi b) = (\text{constant})y + O\left(\frac{y}{\ln y}\right). \tag{323}$$

Summary

Using the above results and the fact that $z(-y) = z(y)$ when $H = 0$, we can now plot $\beta^{-1} z(y)$ schematically for various temperatures. This is shown in Figs. 27–29. One obvious difficulty is that $\beta^{-1} z(y) = 0$ when $T = \infty$ for all $y \neq \pm 1$. However, $z(y)$ is perfectly finite in that case so we have adopted the somewhat unusual expedient of plotting $z(y)$ itself in these figures when $T = \infty$. These are the dashed curves labelled $T = \infty$. The dotted curves in these figures will play a role in the next section.

For $T = \infty$, $z(0) = \frac{3}{2} \ln (\frac{4}{3})$ and the slope of $z(y)$ is infinite at $|y| = 1$. Also, $z(\pm 1) = 0$.

For $T = 0$, $\beta^{-1} z(y)$ is piecewise linear as given in (291) and (293).

In general $z(y)$ is concave in y and

$$\beta^{-1} z(\pm 1) = -\varepsilon_2 + \max(0, -\varepsilon_1), \quad \text{all } T \tag{324}$$

since $b = 0$ when $y = 1$. In our graphs we plot $\beta^{-1}[z(y) - z(1)]$.

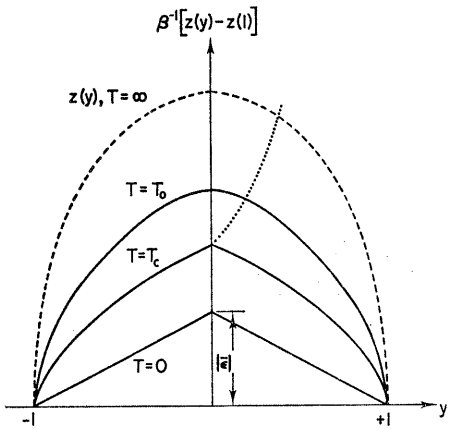

FIG. 29. Schematic plot of $\beta^{-1} z(y)$ for the intrinsically antiferroelectric model with $\bar{\varepsilon} < 0$ and $\varepsilon_1 = 0$. The slope of $z(y)$ is infinite at $y = \pm 1$ at all non-zero temperatures. The dotted curve is the locus of all points with fixed slope whose magnitude is smaller than $|\bar{\varepsilon}|$. The dashed curve denotes $z(y)$ at $T = \infty$.

There are five cases:

(a) $\bar{\varepsilon} = \max(0, \varepsilon_1) - \varepsilon_2 > 0$, $\varepsilon_1 \neq 0$ (Fig. 27)

This is the intrinsically ferroelectric case with positive Δ and $\lim_{T \to 0} \Delta = \infty$. Therefore for $T \leqslant T_0$, corresponding to $\Delta \geqslant 1$, $\beta^{-1}[z(y) - z(1)]$ remains zero for all y. For $T > T_0$, $z(0)$ is given by (187a) and $\beta^{-1}[z(y) - z(1)] = 0(y^2)$. The slope at $|y| = 1$ is finite.

(b) $\bar{\varepsilon} < 0$, $\varepsilon_1 \neq 0$ (Fig. 28)

This is the intrinsically antiferroelectric case with $\Delta < \frac{1}{2}$ and $\lim_{T \to 0} \Delta = -\infty$. Therefore for $T \geqslant T_0$ corresponding to $\Delta \geqslant -1$, $z(y)$ has the same behaviour as in the region $T > T_0$ in (a). However, for $T < T_0$ ($\Delta < -1$) a cusp appears at $y = 0$ with $\beta^{-1} z(y)$ eventually becoming a straight line with slope $\bar{\varepsilon}$ at $T = 0 (\Delta = -\infty)$.

(c) $\bar{\varepsilon} < 0$, $\varepsilon_1 = 0$ (F model, Fig. 29)

This is the antiferroelectric F model. The behaviour of $z(y)$ is the same as in the intrinsically antiferroelectric case with the exception that $z'(1) = -\infty$ for all temperatures. However, $\beta^{-1} [z(y) - z(1)]$ does tend to a straight line at $T = 0$.

(d) $\bar{\varepsilon} > 0$, $\varepsilon_1 = 0$ (IF model)

For small y, $z(y)$ is similar to case (a) except that $T_0 = 0$ because $\frac{1}{2} < \Delta < 1$ for all T. For $|y|$ near 1, $z(y)$ has an infinite slope as in case (c).

(e) $\bar{\varepsilon} = 0$ (IKDP model)

Again $T_0 = 0$ since $0 < \Delta < \frac{1}{2}$ and, for all y, $z(y)$ is as in case (a) for all $T > T_0 = 0$.

E. Thermodynamic properties when $h = 0$ and $v \neq 0$

We are now ready to discuss the thermodynamic properties of the general ice-rule models in the presence of an external field. In this section we shall consider a vertical field only. By restricting the external field to a single component, we are able to make simple comparisons with the properties of the Ising model. The general features of the thermodynamic behaviour of our model is presumably unchanged when a horizontal field is also present. Some results pertaining to this general situation will be given in Section V.F.

Referring to (149), we see that the free energy $\mathscr{F}$, which yields the thermodynamic properties of the system, depends on the optimum choice of y obtained by solving

$$z'(y) = -V = -\beta v. \tag{325}$$

Bearing in mind that $z(y)$ is symmetric and concave, we need only consider $V \geqslant 0$. On the basis of the theorem quoted in Section V.A, a phase transition can occur only when the optimum choice happens to be $y = 0$ or $y = \pm 1$. The behaviour of the model near the transition temperature then follows from the behaviour of $z(y)$ near $y = 0$ and $y = \pm 1$. It is therefore convenient to discuss the cases (a)–(e) of the last section corresponding to Figs. 27–29 separately.

(a) $\bar{\varepsilon} = \max(0, \varepsilon_1) - \varepsilon_2 > 0, \varepsilon_1 \neq 0$ (Fig. 27)

We saw from Fig. 27 that in this case the slope of $z(y)$ is zero at $y = 0$ and non-zero at $y = \pm 1$ for $T > T_0$, where T_0 is the temperature corresponding to $\Delta = 1$. Therefore in zero field ($v = 0$) the optimum choice is always $y = 0$ and $\mathscr{F} = -\beta^{-1} z(0)$. With a positive vertical field, v, the optimum choice for y are located on the dotted curve which is the locus of all points having slope $= -v$ in Fig. 27. As the temperature decreases from infinity, we come down along the dotted line and reach perfect polarization $y = 1$ at some temperature $T_c(v) > T_0$ such that

$$z'(1) = -V, \quad T = T_c(v). \tag{326}$$

When $y = 1$, $\mathscr{F} = -\varepsilon_2 + \max(0, -\varepsilon_1) - v$. If $T < T_c(v)$ then y continues to "stick" at 1 because $-kTz'(1)$ decreases as T decreases. This can be proved for all T and all choices of ε_1 and ε_2 by differentiating (298). Therefore $T_c(v)$ is the transition temperature for a ferroelectric ($y = 1$) transition. Upon using (298), the critical condition (326) can be rewritten as

$$2\Delta = e^{2V}(1 - \eta) + (1 + \eta), \quad T = T_c(v). \tag{327}$$

One sees explicitly from (327) that the transition temperature $T_c(v)$ increases as v increases. This is in contrast to the ferromagnetic Ising model where a non-zero external field removes the phase transition. Our result that $T_c(v)$ increases with v is, however, in agreement with the experimental finding (Reese, 1969) that the transition of KH_2PO_4 (KDP) is indeed shifted to higher temperatures under an external field. The linear shift in T_c for small v, as can be seen from (327), also agrees with the experimental indications (Reese, 1969). We plot in Fig. 30 the phase diagram for the KDP model ($\varepsilon_2 = 0$, $\varepsilon_1 > 0$). The $y = \pm 1$ phases are bounded by the curves defined by

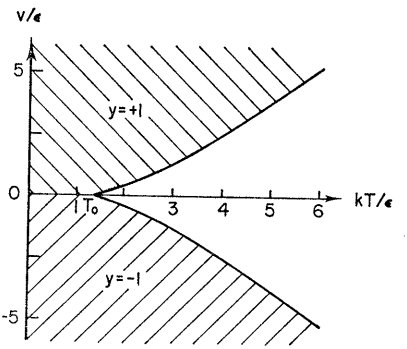

FIG. 30. Phase diagram for the KDP model ($\varepsilon_1 = \varepsilon, \varepsilon_2 = 0$) with a vertical field v. The phase boundaries meet at $T = T_0 = \varepsilon/(k\ln 2)$.

(327). The initial slopes of the boundary for small v is

$$dv/dT_c = \pm k \ln 2 \quad \text{at } v = 0.$$

(b) $\bar{\varepsilon} = \max(0, \varepsilon_1) - \varepsilon_2 < 0$, $\varepsilon_1 \neq 0$

We saw from Fig. 28 that for $\bar{\varepsilon} < 0$ and $\varepsilon_1 \neq 0$ $z(y)$ has zero slope at $y = 0$ for $T \geqslant T_0$, and has a finite, but non-zero derivative at $y = 0$ for $T < T_0$, where T_0 is the temperature corresponding to $\Delta = -1$. $\beta^{-1} z'(0)$ becomes more negative as T decreases from T_0 and reaches a finite value $\bar{\varepsilon}$ (*cf.* (293)) at zero temperature. (The above assertion is undoubtedly true, but we have not done the analysis. We leave this as an unsolved problem for the reader.)

On the other hand the slope of $z(y)$ at $y = 1$ is always finite and decreases in magnitude as the temperature decreases until $\beta^{-1} z'(1) = \bar{\varepsilon}$ at $T = 0$ (*cf.* remark following (326)). Therefore, to find the optimum choice of y we proceed, with $v = 0$, along the y-axis and obtain, as before, $\mathscr{F} = -\beta^{-1} z(0)$. But with $v \neq 0$ we proceed in Fig. 28 along the dotted curves which are the loci of all points with a given fixed slope. Curve (1) is the locus of all points with a fixed slope greater than $\bar{\varepsilon}$, whereas curve (2) represents the locus of all points having a fixed slope less than $\bar{\varepsilon}$ in Fig. 28. For $0 \leqslant v \leqslant -\bar{\varepsilon}$, we come down along the dotted curve (1) as the temperature decreases from $T = \infty$ and eventually reach the cusp at a temperature $T_c(v)$ whose initial slope is precisely $-v$. Further lowering of the temperature reduces the slope and y "sticks" at zero. We have an antiferroelectric phase transition occuring at $T_c(v)$ defined by $\beta^{-1} z'(0) = -v$, or, using (306),

$$V = \Xi(\lambda - \theta_0), \quad v \leqslant -\bar{\varepsilon}, \quad T = T_c(v). \tag{328}$$

Clearly $T_c(v)$ decreases from the zero field value, T_0, as v increases from zero, and reaches absolute zero when v reaches the "critical" value $|\bar{\varepsilon}|$. This is similar to the corresponding situation expected for an antiferromagnet, as seen from the exact solution of a super-exchange antiferromagnetic Ising model (Fisher, 1960). We plot in Fig. 31 the phase diagram of a particular intrinsically antiferroelectric model with $\varepsilon_2 = 2\varepsilon_1 \equiv 2\varepsilon > 0$. The antiferroelectric $y = 0$ phase is bounded by the curves (328).

For $v > -\bar{\varepsilon}$, however, the optimum choice can never be $y = 0$. Instead, we come down along the dotted curve (2) in Fig. 28 until we reach the point $y = 1$ at a temperature $T_c(v)$ again defined by (326, 327). Further lowering of the temperature has no effect on the optimum value of y and we thus have a *ferroelectric* transition.

Summarizing the above results for the intrinsically antiferroelectric model, we see that a non-zero external field has the effect of reducing the transition

temperature until the antiferroelectric transition disappears ($T_c(v) = 0$) at $v = -\bar{\varepsilon}$. Further increase of the field changes the nature of the transition so that a ferroelectric transition begins to appear at a gradually rising $T_c(v)$, which can be made arbitrarily large, and the model is now ferroelectric. This is a unique feature of the antiferroelectric model, not shared by the antiferromagnet, but is what we expect from energetic considerations. Using the vertex energies (93), one easily sees that (for $h = 0$) $v > -\bar{\varepsilon}$ implies either e_1 or e_4 is favoured and we then have a ferroelectric ground state. These $y = \pm 1$ phases are also shown in Fig. 31 by the cross-hatched areas with boundaries given by (327).

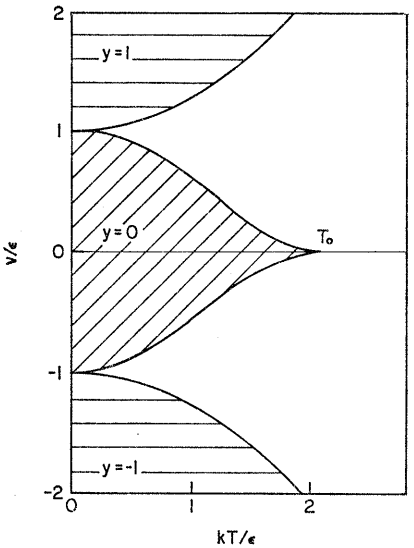

FIG. 31. Phase diagram for the intrinsically antiferroelectric model $\varepsilon_2 = 2\varepsilon_1 \equiv 2\varepsilon > 0$ with a vertical field v. The transition temperature at $v = 0$ is

$$T_0 = \varepsilon\left[k\ln\left(\frac{\sqrt{5}+1}{2}\right)\right]^{-1}.$$

It is interesting to investigate the behaviour of the phase boundaries near $T = 0$ and $T = T_0$. Plainly the slope of the boundaries vanishes exponentially at $T = 0$. In fact we find for the ferroelectric phase boundary (327)

$$v = |\bar{\varepsilon}| + \frac{kT}{2}\exp(-\beta|\varepsilon_1|), \quad T \cong 0+, \tag{329}$$

and for the antiferroelectric phase boundary (328)

$$v = |\bar{\varepsilon}| - kT\exp(-\beta|\varepsilon_1|), \quad T \cong 0+. \tag{330}$$

At T_0- the behaviour of (328) is more subtle and requires careful analysis. It is now convenient to use the expression (307c) for Ξ. Near T_0 we have $\lambda \to 0$ hence, from (176), $\lambda - \theta_0 \to [2/(\eta + 1)\lambda]$. Furthermore, in (307c) $\lambda \to 0$ implies $m \to 1$, $\mathbf{K}' \to \pi/2$ and $\mathbf{K} \to \pi^2/2\lambda$. We thus have

$$V = \cosh^{-1}\left[\mathrm{nd}\left(\frac{\pi}{\eta + 1}\,\middle|\, 1 - m\right)\right], \quad T \cong T_0-. \tag{331}$$

Now for $m \cong 1$ we have from eqns (16.3.3) and (16.13.3) of Milne-Thomson (1964)

$$\mathrm{nd}(u \mid 1 - m) \cong 1 + \tfrac{1}{2}(1 - m)\sin^2 u, \quad m \cong 1.$$

It follows then that

$$V \cong (1 - m)^{\frac{1}{2}} \sin\left(\frac{\pi}{\eta + 1}\right), \quad T \cong T_0-, \tag{332}$$

since

$$\frac{\pi^2}{2\lambda} \cong \mathbf{K} \cong \tfrac{1}{2}\ln\frac{16}{1 - m},$$

where the last expression is taken from eqn (17.3.26) of Milne-Thomson (1964). We finally obtain

$$\begin{aligned} v &\cong 4kT \sin\left(\frac{\pi}{\eta + 1}\right) \mathrm{e}^{-\pi^2/2\lambda} \\ &\propto \exp\left[-(\text{constant})(T_0 - T)^{-1/2}\right], \quad T \cong T_0-, \end{aligned} \tag{333}$$

which also vanishes exponentially.

(c) $\bar{\varepsilon} = -\varepsilon_2 < 0$, $\varepsilon_1 = 0$ (F model)

This model is characterized by the fact that $z(y)$ has an infinite slope at $y = \pm 1$ at all temperatures, while the behaviour of $z(y)$ for small y is the same as in case (b). Therefore, as the field v increases from zero, the transition temperature decreases the same as in case (b) and reaches $T_c = 0$ when $v = -\bar{\varepsilon}$. However, since the $y = 1$ transition never occurs, the transition temperature remains zero for all $v > -\bar{\varepsilon}$ and the complete ferroelectric polarization never appears. Thus the phase diagram which we plot in Fig. 32 looks much like that of an antiferromagnet in a direct magnet field. We can also understand from an energetic consideration why the $y = \pm 1$ polarized phases never occur for the F model *in the absenceof a horizontal field.* For in this case vertices of types (1) and (4) have equal energy, and are both favoured when $v > -\bar{\varepsilon}$. Since the ground state composed of vertices of types (1) and (4) is highly degenerate, a phase transition never materializes.

The phase boundaries in Fig. 32 is given by

$$V = \Xi(\lambda), \quad v \leqslant -\bar{\varepsilon}. \tag{334}$$

Unlike case (b), these boundaries have finite slope at small T. Using (307b), we can compute this slope:

$$v = kT\left[\tfrac{1}{2}\lambda + \sum_{n=1}^{\infty} \frac{(-1)^n}{n} \tanh n\lambda\right] \tag{335}$$

$$k^{-1}\left.\frac{\mathrm{d}v}{\mathrm{d}T}\right|_{T=0} = \sum_{n=1}^{\infty} \frac{(-1)^n}{n} = -\ln 2.$$

The behaviour at T_0- is the same as (333) with $\eta = 1$.

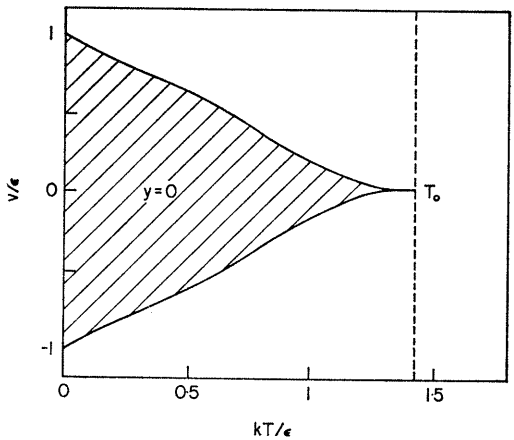

FIG. 32. Phase diagram for the F model $\varepsilon_1 = 0$, $\varepsilon_2 = \varepsilon$ with a vertical field v. The transition temperature at $v = 0$ is $T_0 = \varepsilon/k\ln 2$.

(d) $\bar{\varepsilon} = \max(0, \varepsilon_1) - \varepsilon_2 > 0$, $\varepsilon_1 = 0$ (IF model)

No transition of any kind occurs when $h = 0$ because $\Delta < 1$ always, whereas the slope of $z(y)$ is infinite at $|y| = 1$. Consequently there is no "sticking" at $|y| = 1$ and there are no singularities at $y = 0$. This is the inverted F model.

(e) $\bar{\varepsilon} = 0$ (IKDP model)

A phase transition can occur only with a non-zero field and is of the $|y| = 1$ type as given by (327). The phase diagram is similar to Fig. 30, but with $T_0 = 0$.

Summarizing the above results, we see that there are essentially two kinds of phase transitions in the presence of a vertical field. The $y = 1$, or the ferroelectric transition, occurs for $\bar{\varepsilon} > 0$ and $\varepsilon_1 \neq 0$ and for $\bar{\varepsilon} < 0$, $\varepsilon_1 \neq 0$ with $v > -\bar{\varepsilon}$. In this case the system "sticks" at $y = 1$ (complete polarization) for $T < T_c$. On the other hand the $y = 0$, or the antiferroelectric transition, occurs for $\bar{\varepsilon} < 0$ and $v < -\bar{\varepsilon}$, and the system "sticks" at $y = 0$ (zero polarization) for $T < T_c$.

Let us now discuss the thermodynamic properties in the transition region for these two cases separately.

(i) *Ferroelectric* ($y = 1$) *transition*

For the ferroelectric transition we have $y = 1$ for $T \leqslant T_c$. At $T \cong T_c+$, we use (149) in conjunction with (300) to yield, for y near 1,

$$y \cong 1 - [a(T)/b(T)]^{1/2} \tag{336a}$$

where, for $V > 0$,

$$a(T) = -V + \tfrac{1}{2} \ln \left(\frac{\eta + 1 - 2\Delta}{\eta - 1} \right) \geqslant 0, \tag{336b}$$

$$b(T) = \frac{\pi^2(\eta^2 + 1 - 2\eta\Delta)(\eta - \Delta)}{8(\eta^2 + 1 - 2\Delta)^2(\eta - 1)^2} > 0. \tag{336c}$$

The square root in (336a) is caused by the fact that $\mathrm{d}^2 z/\mathrm{d}y^2 = 0$ at $|y| = 1$. It follows then that

$$\begin{aligned} -\beta \mathscr{F} &= V + 2[a(T)]^{3/2}/3[b(T)]^{1/2}, \quad T \cong T_c+ \\ &= V, \qquad\qquad\qquad\qquad\quad T \leqslant T_c. \end{aligned} \tag{337}$$

The transition temperature, T_c, is of course, given by $a(T_c) = 0$. The internal energy, U, is computed as

$$\begin{aligned} U = \frac{\partial}{\partial \beta}(\beta \mathscr{F}) &\cong -v - \left(\frac{a}{b}\right)^{1/2} \frac{\partial a}{\partial \beta} + \tfrac{1}{3}\left(\frac{a}{b}\right)^{3/2} \frac{\partial b}{\partial \beta}, \quad T \cong T_c+ \\ &= -v, \qquad\qquad\qquad\qquad\qquad\qquad\quad T \leqslant T_c. \end{aligned} \tag{338}$$

The essential point to notice is that $\eta > 1$ and $\Delta \leqslant 1$ imply that $a(T)$ and $b(T)$ are real analytic in T. $a(T_c) = 0$ characterizes the transition temperature and near that point $a(T)$ has a non-vanishing slope while $b(T)$ is always positive. Consequently U is now continuous at T_c and the transition is without

a latent heat. Further differentiation of U leads to the behaviour of the specific heat

$$\begin{aligned} C &\propto (T - T_c)^{-1/2}, \quad T \cong T_c+ \\ &= 0, \qquad\qquad T < T_c. \end{aligned} \tag{339}$$

These conclusions contrast with the zero field result of Section V.C. The transition is now second order although the specific heat singularity remains unaltered.

(ii) *Antiferroelectric* ($y = 0$) *transition*

For the antiferroelectric transition we have $y = 0$ when $T < T_c(v)$. Therefore the thermodynamic properties are *identical* to those with $v = 0$ on the low temperature side of $T_c(v)$. This is a truly striking result because it means that although the field greatly modifies the thermodynamics above $T_c(v)$, as we shall soon see, it has *literally no effect* on the free energy below $T_c(v)$. Of course the region below $T_c(v)$ diminishes as v increases, but the presence of that region is in marked contrast to the Ising model situation.

On the high temperature side of $T_c(v)$ we must use the small y expansion of $z(y)$, namely (304), in maximizing $-\beta\mathscr{F}$ given by (149). Thus we find

$$y \cong [c(T)/\mathrm{d}(T)]^{1/2} \tag{340}$$

with

$$c(T) = V + z'(0) \geqslant 0, \tag{341a}$$

$$d(T) = -\tfrac{1}{2}z'''(0) > 0 \tag{341b}$$

where $z'(0)$ and $z'''(0)$ have been given in (308). It follows then that

$$\begin{aligned} -\beta\mathscr{F} &\cong z(0) + 2[c(T)]^{3/2}/3[\mathrm{d}(T)]^{1/2}, \quad T \cong T_c+ \\ &= z(0), \qquad\qquad T \leqslant T_c. \end{aligned} \tag{342}$$

The transition temperature is again defined by $c(T_c) = 0$. Once again, by direct differentiation, we see that the internal energy is continuous (no latent heat) at T_c while the specific heat diverges as $(T - T_c)^{-1/2}$ at T_c+.

Having discussed the thermodynamic properties, we conclude with a description of the dependence of polarization on field for the various models at fixed temperatures.

(a) Intrinsically Ferroelectric Model $\bar{\varepsilon} > 0$, $\varepsilon_1 \neq 0$

The situation is exhibited in Fig. 33 where various isotherms are shown. The polarization "sticks" at $y = 1$ at the field $v(T)$ specified by (327). Therefore

the isotherm moves towards the right as T increases. For $T \leqslant T_0$, however, a spontaneous polarization appears at zero field and the isotherm for $T < T_0$ becomes a step function. For $T > T_0$ the isotherm near the upper edge is given by (336a) and has a vertical tangent at $y = 1$; namely

$$y \cong 1 - \{\beta [v(T) - v]/b(T)\}^{1/2}, \quad y \cong 1-. \tag{343}$$

Near $y = 0$ the isotherm approaches the origin linearly. We find from (149) and (316) that

$$y \cong \chi v, \quad y \cong 0+ \tag{344a}$$

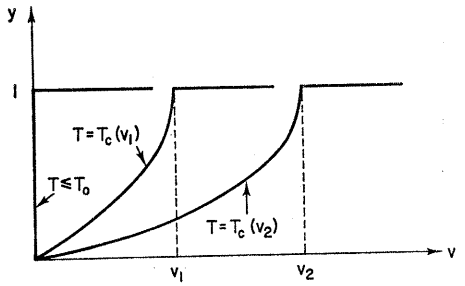

FIG. 33. Vertical polarization *vs.* vertical field for the intrinsically ferroelectric model ($\bar{\varepsilon} > 0$). (Schematic plot.)

where the polarizability, χ, is given by

$$\chi = \frac{2}{kT(\pi - \mu)} \sec\left(\frac{\pi\phi_0}{2\mu}\right). \tag{344b}$$

At high temperatures, we have $\mu \to \frac{2}{3}\pi$, $\phi_0 \to 0$ and (344b) takes the Curie form

$$\chi = \frac{6}{\pi}(kT)^{-1}, \quad T \to \infty. \tag{345}$$

As $T \to T_0+$, we have $\mu \to \pi$ and χ diverges. To compute this divergence to leading order in $T - T_0$ we note from (175) that as $\Delta \to 1$, $\mu \to \pi$, $\phi_0 \to \pi$. If we define $\delta = [k(T - T_0)]^{1/2}$ then $\pi - \mu$ is analytic in δ near $\delta = 0$ with a linear leading term; $\cos(\pi\phi_0/2\mu)$ has the same property with leading term $(\pi - \mu)/(\eta - 1)$. Consequently,

$$\chi = A(T - T_0)^{-1} + B(T - T_0)^{-1/2} + C + \ldots, \quad T \cong T_0 \tag{346a}$$

where A, B and C are constants. For the KDP model

$$A = 2/k \ln 2, \qquad \text{KDP}. \tag{346b}$$

(b) Intrinsically antiferroelectric model $\bar{\varepsilon} < 0$, $\varepsilon_1 \neq 0$

The isotherms in this case are shown in Fig. 34 which should be compared with Fig. 31. At $T = 0$, we have $y = 0$ for $v < |\bar{\varepsilon}|$ and $y = 1$ for $v > |\bar{\varepsilon}|$; y is therefore a step function. For $0 < T < T_0$, it requires a non-zero "critical" field to produce a net polarization, and the polarization saturates at $y = 1$ when the field reaches the value $v(T) > |\bar{\varepsilon}|$ defined by (327). For $T > T_0$, however, it is possible to produce a net polarization with an infinitesimal v. The fact that a non-zero field is required to produce polarization when $T < T_0$

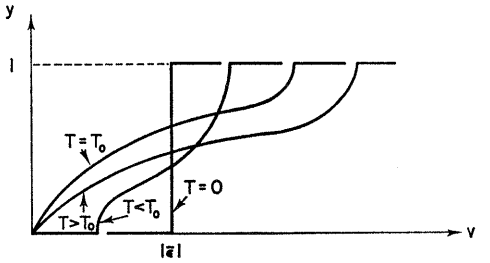

FIG. 34. Vertical polarization *vs.* vertical field for the intrinsically antiferroelectric model ($\bar{\varepsilon} < 0$) with $\varepsilon_1 \neq 0$. (Schematic plot.)

means that the system is "locked in", despite what one might think from the infinite order phase transition described in Section V.C. This state of affairs is strikingly different from the Ising ferromagnet.

The isotherms are again given by (343) near $y = 1-$ where they have vertical tangents. The behaviour of the isotherms at small y is somewhat different. For $T < T_0$, the initial tangent is vertical and, according to (340), the polarization behaves as

$$y \cong \{\beta[v - v_1(T)]/\mathrm{d}(T)\}^{1/2}, \quad y \cong 0+, \quad T < T_0. \tag{347}$$

For $T \geqslant T_0$, we find as in case (a) that the polarizability χ is given by (344b). However for the antiferroelectric models now under consideration we have $-1 < \Delta < \frac{1}{2}$ (see Fig. 13), $0 < \mu < \frac{2}{3}\pi$, hence χ is always finite. Using (322) and (177) we find at T_0,

$$\chi_0 = \frac{2}{\pi k T_0} \sec\left[\frac{\pi(\eta_0 - 1)}{2(\eta_0 + 1)}\right], \quad T = T_0 \tag{348}$$

where η_0 is the value of η at T_0.

As T increases from T_0, χ increases initially, but never diverges and eventually vanishes as $1/T$ precisely as given by (345).

We draw attention to the anomalous non-uniform behaviour of the polarization for small field and T near T_0. Just above T_0 the polarization is linear, while just below T_0 it has a step-function-like behaviour.

(c) F model $\bar{\varepsilon} < 0$, $\varepsilon_1 = 0$

The F model is a special case of the antiferroelectric model with the unique property that the polarization never saturates for finite fields. The isotherms are shown schematically in Fig. 35. For small y, the isotherms behave exactly as in case (b); namely, given by (347) for $T < T_0$ and $y = \chi v$ for $T \geqslant T_0$. Because $\phi_0 \equiv 0$, the polarizability, χ, of (344b) now has the simple expression

$$\chi = \frac{2}{kT(\pi - \mu)}, \quad T \geqslant T_0 \text{ (F model)}. \tag{349}$$

Here, again, $T = T_0$ corresponds to $\mu = 0$. χkT increases monotonically in T and never diverges.

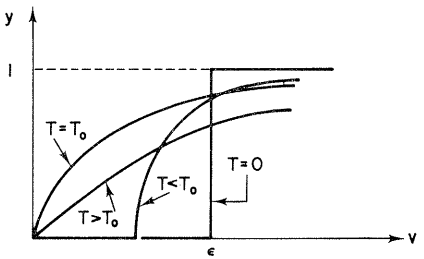

FIG. 35. Vertical polarization *vs.* vertical field for the F model ($\varepsilon_1 = 0$, $\varepsilon_2 = \varepsilon > 0$.) (Schematic plot.)

The behaviour of the polarization near $y = 1$ can be obtained from (302) and (149). We find

$$y \cong 1 - \frac{\pi}{4(1 - \Delta)} \exp(-2\beta v), \quad y \cong 1-. \tag{350}$$

This behaviour of y for large v is the same as for the Ising model (ferro- or antiferromagnetic) and is characteristic of any system with an energy gap for "turning over a spin". However, among the ferroelectrics it occurs only for the F and IF models.

(d) IF Model $\bar{\varepsilon} > 0$, $\varepsilon_1 = 0$

There is no phase transition for the IF model when $h = 0$, and the polarization never saturates. Near $y = 1-$, the polarization behaves as (350) which approaches $y = 1$ exponentially. For small y, the polarization rises linearly in v as in (344a) for all temperatures. However, as $T \to 0$ we have $\mu \uparrow \pi$,

$\phi_0(=3\mu - 2\pi) \downarrow \pi$ and hence the following behaviour of the polarizability:

$$\chi \cong \frac{2}{kT} e^{2|K|}, \quad T \cong 0 \text{ (IF model)}. \tag{351}$$

The situation is demonstrated in Fig. 36.

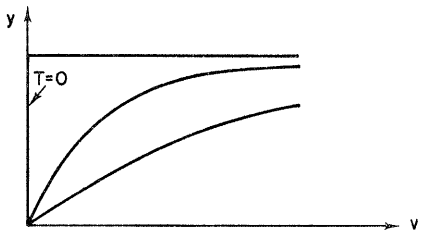

FIG. 36. Vertical polarization *vs.* vertical field for the IF model ($\varepsilon_1 = 0$, $\varepsilon_2 < 0$). (Schematic plot.)

(e) IKDP model $\bar{\varepsilon} = 0$

There is no transition for $v = 0$. For $v > 0$ a $y = 1$ transition occurs at a temperature $T(v)$ defined by (327), which increases from $T(0) = 0$ monotonically in v. Therefore the situation is identical to case (a) but with $T_0 = 0$. However, as $T \to T_0 = 0$, the polarizability is found to behave as

$$\chi_0 \cong \frac{2}{\pi kT} e^{|K|}, \quad T \cong 0 \text{ (IKDP model)}. \tag{352}$$

F. Transition temperature when $h \neq 0$ and $v \neq 0$

In Section V.E. we gave a complete description of the ice rule ferroelectric models when $v \neq 0$ but $h = 0$. We saw that a verticle field caused all phase transitions to become second order and that the transition temperature, T_c, increased for the ferroelectric and decreased for the antiferroelectric. In the latter case T_c vanishes for a finite field such that two of the three pairs of verticles have degenerate energies. A further increase of field causes the system to become a ferroelectric (except in the case of the F and IF models) with a value of T_c that eventually becomes infinite for infinite field.†

The properties of the ferroelectric models can be expected to be qualitatively similar if a horizontal field is also present. The analysis has been sketched in Sutherland *et al.* (1967) but as the details have not yet appeared we shall content ourselves here with a discussion of the dependence of T_c on field. As before, $T < T_c$ for the ferroelectric is characterized by the system "sticking" at $y = 1$ (or $y = -1$) while the antiferroelectric phase

† This behaviour is completely different from that of the Ising model.

means y "sticks" at zero. Part of what is contained here is based on Sutherland *et al.* (1967).

It is convenient to consider various regions of the $h - v$ plane such that within each region a given type of vertex (*cf.* Fig. 1) is favoured. Using the expressions of the vertex energies (93), we obtain the following:

$$
\begin{aligned}
\bar{\varepsilon} > 0: \quad & \text{Region 1:} \quad h > -\tfrac{1}{2}\varepsilon_1, \quad v > -\tfrac{1}{2}\varepsilon_1, \quad h + v > 0, \\
& \text{Region 2:} \quad h < \tfrac{1}{2}\varepsilon_1, \quad v < \tfrac{1}{2}\varepsilon_1, \quad h + v < 0, \\
& \text{Region 3:} \quad h > \tfrac{1}{2}\varepsilon_1, \quad v < -\tfrac{1}{2}\varepsilon_1, \quad h - v > 0, \\
& \text{Region 4:} \quad h < -\tfrac{1}{2}\varepsilon_1, \quad v > \tfrac{1}{2}\varepsilon_1, \quad h - v < 0.
\end{aligned} \tag{353a}
$$

$$
\begin{aligned}
\bar{\varepsilon} < 0: \quad & \text{Region 1:} \quad h > -\tfrac{1}{2}\varepsilon_1, \quad v > -\tfrac{1}{2}\varepsilon_1, \quad h + v > \varepsilon_2 - \varepsilon_1, \\
& \text{Region 2:} \quad h < \tfrac{1}{2}\varepsilon_1, \quad v < \tfrac{1}{2}\varepsilon_1, \quad h + v < \varepsilon_1 - \varepsilon_2, \\
& \text{Region 3:} \quad h > \tfrac{1}{2}\varepsilon_1, \quad v < -\tfrac{1}{2}\varepsilon_1, \quad h - v > \varepsilon_2, \\
& \text{Region 4:} \quad h < -\tfrac{1}{2}\varepsilon_1, \quad v > \tfrac{1}{2}\varepsilon_1, \quad h - v < -\varepsilon_2, \\
& \text{Region 5:} \quad \varepsilon_1 - \varepsilon_2 < h + v < \varepsilon_2 - \varepsilon_1, \quad -\varepsilon_2 < h - v < \varepsilon_2.
\end{aligned} \tag{353b}
$$

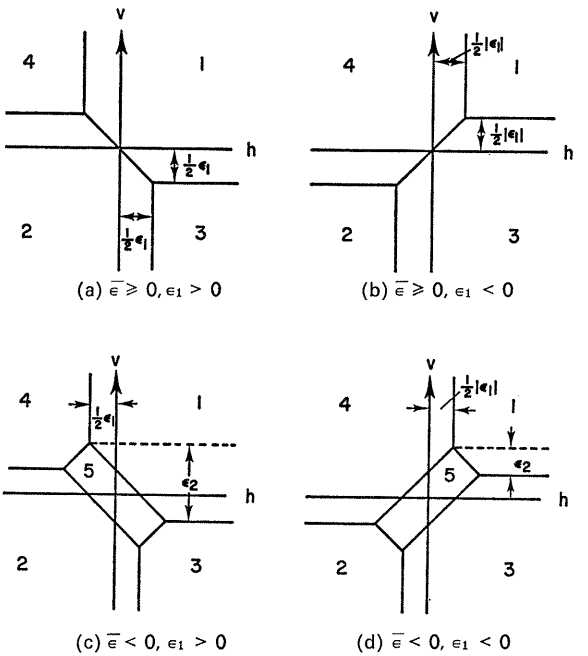

FIG. 37. Different regions in the (h, v) plane for the ice rule models. (a) and (b) are the intrinsically ferroelectric cases including the IKDP ($\bar{\varepsilon} = 0$) and IF($\varepsilon_1 = 0$) models; (c) and (d) are the intrinsically antiferroelectric cases.

In (353), the ith region is characterized by $e_i \leqslant e_j$ for $j \neq i$. Note that the antiferroelectric region 5 exists only when $\bar{\varepsilon} < 0$. These regions are exhibited in Fig. 37. We consider the $y = 1$ (or $y = -1$) and $y = 0$ transitions separately.

(a) *The Ferroelectric Transition at* $y = 1$

The ferroelectric transition occuring at $y = 1$ is characterized by a complete polarization in the vertical direction. Referring to Fig. 1 we see that only the vertices of types (1) and (4) have a positive vertical polarization. Therefore the $y = 1$ transition occurs in either region 1 or region 4 and when the vertical field is sufficiently positive.

To obtain the temperature at which this transition occurs, we recall from (81) that $y \sim 1$ corresponds to $n \sim 0$ where n is the number of down arrows of any row of the lattice. The n numbers $\{k\} = \{k_1, \ldots, k_n\}$ appearing in the Bethe ansatz (140) satisfy (147). For small n, at least, we shall suppose that (147) has a solution, even when $H \neq 0$, and that this solution, as in the $H = 0$ case, has the property that the k's cluster near the origin in the complex k plane. Admittedly a rigorous proof is lacking. That being the case, we can evaluate $z(y)$ to leading order in $y - 1$ by setting $k_1, \ldots, k_n = 0$ in (141);

$$\frac{1}{N} \ln \Lambda_R(y) = Vy - K_2 + H + \tfrac{1}{2}(1 - y) \ln \left[\frac{e^{-K_1} - e^{2K_2 - K_1} - e^{2H}}{1 - e^{K_1 + 2H}} \right], \tag{354a}$$

$$\frac{1}{N} \ln \Lambda_L(y) = Vy - K_1 - K_2 - H + \tfrac{1}{2}(1 - y) \ln \left[\frac{e^{K_1} - e^{2K_2 - K_1} - e^{-2H}}{1 - e^{-K_1 - 2H}} \right], \tag{354b}$$

and

$$\Lambda(y) = \Lambda_R(y) + \Lambda_L(y).$$

In the thermodynamic limit the system "sticks" at $y = 1$ if $\Lambda'(1) \geqslant 0$ [*cf.* eqns (148, 149)]. We are here making use of the fundamental thermodynamic fact that $z(y)$ must be a concave function of y so that $\Lambda'(1) > 0$ implies that $\max_{|y| \leqslant 1} z(y)$ occurs at $y = 1$. This is equivalent to $\Lambda_R'(1) \geqslant 0$ if $\Lambda_R(1) > \Lambda_L(1)$ or $\Lambda'_L(1) \geqslant 0$ if $\Lambda_R(1) < \Lambda_L(1)$. Now $\Lambda_R(1) = \Lambda_L(1)$ means $\varepsilon_1 + 2h = 0$ which is precisely the vertical boundary between regions 1 and 4. Thus, the maximizing y "sticks" at $+1$ for $\Lambda_R(1) \geqslant 0$ in region 1 and $\Lambda_L(1) \geqslant 0$ in region 4. This is the condition

$$\begin{aligned} &(e^{2H + K_1} - 1)(e^{2V + K_1} - 1) \geqslant e^{2K_2}, \quad \text{region 1} \\ &(e^{-2H} - e^{K_1})(e^{2V} - e^{K_1}) \geqslant e^{2K_2}, \quad \text{region 4.} \end{aligned} \tag{355a}$$

Eqn (355a) (with equality) also reduces to (327) on taking $H = 0$, as it should (the first equation is for $\varepsilon_1 > 0$ and the second for $\varepsilon_1 < 0$). When $\bar{\varepsilon} > 0$ and $\varepsilon_1 = 0$ (IF model) no transition is possible using one field alone.

(b) *The Ferroelectric Transition at* $y = -1$

By symmetry, the maximizing y "sticks" at $y = -1$ for

$$\begin{aligned} &(e^{-2H+K_1} - 1)(e^{-2V+K_1} - 1) \geqslant e^{2K_2}, && \text{region 2} \\ &(e^{2H} - e^{K_1})(e^{-2V} - e^{K_1}) \geqslant e^{2K_2}, && \text{region 3} \end{aligned} \tag{355b}$$

(355a, b) reduce to the condition (156a, b) by taking $\Delta = 0$ or $e^{2K_2} = e^{2K_1} + 1$. The equality sign in (355a, b) defines the temperature $T_c(h, v)$ at which the $|y| = 1$ transition occurs.

It is interesting to plot the constant T_c contours in the $h - v$ plane. We have done this for two models. In Fig. 38 the T_c contours are plotted for the ferroelectric Slater KDP model. In Fig. 39 the constant T_c contours are plotted for an antiferroelectric model with $\varepsilon_2 = 2\varepsilon_1 = \varepsilon$. The transition temperature in region 5 will be given presently.

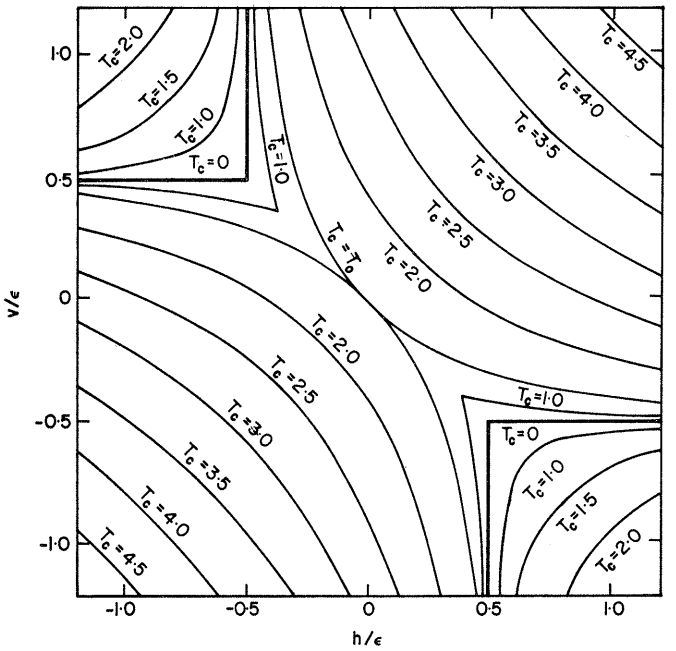

FIG. 38. Constant T_c contours in the (h, v) plane for the KDP model ($\varepsilon_1 = \varepsilon > 0$, $\varepsilon_2 = 0$). T_c is measured in units of ε/k and $T_0 = 1/(\ln 2) = 1{\cdot}44$ is the transition temperature in zero field.

We note that $T_c = 0$ on the boundaries between all regions except those between regions 1 and 2 (Fig. 37a) or 3 and 4 (Fig. 37b). Along these latter boundaries T_c is not even constant, as is seen from Fig. 38. The one exceptional case occurs for the IKDP models defined by $\bar{\varepsilon} = 0$. For these models Figs. 37a and 37c (resp. 37b and 37d) merge into each other and $T_c = 0$ along the 1–2 (resp. 3–4) boundary. The fact that $T_c = 0$ on the other boundaries is a consequence of the degeneracy of the lowest vertex energies.

(c) *The Antiferroelectric Transition at* $y = 0$

We have seen in the previous section that, for the intrinsically antiferroelectric model ($\bar{\varepsilon} < 0$) with a vertical field only, the maximizing y "sticks" at $y = 0$ for $T < T_c(v)$ defined by (328). $T_c(v)$ is then the transition temperature. The situation is basically the same when a horizontal field is included. The transition temperature $T_c(h, v)$ is defined as the temperature below which both the horizontal and vertical polarization x and y "stick" at zero. Sutherland *et al.* (1967) have shown that this occurs only for $\Delta < -1$ and the point $x = y = 0$ corresponds to a *region* in the $h - v$ plane bounded by the closed curve parametrically defined as:

$$H = \Xi(s)$$
$$V = \Xi(\lambda - \theta_0 + s), \quad |s| \leqslant 2\lambda. \tag{356}$$

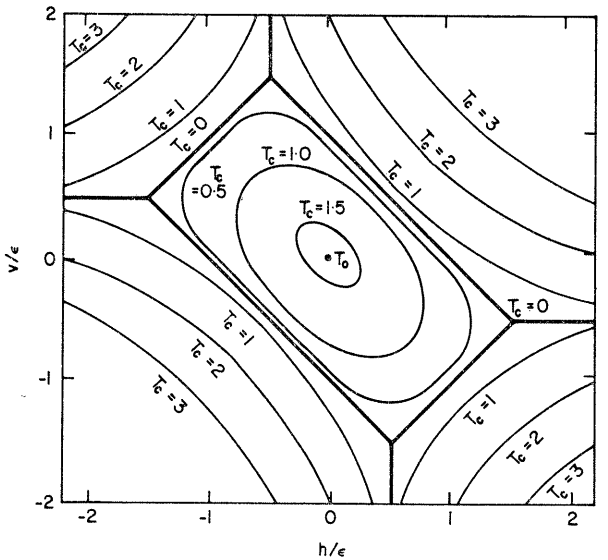

FIG. 39. Constant T_c contours in the (h, v) plane for the intrinsically antiferroelectric model with $\varepsilon_2 = 2\varepsilon_1 = 2\varepsilon > 0$. T_c is measured in units of ε/k and $T_0 = 1/\ln[\frac{1}{2}(\sqrt{5}+1)] = 2{\cdot}08$ is the transition temperature in zero field.

Here $\Xi(\phi)$ is defined by (307a) for $|\phi| < 3\lambda$, and θ_0 is defined by (176). Therefore, the temperature $T_c(h, v)$ at which the $x = y = 0$ transition occurs is given precisely by (356). For $H = 0$ we have $s = 0$ and (356) reduces to (328) as it should. If, in addition, we also have $V = 0$, the transition temperature is $T_c(0, 0) = T_0$ defined by $\lambda = \theta_0 = 0$ or $\Delta = -1$. One can also see from (356) that $T_c(h, v) \to 0$ as one approaches the boundary of the antiferroelectric region 5 defined in (353b). This limit is characterized by $\lambda \to 2K_2 - K_1 \to \infty$; $\theta_0 \to |K_1| \to \infty$; $\lambda - \theta_0 \to \infty$.

The constant T_c contours in this region are plotted in Fig. 39 for the case $\varepsilon_2 = 2\varepsilon_1 = \varepsilon$.

G. The modified KDP model

In the previous sections we have considered the ice rule models using the method of the transfer matrix introduced in Section IV.A. The solution is based on the assumption of the Bethe *ansatz* which eventually led us to the integral equation (174a). In general the integral equation cannot be solved for arbitrary y. For $\Delta = 0$, the kernel of the integral equation vanishes and the solution is trivial. The solution in this case has been given in Section IV.E.

An independent method which, when applicable, sometimes provides a more direct route to the solution of the ferroelectric problem is the Pfaffian method. In Section VI we shall see that the Pfaffian method can be used whenever the condition (392) is fulfilled. It is then a simple matter to see that $\Delta = 0$ is precisely this solubility condition (392). Thus we are led via two different routes to the same soluble cases. In this sense the transfer matrix method with the Bethe *ansatz* assumption is more powerful because it also yields solutions for $\Delta \neq 0$ in many cases.

The condition $\Delta = 0$ (see eqn (153)) means a fixed temperature for given ε_1 and ε_2. This solution is limited, although it is interesting because when $\Delta = 0$ the problem can be simply solved for arbitrary fields and at the same time the $\Delta = 0$ isotherm is typical of the entire region $-1 < \Delta < 1$. However, examination of (153) indicates that, for $\varepsilon_1 = -\infty$ and $\varepsilon_2 = 0$, $\Delta = 0$ is valid at all temperatures. This limit is not as pathologic as it sounds and leads to a physically interesting model which we shall now describe.

The modified KDP model (Wu, 1967, 1968) is specified by the following conditions on the vertex energies (94):

$$e_1 = \infty, \tag{357}$$

$$e_3 + e_4 = e_5 + e_6, \tag{358}$$

and e_2, e_3, e_4, $e_5 = e_6$ otherwise being arbitrary. It can be interpreted as the

Slater KDP model with the additional constraint that type (1) vertices are forbidden. It is possible to solve this model by taking certain limits in the general ice rule models (Sutherland *et al.*, 1967). Examination of (94) shows that the appropriate limits to take are $\varepsilon_1 \to -\infty$, $\varepsilon_2 \to 0$, $\Delta \to 0$, $h \to -\infty$ and $v \to -\infty$. The manipulation is rather delicate, however, since these limits are obviously related. Fortunately in this case the Pfaffian approach is more effective. It suffices to say here that the conditions (357, 358) again satisfy the solubility condition (392) below. Thus we may simply use (393) which gives the free energy, $\mathscr{F}$, per vertex as

$$
\begin{aligned}
-\beta\mathscr{F} &\equiv \lim_{\substack{M\to\infty \\ N\to\infty}} (MN)^{-1} \ln Z \\
&= \frac{1}{8\pi^2}\int_{-\pi}^{\pi} d\theta \int_{-\pi}^{\pi} d\phi \ln[\omega_2{}^2 + \omega_3{}^2 + \omega_4{}^2 + 2\omega_3\omega_2 \cos\theta + 2\omega_2\omega_4 \\
&\qquad \times \cos\phi + 2\omega_3\omega_4 \cos(\theta - \phi)] \\
&= \frac{1}{4\pi}\int_{-\pi}^{\pi} d\theta \ln \max\{\omega_4{}^2, \omega_2{}^2 + \omega_3{}^2 - 2\omega_2\omega_3 \cos\theta\} \qquad (359)
\end{aligned}
$$

where $\omega_i = \exp(-\beta e_i)$, and the last expression is obtained by carrying out the ϕ integration.

Clearly, explicit evaluation of (359) depends on whether ω_2, ω_3 and ω_4 are the sides of a triangle. For given e_2, e_3 and e_4, all distinct, there always exists a temperature T_c defined by

$$\omega_2 + \omega_3 + \omega_4 = 2 \max\{\omega_2, \omega_3, \omega_4\}, \quad T = T_c, \qquad (360)$$

such that below T_c the maximum ω_i dominates and there is no triangular relationship. Under this circumstance we find

$$-\beta\mathscr{F} = -\beta \min\{e_2, e_3, e_4\}, \quad T \leqslant T_c, \qquad (361)$$

and hence the energy per vertex

$$U = \frac{\partial}{\partial\beta}(\beta\mathscr{F}) = \min\{e_2, e_3, e_4\}, \quad T \leqslant T_c. \qquad (362)$$

In other words, the system is in a completely polarized state. Above T_c, however, the triangular inequalities $\omega_2 + \omega_3 > \omega_4$, $\omega_2 + \omega_4 > \omega_3$ and $\omega_3 + \omega_4 > \omega_2$ hold, and the integral (359) cannot be evaluated in closed form. By differentiating, we find the following expression for the energy,

$$U = \frac{1}{\pi}(e_2\theta_2 + e_3\theta_3 + e_4\theta_4), \quad T \geqslant T_c, \qquad (363)$$

where θ_i is the angle opposite to the side ω_i in a triangle whose sides are ω_2, ω_3 and ω_4.

We note that the energy U is continuous at T_c as the θ's go to 0 or π smoothly at T_c. The specific heat C can now be computed. We find

$$C = 0, \quad T \leqslant T_c,$$
$$C \propto (T - T_c)^{-1/2}, \quad T \cong T_c+. \tag{364}$$

Thus the model exhibits a second-order phase transition with no latent heat.

For the modified KDP model we have

$$\begin{aligned} e_1 &= \infty, \\ e_2 &= h + v, \\ e_3 &= \varepsilon - h + v, \\ e_4 &= \varepsilon + h - v, \\ e_5 &= e_6 = \varepsilon. \end{aligned} \tag{365}$$

As in Section V.F it is again convenient to consider various regions of the $h - v$ plane such that within each region a given type of vertex is favoured. We find that:

$$\begin{aligned} &\text{Region 2:} \quad h < \tfrac{1}{2}\varepsilon, \quad v < \tfrac{1}{2}\varepsilon, \\ &\text{Region 3:} \quad h > \tfrac{1}{2}\varepsilon, \quad h - v > 0, \\ &\text{Region 4:} \quad v > \tfrac{1}{2}\varepsilon, \quad h - v < 0, \end{aligned} \tag{366}$$

where the ith region is characterized by $e_i \leqslant e_j$ for $j \neq i$. A plot of these regions is given in Fig. 40. The transition temperature T_c is now given explicitly by

$$\begin{aligned} \mathrm{e}^{K} &= \mathrm{e}^{2H} + \mathrm{e}^{2V}, \quad \text{region 2}, \\ \mathrm{e}^{2H} &= \mathrm{e}^{K} + \mathrm{e}^{2V}, \quad \text{region 3}, \\ \mathrm{e}^{2V} &= \mathrm{e}^{K} + \mathrm{e}^{2H}, \quad \text{region 4}, \quad T = T_c, \end{aligned} \tag{367}$$

where $K = \beta\varepsilon$, $H = \beta h$, $V = \beta v$. We observe that $T_c \to \infty$ as either $|h|$ or $|v| \to \infty$. Also $T_c = 0$ on the boundaries between the regions. This is also a consequence of the fact that the lowest configuration is highly degenerate.

The critical condition (367) should be compared with that of the KDP model, eqns (355a, 355b). While the conditions of the two models are different in regions 3 and 4, they are identical in region 2. This indicates that the

effect of type (1) vertices is insignificant when vertex (2) is favoured; namely, there is not much difference between the regular and the modified models, at least near the region of the transitions. This is what one expects intuitively because the ice rule dictates that no type (1) vertex can be inserted in the ground state without affecting at least two chains of vertices running across the entire lattice.

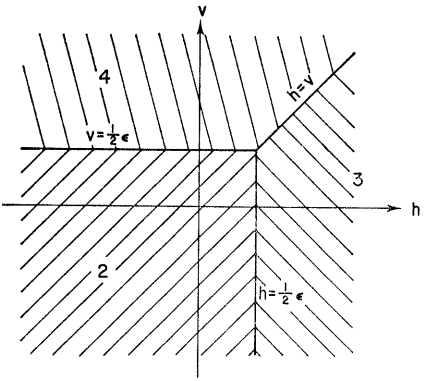

FIG. 40. Different regions in the (h, v) plane for the modified KDP model.

We can now introduce (365) into (359) to compute the polarizations $x = -\partial\mathscr{F}/\partial h$, $y = -\partial\mathscr{F}/\partial v$. One finds complete polarization below T_c, namely

$$\left.\begin{aligned}(x, y) &= (-1, -1), \quad \text{region 2},\\ &= (+1, -1), \quad \text{region 3},\\ &= (-1, +1), \quad \text{region 4.}\end{aligned}\right\} \; T \leqslant T_c \tag{368a}$$

Also

$$x = \frac{2}{\pi}\theta_3 - 1, \qquad T \geqslant T_c, \tag{368b}$$

$$y = \frac{2}{\pi}\theta_4 - 1,$$

where θ_i is the same as in (363). In particular we find that in zero field the polarizations do not vanish,

$$x = y = \frac{2}{\pi}\cos^{-1}(\tfrac{1}{2}e^{K}) - 1, \quad h = v = 0. \tag{369}$$

This reflects the fact that the modified model lacks the inversion symmetry of the Slater KDF model.

The phase diagram of this model is best visualised in the $h - v$ plane. In Fig. 41 the heavy curves show the phase boundaries (367) at a given temperature T. These curves move out as T increases and converges toward the region boundaries as T decreases to zero. It is now possible to investigate the dependence of the polarization, y, for example, on both h and v. Either (386b) or Fig. 41 shows that as a function of v, for h fixed, y increases mono-

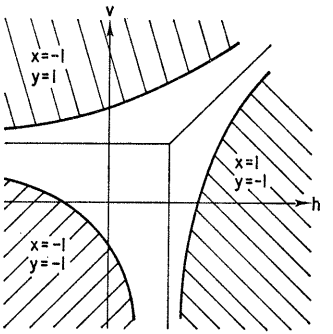

FIG. 41. Phase boundaries of the modified KDP model at a fixed temperature. The lattice is completely polarized in the shaded regions. (Schematic plot.)

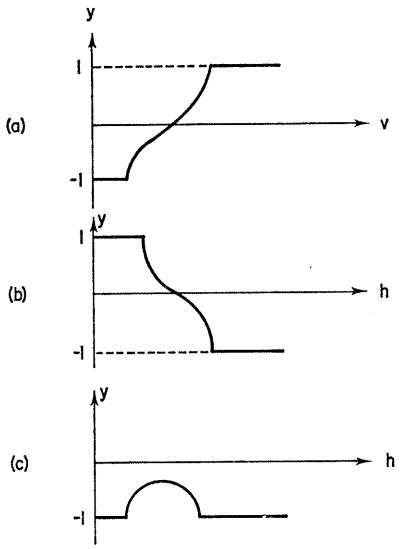

FIG. 42. Vertical polarization *vs.* external field for the modified KDP model. (a) y as a function of the vertical field v. (b) y as a function of the horizontal field h for $v > \frac{1}{2}\varepsilon$, (c) y as a function of h for $v < \frac{1}{2}\varepsilon$. (Schematic plot.)

tonically from -1 to 1 as shown in Fig. 42a. As a function of h, for v fixed, the behaviour of y depends on whether $v > \frac{1}{2}\varepsilon$ or $v < \frac{1}{2}\varepsilon$. For $v > \frac{1}{2}\varepsilon$, as shown in Fig. 42b, y decreases monotonically from 1 to -1 as h increases. For $v < \frac{1}{2}\varepsilon$, however, y increases initially from -1, but never reaches zero, and eventually returns to the value -1. This situation is shown in Fig. 42c. It is easy to compute the maximum polarization in this case,

$$y_{\max} = \frac{2}{\pi}\tan^{-1}\{\exp[2(V - \hat{H})]\} - 1, \tag{370}$$

where $\hat{H}$ is given by

$$4\hat{H} = \ln(e^{2K} - e^{4V}). \tag{371}$$

These isotherms have vertical tangents at $y = \pm 1$. The slope is found to diverge as $|v - v_0|^{-1/2}$ or $|h - h_0|^{-1/2}$ as the critical field h_0 or v_0 is approached. This behaviour is similar to that of the regular ice rule models as given by (343) and (347).

The modified KDP model can also be solved with a staggered field and the phase diagram in a staggered field is found to be similar to that of the F model in a direct field. (Wu, 1971a).

Finally, we mention that the modified KDP model is completely equivalent to the problem of close-packed dimers on a hexagonal lattice. The equivalence can be most simply established if one treats the modified KDP model by the method of dimers (Wu, 1968). We shall omit the details here and give only the result. Let Z_D be the generating function for the close-packed dimer configurations on a hexagonal lattice of N vertices and having activities ω_2, ω_3 and ω_4 along the three principal axes. Then

$$\lim_{N\to\infty} N^{-1} \ln Z_D = -\tfrac{1}{2}\beta\mathscr{F} \tag{372}$$

where $\beta\mathscr{F}$ is given by (359). The existence of a phase transition for the hexagonal dimer lattice was first pointed out by Kasteleyn (1963). The number of close-packed dimer configurations on a hexagonal lattice can be computed from this generating function by setting $\omega_2 = \omega_3 = \omega_4 = 1$. The result has been given in (23).

H. Other ice rule models

1. *The F Model with a Staggered Field when $\Delta = 0$*

As we have remarked earlier in Section IV.E (see also Section VIII), one of the outstanding unsolved problems for the ferroelectrics is the problem of inclusion of a staggered field. However, at a particular temperature corres-

ponding to $\Delta = 0$, the partition function can be evaluated in closed form using the method of Pfaffians (Baxter, 1970b). For the Rys F model $\Delta = 0$ corresponds to the temperature

$$T = 2\varepsilon/k \ln 2 = 2T_0. \tag{373}$$

Baxter's expression of the free energy of the F model with both direct and staggered fields at this temperature has been given in (157). We refer the readers to Baxter (1970b) for detailed analysis and quote here only the main findings:

(1) For a non-zero staggered field, s, there is no direct polarization unless the direct fields are sufficiently large. Thus, although $T(= 2T_0)$ lies above the critical temperature T_0 of the zero-field F model, application of a staggered field makes the direct polarization behave similarly to the $T < T_0$ case.

(2) In zero direct fields, the staggered polarizability, $\partial^2\mathscr{F}/\partial s^2$ diverges as $\ln|s|$ near $s = 0$ indicating a non-analytic transition from positive to negative staggered fields. $\mathscr{F}$ is analytic in s when $s \neq 0$. Further, at $s = 0$ the correlation between two vertical arrows on the same row a large distance r apart are found to decay only as r^{-2}.

(3) Complete direct polarization, and zero staggered polarization, can be achieved by applying sufficiently strong, but finite, direct fields in both the horizontal and vertical directions. However, if one of these fields is zero, complete polarization is achieved only when the other is infinite.

2. *The Ferrielectric Model*

There is one example of a staggered model that can be solved generally (provided the horizontal field is zero) and this model—the ferrielectric model —is not without physical interest. The vertex energies are chosen to be constant within any row, but alternate from row to row. On the odd rows let the energies be as given in (93). On the even rows make the replacement

$$\varepsilon_1 \to \hat{\varepsilon}_1 = -\varepsilon_1; \quad \varepsilon_2 \to \hat{\varepsilon}_2 = \varepsilon_2 - \varepsilon_1 \tag{374}$$

while h and v remain unaltered. If we add a (trivial) constant energy $2\varepsilon_1$ to every vertex on the even rows, it will be seen that, for zero horizontal field, the even and odd rows are identical except for the interchanges of vertex 1 with 4 and vertex 2 with 3. Consequently, the value of Δ is the same for all rows. If we are in the intrinsically ferroelectric situation so that vertex 1, say, is preferred on the odd rows, then vertex 4 will be preferred on the even rows and the ordered state will be one in which the polarization is alternately northeast and northwest on the odd and even rows. (See Fig. 43). Thus, in the

vertical direction the system appears to be a ferroelectric while in the horizontal direction it appears to be an antiferroelectric. Such systems have been considered by experimentalists (Jona and Shirane, 1962).

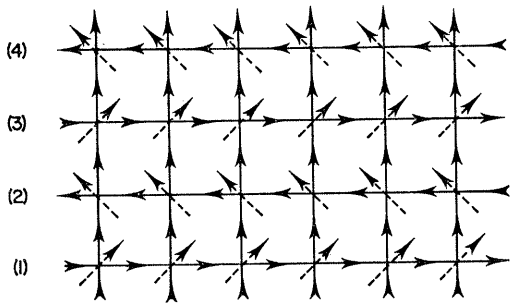

FIG. 43. The ordered state of the ferrielectric model in which the vertex energies alternate from row to row. The case in which vertex (1) is preferred on odd rows and vertex (4) is preferred on even rows is shown here. The dashed arrows are the net polarization at each vertex.

The astounding fact is that *all thermodynamic properties of the ice rule ferrielectric without horizontal field are exactly the same as for the ferroelectric model before we prescribe the alternation given by* (374). This is so for all ε_1 and ε_2. The reader may feel that this result can be simply verified by establishing an energy preserving isomorphism between configurations for the two models. If such an isomorphism exists we have been unable to find it.

We are not able to solve the problem when a horizontal field is present, even if there is no vertical field and even if we rotate the lattice by 90°. We leave this as a challenging unsolved problem which we believe is in the realm of the possible. In the following we shall always assume $h = 0$.

Returning to Section IV.C we note that D^V, (97), is the same for all rows and satisfies (91). If we use a $\hat{}$ to designate quantities on the even rows we see that

$$e^{2K_1N} D_R{}^F(\mathbf{X}, \mathbf{Y}) D_R{}^{KDP}(\mathbf{X}, \mathbf{Y}) = \hat{D}_L{}^F(\mathbf{Y}, \mathbf{X}) \hat{D}_L{}^{KDP}(\mathbf{Y}, \mathbf{X}), \tag{375}$$

and the same is true if L and R are interchanged. Thus, from (91),

$$e^{2K_1N} T^\dagger = \hat{T} \tag{376}$$

where † means adjoint. Now, if M is even for convenience,

$$Z = \mathrm{Tr}(\hat{T}\, T)^{M/2} \tag{377}$$

and we require the largest eigenvalue of $\hat{T}\, T$. On the other hand, since $\Delta = \hat{\Delta}$, (142, 143) show that every eigenvector of T of the Bethe *ansatz*

form is also an eigenvector of $\hat{T}$. Moreover, the eigenvalues are essentially the same since $\hat{\Lambda}_R = \Lambda_L e^{2K_1 N}$ and $\hat{\Lambda}_L = \Lambda_R e^{2K_1 N}$. This remark proves the assertion that $\mathscr{F}$ is the same for the ferroelectric and ferrielectric models except that the latter has an additional term ε_1.

As a by-product we are thus led to the following:

Conjecture: T *is a normal matrix, i.e.* $[T, T^\dagger] = 0$.

If we knew that T had a complete set of eigenvectors and if all were of the Bethe type, the conjecture would be proved. The conjecture is consistent with the assertion of Section IV.D that $[T, H] = 0$ where H is a Hermitian linear Hamiltonian. If all the eigenvalues of H were non-degenerate the conjecture would also be proved. The conjecture is certainly true when $\Delta = 0$ because the discussion given prior to (151) easily generalizes to the following: Any set $\{k\}$ in which the k's are distinct and of the form $2\pi(\text{integer})/N$ (n odd) or $2\pi(\text{integer})N + \pi/N$ (n even) satisfies (147). These sets generate a complete orthonormal set of determinantal eigenfunctions.

The significance of the conjecture is that T would have a spectral decomposition:

$$T(\mathbf{X}, \mathbf{Y}) = \sum_{j=1}^{2^N} \Lambda_j \psi_j(\mathbf{X}) \bar{\psi}_j(\mathbf{Y}) \tag{378}$$

with the $\{\psi_j\}$ orthonormal but the $\{\Lambda_j\}$ not necessarily real. The spectral decomposition would be useful for discussing correlation functions to which we shall turn in the next section.

I. Correlation functions when $\Delta = 0$

Of the many correlation functions that can be defined, we shall restrict ourselves here to the correlation of two vertical arrows separated by $\mathbf{r} = (a, b)$, with a and b integers, i.e.

$$G(\mathbf{r}) = \langle \sigma_0^z \sigma_\mathbf{r}^z \rangle. \tag{379}$$

The evaluation of G in general defies analysis, even when the arrows are on the same row, because the maximum eigenvector (140) is too complicated. For $\Delta = 0$, however, the calculation can be performed because all eigenvectors of T are determinantal, as remarked in Section V.H; this was done by Sutherland (1968). On thermodynamic grounds the point $\Delta = 0$ is not atypical. Although we have no proof, we are convinced that the following statements about $G(\mathbf{r})$ are qualitatively valid for the entire region

$-1 < \Delta < 1$. Since T has the form (378) we can easily derive, for $M \to \infty$, that

$$G(\mathbf{r}) = \sum_{j=0}^{2^N-1} \langle 0|\sigma_0^z|j\rangle\langle j|\sigma_a^z|0\rangle \left(\frac{\Lambda_j}{\Lambda_0}\right)^b, \tag{380}$$

where the $\{|j\rangle\}$ are a complete set of orthonormal determinantal eigenfunctions and $|0\rangle$ is the one with maximum eigenvalue. Although the eigenfunctions are determinants only in the region (83) we can note that the inner products in (380) always involve the product of two determinants so that we can ignore the restriction (83) and pretend the particles are fermions. In that case

$$\sigma_a^z = 2c_a^\dagger c_a - 1 = \frac{2}{N}\sum_k \sum_q d_k^\dagger d_q \exp[i(k-q)a] - 1, \tag{381}$$

where the $\{c_a\}$ are fermion operators and the $\{d_k\}$ are their Fourier transforms. The evaluation of (380) is well known from solid state physics except for the following remarks:

(1) Since $y = 1 - 2n/N$ is invariant we can evaluate G for each y subspace separately. The appropriate y to use is determined by (149).

(2) One possible intermediate state in (380) is $|0\rangle$ and this comes from the diagonal term in (381). It gives rise to a term y^2. The other relevant states are obtained by promoting a "particle" of momentum k in the "Fermi sea" $|k| < \frac{1}{2}\pi(1-y)$ to a momentum q in the complement of the "Fermi sea". The factor Λ_j/Λ_0 is then simply $\lambda_R(q; K_1, K_2, H)/\lambda_R(k; K_1, K_2, H)$ since, as we remarked in Section IV.E, $\lambda_R = -\lambda_L$ when $\Delta = 0$.

In the usual way we pass from sums to integrals as $N \to \infty$ and obtain, for fixed y,

$$G_y(a, b) = y^2 + \pi^{-2} I_1 I_2 \tag{382}$$

where

$$I_1 = \int_{-\frac{1}{2}\pi(1-y)}^{\frac{1}{2}\pi(1-y)} \left[\frac{\exp(2H + K_1 + ik) - 1}{\exp(K_1) + \exp(2H + iK)}\right]^b \exp(-ika)\,\mathrm{d}k,$$

$$I_2 = \int_{\frac{1}{2}\pi(1-y)}^{\frac{1}{2}\pi(3+y)} \left[\frac{\exp(K_1) + \exp(2H + iq)}{\exp(2H + K_1 + iq) - 1}\right]^b \exp(iqa)\,\mathrm{d}q. \tag{383}$$

I_1 is the integral over the "Fermi sea" while I_2 is the integral over its complement.

When $b = 0$ (arrows on the same row)

$$G_y(a, 0) = y^2 - \left\{\frac{2}{\pi a}\sin\left[\frac{\pi a}{2}(1-y)\right]\right\}^2. \tag{384}$$

This is an unusual result for several reasons.

(1) The non-constant part of G decays asymptotically with a power law instead of an exponential;

(2) In a field (so that $y \neq 0$), the periodicity of G is unrelated to that of the lattice;

(3) With no field, $y = 0$ and $G \equiv 0$ when b is even;

(4) In all cases, G never exceeds its asymptotic value.

For further details the reader is referred to Sutherland (1968). For large $r = (a^2 + b^2)^{1/2}$ he asserts that:

(1) $G_y(\mathbf{r}) - y^2$ decays as r^{-2} with an angle dependent factor;

(2) For the F model in zero field ($y = 0$) the asymptotic form is

$$G_0(\mathbf{r}) \sim \left[\frac{2}{\pi r}\sin\psi\right]^2, \quad a + b \text{ even}$$

$$\sim -\left[\frac{2}{\pi r}\cos\psi\right]^2, \quad a + b \text{ odd} \tag{385}$$

where (r, ψ) is the polar coordinate representation of (a, b). The fact that $|G_0(\mathbf{r})|$ has a logarithmically divergent spatial integral is consistent with the logarithmically divergent zero field staggered susceptibility mentioned in Section V.H1.

J. List of constants

We list here some constants pertaining to the ferroelectric models.

KDP Model

$\varepsilon/kT_0 \quad = \ln 2 \quad = 0{\cdot}693147180\ldots$

$\frac{1}{\varepsilon}U(T = \infty) \quad = \frac{3}{4}\sqrt{3} - \frac{1}{2\pi}\sqrt{3} - \frac{1}{3} = 0{\cdot}690040324\ldots$

$\frac{1}{\varepsilon}U(T = T_0+) = \frac{1}{2}$

$\frac{1}{k}S(T = T_0+) = \frac{1}{2}\ln 2 \quad = 0{\cdot}346573590\ldots$

$\frac{1}{k}S(T = \infty) \quad = \frac{3}{2}\ln\frac{4}{3} \quad = 0{\cdot}431523108\ldots$

F Model

$$\varepsilon/kT_0 = \ln 2 = 0{\cdot}693147180\ldots$$

$$\frac{1}{\varepsilon}U(T=\infty) = \tfrac{8}{3} + \frac{\sqrt{3}}{\pi} - \tfrac{3}{2}\sqrt{3} = 0{\cdot}619919351\ldots$$

$$\frac{1}{\varepsilon}U(T=T_0) = \tfrac{1}{3}$$

$$\frac{1}{k}C(T=T_0) = \tfrac{2}{4}\tfrac{8}{5}(\ln 2)^2 = 0{\cdot}29894854\ldots$$

$$\frac{1}{k}S(T=T_0) = 2\ln[\Gamma(\tfrac{1}{4})/\Gamma(\tfrac{3}{4})] - \tfrac{8}{3}\ln 2 = 0{\cdot}3210966\ldots$$

$$\frac{1}{k}S(T=\infty) = \tfrac{3}{2}\ln\tfrac{4}{3} = 0{\cdot}431523108\ldots$$

Ice Model

Average fraction of types (5) plus (6) vertices

$$= \sqrt{3}\left(\frac{3}{2} - \frac{1}{\pi}\right) - \tfrac{5}{3} = 0{\cdot}380080648\ldots .$$

In these expressions S is the entropy per vertex. Some of these constants have been given in the text; others can be obtained directly by differentiating (192), the free energy of the KDP model in zero field. The average fraction of types (5) and (6) vertices was first evaluated by Wu and reported in Ref. 74 of Lebowitz (1968). A typographical error of a missing square root sign was contained in the expression quoted there, however.

VI. General Lattice Model on a Square Lattice

Up to now we have considered the ice rule ferroelectric models defined on a square lattice. The ice rule has the important consequence that the number of down arrows along a row of vertical lattice bonds is conserved; this in turn allows us to use Bethe ansatz for the solution.

In Section II.D we introduced the general ferroelectric model which in general does not obey the ice rule. This means that we must now consider all sixteen vertices shown in Fig. 10. This is a much more difficult problem to solve and, needless to say, no general solution is known to date. It is possible, however, to learn a great deal about the behaviour of these models

by some general considerations as well as particular consideration of a number of soluble cases which shall concern us in this section.

A. The eight vertex problem

The eight vertex problem is a first step generalization of the ice rule models by inclusion of the vertices of types (7) and (8), in addition to the six ice rule vertices (*cf.* Fig. 10). The partition function in this problem has been given in (25).

First we can write down a number of symmetry relations on the partition function without actually solving the problem (Fan and Wu, 1970). Because vertices (5) and (6) or (7) and (8) occur in pairs globally, we may take $\omega_5 = \omega_6 = a$, $\omega_7 = \omega_8 = b$ and observe the relation

$$Z \equiv Z(a, b) = Z(-a, b) = Z(a, -b). \tag{386}$$

If we reverse all horizontal arrows and then look at the lattice in a mirror we deduce that

$$Z(a, b) = Z(b, a). \tag{387}$$

Let us now temporarily disregard the weights a and b and write $Z = Z_{1234}$, where each subscript $\xi(=1, 2, 3, 4)$ stands for the dependence on the vertex weight ω_ξ. Since Z, being a sum over all configurations, is invariant if the vertical or horizontal arrows be reversed in the enumeration of the configurations, we have the obvious symmetry relation

$$Z \equiv Z_{1234} = Z_{3412} = Z_{2143} = Z_{4321}. \tag{388a}$$

Futhermore, by rotating the lattice 90° we also obtain

$$Z_{1234} = Z_{1243} = Z_{3421} = Z_{2134} = Z_{4312}. \tag{388b}$$

Note that these are symmetry relations involving the interchanging of the vertex weights ω_1, ω_2, ω_3 and ω_4; no changes between the weights ω_1, ω_2, ω_3, ω_4 and ω_5, ω_6, ω_7, ω_8 are involved.

If the vertex weights satisfy

$$\begin{aligned} &\omega_1 = \omega_2 = u_1, \quad \omega_3 = \omega_4 = u_2, \\ &\omega_5 = \omega_6 = u_3, \quad \omega_7 = \omega_8 = u_4, \end{aligned} \tag{389}$$

which can be considered as the basic eight vertex problem without a field, it is then possible to obtain symmetry relations which involves interchanges

between the first four and last four weights. From a consideration of reversing all arrows along some zigzag paths, one obtains (Fan and Wu, 1970)

$$Z \equiv Z(u_1, u_2; u_3, u_4) = Z(u_3, u_4; u_1, u_2). \tag{390}$$

Another useful symmetry relation can be obtained by applying to the series expansion of the partition function a rearrangement procedure, known as the weak graph expansion. (See the discussion on the application of the weak graph expansion method to the ferroelectric models by J. F. Nagle elsewhere in this book.) One finds (Wu, 1969b)

$$Z(u_1, u_2; u_3, u_4) = Z(\tfrac{1}{2}(u_1 + u_2 + u_3 + u_4), \tfrac{1}{2}(u_1 + u_2 - u_3 - u_4);$$
$$\tfrac{1}{2}(u_1 - u_2 + u_3 - u_4), \tfrac{1}{2}(u_1 - u_2 - u_3 + u_4)). \tag{391}$$

It must be remembered from (386) that Z is also invariant under the replacement $u_i \to -u_i$ for any one i. In fact, further iterations of (391) yield precisely relations differing from (391) only by these sign changes. If we substitute $u_1 = u_2 = u_3 = 1$ and $u_4 = 0$ into (391), the left-hand side is Z_0 of (3). The right-hand side is $(\frac{3}{2})^N Z(1, \frac{1}{3}, \frac{1}{3}, \frac{1}{3})$. Recalling the interpretation of Z in terms of polygons as given in Section II.B and Fig. 10 we deduce formula (18).

Having discussed the symmetry relations of the partition function Z, we now ask under what condition can Z be evaluated in closed form? A partial answer to this question has been provided by Hurst and Green (1964) from a somewhat different point of view. In their consideration of the most general planar Ising lattice, they introduce a sublattice at each vertex of a simple square lattice. In the high temperature hyperbolic tangent series expansion of this extended Ising model, each sublattice carries a weight which depends on the "terminal configuration" of the sublattice. One then has precisely an eight vertex problem. Hurst and Green obtained the following condition under which this problem is solvable with the Pfaffian method:

$$\omega_1\omega_2 + \omega_3\omega_4 = \omega_5\omega_6 + \omega_7\omega_8. \tag{392}$$

In the S-matrix formulation (Hurst and Green, 1960) of the eight vertex problem, this condition is equivalent to the consideration of a non-interacting many-fermion system (Fan and Wu, 1969). Therefore we shall refer to (392) as the *free-fermion condition* and the model satisfying (392) as the *free-fermion model.*

The Free-Fermion model

The partition function of the free-fermion model was first evaluated by Hurst and Green (1963). It has also been rederived by the S-matrix method (Fan

and Wu, 1969) and by the method of dimers (Fan and Wu, 1970). The expression of the free energy $\mathscr{F}$ is

$$-\beta\mathscr{F} = \frac{1}{8\pi^2}\int_{-\pi}^{\pi} d\theta \int_{-\pi}^{\pi} d\phi \ln [a + 2b\cos\theta + 2c\cos\phi + 2f\cos(\theta - \phi) + 2g\cos(\theta + \phi)], \tag{393a}$$

where

$$\begin{aligned} a &= \omega_1^2 + \omega_2^2 + \omega_3^2 + \omega_4^2, \\ b &= \omega_1\omega_3 - \omega_2\omega_4, \\ c &= \omega_1\omega_4 - \omega_2\omega_3, \\ f &= \omega_3\omega_4 - \omega_7\omega_8, \\ g &= \omega_1\omega_2 - \omega_5\omega_6. \end{aligned} \tag{393b}$$

As one easily checks, the symmetry relations derived earlier hold for this solution.

Before we proceed to discuss the thermodynamics of this free-fermion model, we pause to ask what the free-fermion models of interest are. Since the vertex weights are Boltzmann factors $\omega_i = \exp(-\beta e_i)$, a meaningful model requires the following identity to hold:

$$\{e_1 + e_2, e_3 + e_4\} = \{e_5 + e_6, e_7 + e_8\}. \tag{394}$$

Therefore the modified KDP model is an example of the free-fermion model. Also we have shown in Section II.D that the eight vertex model is completely equivalent to an Ising model with 2 and 4 body interactions. In particular the square lattice Ising model with first-neighbour interactions $-J_1$, $-J_2$ and second-neighbour interactions $-J$, $-J'$ is equivalent to an eight vertex model with energies

$$\begin{aligned} e_1 &= -J_1 - J_2 - J - J', & e_2 &= J_1 + J_2 - J - J', \\ e_3 &= J_1 - J_2 + J + J', & e_4 &= -J_1 + J_2 + J + J', \\ e_5 &= e_6 = J' - J, & e_7 &= e_8 = J - J'. \end{aligned} \tag{395}$$

These values are obtained by setting $J_0 = J_4 = 0$ in (29). Clearly (395) does not satisfy the condition (394), consistent with the well-known result that the next-neighbour Ising model cannot be solved using the Pfaffian method. However, these energies do satisfy the free-fermion condition if we put one of the second-neighbour interactions, say, $J' = 0$. The resulting Ising lattice is a triangular one with three parameters J_1, J_2 and J. Thus the free-fermion

model, which is also specified by three energy parameters, is equivalent to the Ising model on a triangular lattice.

It is not necessary, of course, to restrict our considerations to the condition (394). In fact, for any eight vertex problem, the free-fermion condition is always satisfied at a temperature defined by (392). Thus we can evaluate the partition function of the general eight vertex problem at one *fixed* temperature. For the ice rule models, (392) together with $e_7 = e_8 = \infty$ lead to precisely the expression given by (149) and (154).

We now return to the expression (393) of the free energy. One of the two integrations can be carried out to yield

$$-\beta\mathscr{F} = \frac{1}{4\pi}\int_{-\pi}^{\pi} d\phi \ln \{A(\cos\phi) + [Q(\cos\phi)]^{1/2}\}, \tag{396}$$

where $A(x)$ and $Q(x)$ are, respectively, polynomials linear and quadratic in x. The analytic properties of $\mathscr{F}$ depend on whether or not $Q(x)$ is a complete square for all T. The main results are summarized below (Fan and Wu, 1970):

(a) $Q(x)$ *is a complete square*

We have either the modified KDP model or the physically uninteresting cases which show no phase transition

$$\{e_1, e_2\} = \{e_3, e_4\} \text{ for which } -\beta\mathscr{F} = \tfrac{1}{2}\ln[2(\omega_1^2 + \omega_2^2)], \tag{397a}$$

$$\{e_1, e_3\} = \{e_2, e_4\} \text{ for which } -\beta\mathscr{F} = \tfrac{1}{2}\ln[2(\omega_1^2 + \omega_3^2 + \omega_1\omega_3)]. \tag{397b}$$

(b) $Q(x)$ *is not a complete square*

The model is equivalent to an Ising model on a triangular lattice. The transition temperature is given by

$$\omega_1 + \omega_2 + \omega_3 + \omega_4 = 2\max\{\omega_1, \omega_2, \omega_3, \omega_4\}, \quad T = T_c. \tag{398}$$

The specific heat diverges as $\ln|T - T_c|$, as compared with the inverse square root singularity (364) of the modified KDP model. The energy can be expressed in terms of complete elliptic integrals. However, the explicit expressions are different for temperatures above and below a certain temperature which is different from T_c. This temperature turns out to coincide with the disorder temperature T_D of the antiferromagnetic triangular Ising lattice (Stephenson, 1969 and 1970). Nevertheless, T_D is an analytic point and is defined by the condition

$$\omega_\alpha + \omega_\delta = \omega_\beta + \omega_\gamma, \tag{399}$$

where $\omega_\alpha \leqslant \omega_\beta \leqslant \omega_\gamma \leqslant \omega_\delta$ are the vertex weights ω_1, ω_2, ω_3 and ω_4 arranged according to their magnitudes. This condition is equivalent to setting $Q(x)$

in (396) to be a complete square (Stephenson, 1969) which can be realized for anisotropic antiferromagnetic triangular Ising lattices only.

The polarizations can also be computed for the free-fermion model. One finds that the polarization is continuous and does not saturate in a finite field.

Other Exact Results

There are very few exact results on the general eight vertex problem. For the basic eight vertex problem without a field* defined by (389), Sutherland (1970) was able to locate the transition temperature using an argument similar to that of Kramers and Wannier (1941); the argument is based on two plausible assumptions. We saw in Section IV.D that the transfer matrix of the basic eight vertex problem commutes with the Hamiltonian of a one-dimensional spin system. While the eigenvalues are different, the largest eigenvectors, which determine the nature of the long-range order, are the same in these two systems. It is then plausible to assume that the singularity in the free energy for the ferroelectric problem corresponds to the singularity in the ground state energy of the spin system. If one further assumes the uniqueness of this singularity (Kramers and Wannier, 1941), it is then possible to determine its location. Sutherland considers the ferroelectric (vertices 1, 2 or 3, 4 favoured) and the antiferroelectric (vertices 5, 6 or 7, 8 favoured) cases separately. However we see from (390) that these two cases are actually equivalent when there is no field. In fact, Sutherland's conjecture on the transition temperature can be put in the following symmetric form:

$$u_1 + u_2 + u_3 + u_4 = 2 \max \{u_1, u_2, u_3, u_4\}, \quad T = T_0. \tag{400}$$

This relation reduces, of course, to the result (195a) of Section V.B for the ice rule models in the absence of an external field when one of the u's is set equal to zero. We also note the striking resemblance to the critical condition (398) for the free-fermion model.

It is interesting to investigate the equivalent Ising lattice. (See also Wu, 1971b). For the basic model let

$$e_1 = e_2 = \varepsilon_1, \quad e_3 = e_4 = \varepsilon_2, \quad e_5 = e_6 = \varepsilon_3, \quad e_7 = e_8 = \varepsilon_4. \tag{401}$$

It is then easy to see from (30) that the corresponding Ising lattice has a four-body interaction:

$$\begin{aligned} J_0 &= -\tfrac{1}{4}(\varepsilon_1 + \varepsilon_2 + \varepsilon_3 + \varepsilon_4), \\ J_1 &= J_2 = 0, \\ J' &= \tfrac{1}{4}(-\varepsilon_1 + \varepsilon_2 + \varepsilon_3 - \varepsilon_4), \\ J &= \tfrac{1}{4}(-\varepsilon_1 + \varepsilon_2 - \varepsilon_3 + \varepsilon_4), \\ J_4 &= \tfrac{1}{4}(-\varepsilon_1 - \varepsilon_2 + \varepsilon_3 + \varepsilon_4). \end{aligned} \tag{402}$$

**Added in proof.* The basic eight vertex problem without a field has been solved by Baxter (1971b, 1972).

The four-body interaction J_4 vanishes if we have the further constraint

$$\varepsilon_1 + \varepsilon_2 = \varepsilon_3 + \varepsilon_4. \tag{403}$$

The Ising lattice now decomposes into two independent simple square lattices with interaction $J' = \frac{1}{2}(-\varepsilon_1 + \varepsilon_3)$, $J = \frac{1}{2}(\varepsilon_2 - \varepsilon_3)$. Consequently the model is now exactly soluble. The critical condition $\sinh|2\beta J| \sinh|2\beta J'| = 1$ reduces, of course, to (400) upon introducing (403). Furthermore, the free energy for the basic ferroelectric model specified by (401, 403) is given by

$$\mathscr{F} = -\tfrac{1}{2}(\varepsilon_1 + \varepsilon_2) + \mathscr{F}_{\text{Ising}}(J, J'). \tag{404}$$

A special case is the *modified F model* (Wu, 1969b) with $\varepsilon_1 = \varepsilon_2 = \varepsilon$, $\varepsilon_3 = 0$, $\varepsilon_4 = 2\varepsilon$, which can be considered as the Rys F model modified by introducing vertices (7) and (8) with energy 2ε. We see that the infinite order transition of the F model now goes over to an Ising type transition with a logarithmic singularity in the specific heat. The transition temperature is given by

$$\frac{kT_0}{\varepsilon} = 1/\ln(\sqrt{2} + 1) = 1{\cdot}13459\ldots. \tag{405}$$

B. The sixteen vertex problem

The partition function Z for the sixteen vertex problem has been given in (25). Again, as in Section VI.A, we may obtain a number of symmetry relations for Z by some general considerations. From the fact that Z, being a sum over all configurations, is invariant if the arrows in a given direction are reversed in the enumeration of the configurations, we obtain

$$\begin{aligned} Z \equiv\ & Z(1,2,3,4,5,6,7,8;9,10,11,12,13,14,15,16) \\ =\ & Z(3,4,1,2,8,7,6,5;11,16,9,14,15,12,13,10) \\ =\ & Z(4,3,2,1,7,8,5,6;15,12,13,10,11,16,9,14) \\ =\ & Z(2,1,4,3,6,5,8,7;13,14,15,16,9,10,11,12), \end{aligned} \tag{406}$$

where each numeral ξ stands for the dependence on the weight ω_ξ. Also Z is invariant if all horizontal arrows are reversed and at the same time left and right are interchanged (looking in a mirror), and similarly for the vertical arrows. We find

$$\begin{aligned} Z =\ & Z(1,2,3,4,7,8,5,6;9,12,11,10,13,16,15,14) \\ =\ & Z(1,2,3,4,8,7,6,5;11,10,9,12,15,14,13,16) \\ =\ & Z(1,2,4,3,5,6,8,7;12,11,10,9,16,15,14,13) \\ =\ & Z(1,2,4,3,6,5,7,8;10,9,12,11,14,13,16,15). \end{aligned} \tag{407a}$$

By rotating the lattice 90°, we also obtain from (406)

$$\begin{aligned} Z &= Z(1,2,4,3,7,8,6,5;10,11,12,9,14,15,16,13) \\ &= Z(3,4,2,1,6,5,7,8;16,9,14,11,12,13,10,15) \\ &= Z(4,3,1,2,5,6,8,7;12,13,10,15,16,9,14,12) \\ &= Z(2,1,3,4,8,7,5,6;14,15,16,13,10,11,12,9). \end{aligned} \tag{407b}$$

We can also apply the weak graph series expansion to Z and obtain the result that Z is invariant under the change $\omega_i \to \omega_i'$, where, in an obvious notation,

$$\begin{aligned}
\omega_1' &= \tfrac{1}{4}[\omega_1+\omega_2+\omega_3+\omega_4+\omega_5+\omega_6+\omega_7+\omega_8+\omega_9+\omega_{10}+\omega_{11}+\omega_{12} \\
&\qquad +\omega_{13}+\omega_{14}+\omega_{15}+\omega_{16}] \\
\omega_2' &= \tfrac{1}{4}[(1+2+3+4+5+6+7+8)-(9+10+11+12+13+14+15+16)] \\
\omega_3' &= \tfrac{1}{4}[(1+2+3+4)-(5+6+7+8)+(10+12+14+16) \\
&\qquad -(9+11+13+15)] \\
\omega_4' &= \tfrac{1}{4}[(1+2+3+4)-(5+6+7+8)-(10+12+14+16) \\
&\qquad +(9+11+13+15)] \\
\omega_5' &= \tfrac{1}{4}[(1+2+5+6)-(3+4+7+8)-(9+12+13+16) \\
&\qquad +(10+11+14+15)] \\
\omega_6' &= \tfrac{1}{4}[(1+2+5+6)-(3+4+7+8)+(9+12+13+16) \\
&\qquad -(10+11+14+15)] \\
\omega_7' &= \tfrac{1}{4}[(1+2+7+8)-(3+4+5+6)-(9+10+13+14) \\
&\qquad +(11+12+15+16)] \\
\omega_8' &= \tfrac{1}{4}[(1+2+7+8)-(3+4+5+6)+(9+10+13+14) \\
&\qquad -(11+12+15+16)] \\
\omega_9' &= \tfrac{1}{4}[(2+3+5+7)-(1+4+6+8)-(10+11+12+13) \\
&\qquad +(9+14+15+16)] \\
\omega_{10}' &= \tfrac{1}{4}[(2+4+6+7)-(1+3+5+8)-(9+11+12+14) \\
&\qquad +(10+13+15+16)] \\
\omega_{11}' &= \tfrac{1}{4}[(2+3+6+8)-(1+4+5+7)-(9+10+12+15) \\
&\qquad +(11+13+14+16)] \\
\omega_{12}' &= \tfrac{1}{4}[(2+4+5+8)-(1+3+6+7)-(9+10+11+16) \\
&\qquad +(12+13+14+15)] \\
\omega_{13}' &= \tfrac{1}{4}[(2+3+5+7)-(1+4+6+8)+(10+11+12+13) \\
&\qquad -(9+14+15+16)] \\
\omega_{14}' &= \tfrac{1}{4}[(2+4+6+7)-(1+3+5+8)+(9+11+12+14) \\
&\qquad -(10+13+15+16)] \\
\omega_{15}' &= \tfrac{1}{4}[(2+3+6+8)-(1+4+5+7)+(9+10+12+15) \\
&\qquad -(11+13+14+16)] \\
\omega_{16}' &= \tfrac{1}{4}[(2+4+5+8)-(1+3+6+7)+(9+10+11+16) \\
&\qquad -(12+13+14+15)].
\end{aligned} \tag{408}$$

This relation reduces to (391) if $\omega_{2n-1} = \omega_{2n}$ for $n = 1, 2, 3, 4$ and $\omega_n = 0$ for $n > 8$.

We saw in Section II.D that the most general sixteen vertex problem is equivalent to an Ising model with 2, 3 and 4 body interactions and with an external magnetic field. Consequently the evaluation of Z in the most general case is extremely difficult. This equivalence with an Ising model, however, does provide us with a means to deduce useful information about the ferroelectrics. In particular, the ferroelectric problem is soluble if the corresponding Ising model has a known solution. Most of our understanding of the general ferroelectric models is based on this kind of reasonings (Wu, 1969a, 1970). We summarize the main results in the following (see also Wu, 1972):

(1) The modified F model mentioned at the end of the last section is also soluble if the vertices (9)–(16) are included with an energy ε. The energies of this general F model is given by (33) with $E_0 = E_4 = E_2 = \varepsilon$, $E_2' = 0$, $E_2'' = 2\varepsilon$ and $E_1 = E_3 = \varepsilon$. It is then easy to see from (36) that the corresponding Ising lattice is a simple square one with interactions $+\frac{1}{4}\varepsilon$ and $-\frac{1}{4}\varepsilon$ along the two axes respectively. This general F model therefore has an Ising-type transition. In particular, the specific heat has a logarithmic singularity near the transition temperature given by

$$kT_0/\varepsilon = 1/2 \ln (\sqrt{2} + 1) = 0{\cdot}567296 \ldots . \tag{409}$$

(2) If we consider the F model and include other types of vertices with energies

$$\begin{aligned} e_7 &= e_8 = b\varepsilon, \\ e_9 &= e_{10} = \ldots = e_{16} = a\varepsilon \end{aligned} \tag{410}$$

but with $b = 4a - 2$ and arbitrary a, the equivalent Ising interactions can be computed from (36) with $E_0 = E_2 = E_4 = \varepsilon$, $E_2' = 0$, $E_1 = E_3 = a\varepsilon$ and $E_2'' = (4a - 2)\varepsilon$. We find

$$\begin{aligned} J_0 &= -a\varepsilon, \\ J_1 &= J_3 = J_4 = 0, \\ J_2' &= -J_2'' = \tfrac{1}{4}(2a - 1)\varepsilon, \\ J_2 &= \tfrac{1}{2}(a - 1)\varepsilon. \end{aligned} \tag{411}$$

The resulting Ising lattice has two-body interactions only, but with crossed bonds, and is shown in Fig. 44. For $a = 1$ or $J_2 = 0$, the Ising model is exactly soluble; this is the case considered in (1) above. For $a \neq 1$, the Ising model cannot be solved exactly. However, it is generally believed, and strongly supported by results of numerical analysis (Dalton and Wood, 1969), that

the critical behaviour of the Ising model is essentially unchanged for short-range two-body interactions. Therefore we may infer that the behaviour of this class of general antiferroelectrics is the same as the Ising model. In particular the specific heat exhibits a logarithmic singularity.

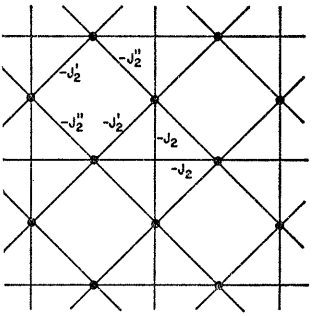

FIG. 44. The equivalent Ising lattice for the general KDP and F models. The dots denote the spins and the lines denote the interactions.

(3) If we consider the KDP model and include other types of vertices with energies (410) with $b = 4a - 2$, the equivalent Ising lattice is again that given in Fig. 44. From (36) and $E_0 = E_4 = 0$, $E_2 = E_2' = \varepsilon$, $E_1 = E_3 = a\varepsilon$, $E_2'' = (4a - 2)\varepsilon$, we find

$$\begin{aligned} J_0 &= -a\varepsilon, \\ J_1 &= J_3 = J_4 = 0, \\ J_2 &= J_2' = \tfrac{1}{4}(2a - 1)\varepsilon, \\ J_2'' &= -\tfrac{1}{2}(a - 1)\varepsilon. \end{aligned} \tag{412}$$

As in (2) above, we conclude that the critical behaviour of this class of general ferroelectrics is the same as for the Ising model.

Several interesting observations emerge from these results. For both the KDP and the F models, the inclusion of the energies (410) for finite a and b always appears to lead to an Ising-type transition. On the other hand, the exact solution for $a = b = \infty$ (the ice rule) is known; the F model has a peculiar infinite order transition and the KDP model has a first-order transition. Thus the critical behaviour is drastically changed when the ice rule is relaxed.

Two cases of the general antiferroelectric F model are exactly soluble. For $a = \infty$, $b = 2$ we have the solution (404). For $a = 1$, $b = 2$ the model is soluble as discussed in (1) above. Furthermore for $a = \frac{1}{2}$, $b = 0$ we have

$T_0 = 0$ since (411) reduces to a linear Ising chain. It is then instructive to compare the behaviour of the specific heat in these soluble cases. In general we expect the transition temperature to rise with a and b. This is so because, as a or b increases, the disordered states will carry smaller statistical weights. As a result, the transtion temperature cannot decrease. This is certainly the case in these soluble cases as shown in Fig. 45 where we plot the specific heat. Our result seems to suggest that, as $a \to \infty$, $b \to \infty$, the width of the "spike" in the specific heat eventually disappears. As a consequence, the phase transition becomes an infinite order one. The dashed curve in Fig. 45 illustrates one residual "spike" expected for some large a and b.

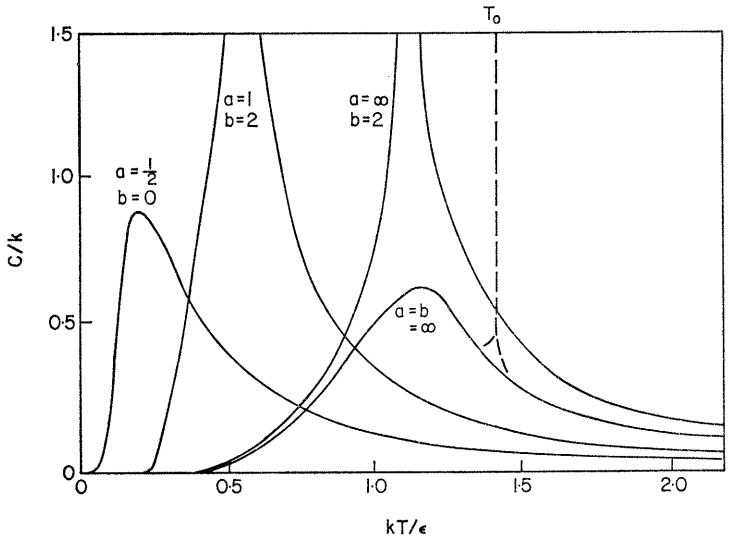

FIG. 45. The specific heat per vertex for the general F model described by $\varepsilon_1 = 0$, $\varepsilon_2 = \varepsilon$ and (410). The dashed curve illustrates the residual "spike" expected for some large a and b at $kT_0/\varepsilon = 1/(\ln 2) = 1{\cdot}44$. $e_7 = e_8 = b\varepsilon$ and $e_9 = \ldots = e_{16} = a\varepsilon$. (From Wu, 1969a.)

For the KDP model with the ice rule, however, the specific heat vanishes identically below T_0 and has a $(T - T_0)^{-1/2}$ singularity above T_0 in the limit $a \to \infty$, $b \to \infty$. This singularity is highly asymmetric about T_0. Therefore at least for some large values of a and b, the specific heat also has a highly asymmetric appearance. Furthermore, since the equivalence of the general ferroelectric model with an Ising model is not restricted to two-dimensional models, one may then use the experimentally observed critical behaviour of the ferroelectrics to deduce some useful information on the three-dimensional Ising model. Thus, if one believes that the model described here adequately describes the hydrogen-bonded ferroelectrics, then the logarithmic diver-

gence (Reese, 1969) observed in the heat capacity of KH_2PO_4 (KDP) for $T \cong T_0-$ may be taken to indicate that the specific heat of the three-dimensional Ising model also possesses a logarithmic singularity ($\alpha' = 0$). This is certainly not far from the value $\alpha' = 1/16$ determined by numerical analysis.

VII. Other Lattice Models (Rodney J. Baxter, *Department of Theoretical Physics I.A.S., The Australian National University, Canberra, A.C.T., Australia*)

In this section we outline some other lattice models which can also be solved by using a Bethe-type *ansatz* for the eigenvector of the transfer matrix.

A. The general three colour problem on a square lattice

As has been pointed out in Section II (and Baxter, 1970c), the solution of the ice model also gives the number of ways of colouring all the faces of a square lattice with three colours A, B, C (or simply 1, 2, 3) so that no two adjacent faces are coloured alike.

We can regard these colours as three types of particles and associate activities z_1, z_2, z_3 with them. The problem then becomes to evaluate the generating function (grand-partition function)

$$Z = \sum z_1^{N1} z_2^{N2} z_3^{N3}\, G(N_1, N_2, N_3), \tag{413}$$

where $G(N_1, N_2, N_3)$ is the number of allowed colourings such that N_1 faces are coloured 1, N_2 are coloured 2, and N_3 are coloured 3. The summation is over all non-negative integers N_1, N_2, N_3 such that

$$N_1 + N_2 + N_3 = N_t, \tag{414}$$

where N_t is the total number of faces of the lattice.

1. *Transfer Matrix*

We consider a lattice of M rows and N columns wound on a torus (so that $N_t = MN$). Using the three-to-one morphism between colourings of the lattice and ice configurations, we can verify that Z is again given by (74)–(78). However, the activities z_1, z_2, z_3 must now be included in the transfer matrix, and to specify a colouring ϕ of a row it is necessary to know not only the locations $x_1, \ldots, x_n$ of the down arrows, but also the colour of one of the faces.

Let σ (= 1, 2, or 3) be the colour of the extreme end face of a row, between columns N and 1, and let $f_\sigma(\mathbf{X})$ be the element of ψ corresponding to this state. Then the transfer matrix equation analogous to (78) is

$$\Lambda f_\sigma(\mathbf{X}) = D_\sigma(\mathbf{X})\,\{\textstyle\sum_R f_{\sigma+1}(\mathbf{Y}) + \sum_L f_{\sigma+2}(\mathbf{Y})\}, \tag{415}$$

where we adopt the obvious modulo 3 convention

$$f_{\sigma+3}(\mathbf{X}) \equiv f_\sigma(\mathbf{X}) \tag{416}$$

and $D_\sigma(\mathbf{X})$ is the product of the activities in the row. We find that

$$D_\sigma(\mathbf{X}) = (z_1 z_2 z_3)^{N/3} \prod_{j=1}^{n} \zeta(x_j + j + \sigma) \tag{417}$$

where

$$\zeta(\sigma) = \frac{z_\sigma z_{\sigma+1}}{(z_1 z_2 z_3)^{2/3}} \equiv \zeta(\sigma + 3). \tag{418}$$

We note also that for the colouring to be consistent with the toroidal boundary conditions, N and n must be such that

$$N - 2n = 3 \times \text{integer}. \tag{419}$$

2. *Bethe Ansatz*

Some inspection of equations (415)–(417) suggests that the appropriate analogue of Bethe ansatz for this model is to try

$$f_\sigma(\mathbf{X}) = \sum_P \mathfrak{A}'(P) \prod_{j=1}^{n} \phi_{Pj}(x_j + j + \sigma), \tag{420}$$

where $\{P1, P2, \ldots, Pn\}$ is some permutation P of the integers $\{1, 2, \ldots, n\}$, and the summation is over all $n!$ such permutations. The coefficients $\mathfrak{A}'(P)$ and the single-particle functions $\phi_1(x), \ldots, \phi_n(x)$ are yet to be determined.

We can ensure that the condition (416) is satisfied by requiring that there exist wave numbers $k_1, \ldots, k_n$ such that

$$\phi_j(x + 3) = \phi_j(x) \exp(3ik_j) \tag{421}$$

and

$$k_1 + \ldots + k_n = 0. \tag{422}$$

Thus $\phi_j(x)$ can be regarded as a plane wave modulo 3. The condition (422) implies that we are seeking a translation–invariant eigenvector of the transfer matrix, which we expect to correspond to the maximum eigenvalue.

When $z_1 = z_2 = z_3$ we regain the ice problem and expect the functions $\phi_j(x)$ to be pure plane waves. To maintain the analogy between the models it is convenient to work not with the coefficients $\mathfrak{A}'(P)$, but rather a new set

$$\mathfrak{A}(P) = \mathfrak{A}'(P) \exp\left\{ i \sum_{j=1}^{n} j k_{Pj} \right\}. \tag{423}$$

When $z_1 = z_2 = z_3$ these coefficients $\mathfrak{A}(P)$ should reduce to those of the ice model.

Inserting (420) into (415), we find that the right-hand side can be classified into "wanted" terms, "unwanted internal terms" and "unwanted boundary terms" in the same way as the ferroelectric problems. The wanted terms on both sides of the equation are equal (for n even) provided

$$\Lambda = 2(z_1 z_2 z_3)^{N/3} \gamma_1 \dots \gamma_n, \tag{424}$$

where γ_j and $\phi_j(x)$ are defined in terms of the wave number k_j by (421) and

$$\gamma_j \left\{ \frac{\phi_j(x)}{\zeta_j(x)} - \frac{\phi_j(x+1)}{\zeta_j(x+1)} \right\} = \phi_j(x+2). \tag{425}$$

Equations (421) and (425) form a cubic eigenvalue equation for γ_j in terms of k_j, the solution of which can be written as $\gamma_j = \gamma(k_j)$, where

$$\gamma(k) = \frac{i}{g(k)} e^{3ik/2} \tag{426}$$

and the function $g = g(k)$ is defined by

$$g^3 - 3Sg + 2 \sin(3k/2) = 0. \tag{427}$$

The constant S is given by

$$\begin{aligned} 3S &= \zeta(1) + \zeta(2) + \zeta(3) \\ &= \frac{z_2 z_3 + z_3 z_1 + z_1 z_2}{(z_1 z_2 z_3)^{2/3}}. \end{aligned} \tag{428}$$

The requirement that the unwanted internal terms cancel again leads to equations of the form (142), i.e.

$$\mathfrak{A}(P) = \mathfrak{A}(Q) B(k_l, k_m) \tag{429}$$

for all permutations $P = \{\dots, l, m, \dots\}$ and associated permutations $Q = \{\dots, m, l, \dots\}$ (i.e. P and Q differ only in the interchange of two successive indices). At first sight it appears in this problem that there are three conditions of this type, but some investigation reveals that they are identical, and that in each case

$$B(p, q) = -s(q, p)/s(p, q), \tag{430}$$

where

$$s(p, q) = g(p) \exp\left\{ i\left(q + \frac{p}{2} \right) \right\} + g(q) \exp\left\{ -i\left(p + \frac{q}{2} \right) \right\}. \tag{431}$$

Solving (429) for the coefficients $\mathfrak{A}(P)$ and substituting the result into the condition that the unwanted boundary terms vanish, we obtain the equations

$$\exp(iNk_j) = \prod_{\substack{i=1 \\ \neq j}}^{n} B(k_j, k_i), \qquad j = 1, \ldots, n. \tag{432}$$

The equations (432) define the k's, from which the eigenvalue Λ is given by (424, 426, 427). Notice that the activities z_1, z_2, z_3 enter these equations in a non-trivial way only through the single parameter S. Why this should be so is not apparent.

When $z_1 = z_2 = z_3$, $S = 1$ and (427) has the solution $g(p) = -2\sin(p/2)$. Substituting this into the above equations, the ice-model results are regained.

3. *The Limit $N \to \infty$*

As with the square lattice ferroelectric models, we assume that in the limit of N large the k's fill some interval $-Q \leqslant k \leqslant Q$, so that the number of k's between k and $k + \mathrm{d}k$ is $N\rho(k)\,\mathrm{d}k$. Setting

$$B(p, q) = -\exp[-i\theta(p, q)], \tag{433}$$

it follows as before that (432) leads to the integral equation (167) for $\rho(k)$, namely

$$1 = 2\pi\rho(k) - \int_{-Q}^{Q} \frac{\partial\theta(k, q)}{\partial k}\rho(q)\,\mathrm{d}q, \tag{434}$$

while Q is given by the condition (165), namely,

$$\tfrac{1}{2}(1 - y) \equiv \frac{n}{N} = \int_{-Q}^{Q} \rho(q)\,\mathrm{d}q. \tag{435}$$

Also, in this limit (76) and (424) for Z and Λ become

$$\begin{aligned} z(y) &= \lim_{\substack{M\to\infty \\ N\to\infty}} \frac{1}{MN} \ln Z = \lim_{N\to\infty} \frac{1}{N} \ln \Lambda(y) \\ &= \tfrac{1}{3}\ln(z_1 z_2 z_3) + \int_{-Q}^{Q} \rho(k) \ln \gamma(k)\,\mathrm{d}k. \end{aligned} \tag{436}$$

Still pursuing the analogy with the ferroelectric models, we look for a change of variables that reduces (434) to an integral equation with a difference

kernel and find that one exists, namely a transformation from k to a variable α defined by

$$\frac{\mathrm{d}\alpha}{\mathrm{d}k} = \frac{L}{S - g^2(k)}, \tag{437}$$

where L is a constant.

Choosing $\alpha = 0$ when $k = 0$ and writing α as a function of k as $\alpha(k)$, and k as a function of α as $k\{\alpha\}$, we find that

$$\theta(p, q) = k\{\alpha(p) - \alpha(q)\}. \tag{438}$$

Defining a density function $R(\alpha)$ such that $R(\alpha)\,\mathrm{d}\alpha = 2\pi\rho(k)\,\mathrm{d}k$, the integral equation (434) in the transformed variables becomes

$$R(\alpha) = \xi(\alpha) + \frac{1}{2\pi}\int_{-b}^{b} \xi(\alpha - \beta)\, R(\beta)\,\mathrm{d}\beta, \tag{439}$$

where

$$\xi(\alpha) = \frac{\mathrm{d}k}{\mathrm{d}\alpha} = \frac{1}{L}\{S - g^2\} \tag{440}$$

(regarding g now as a function of α, rather than k).

Also, (435) and (436) become

$$\pi(1 - y) = \int_{-b}^{b} R(\alpha)\,\mathrm{d}\alpha, \tag{441}$$

$$z(y) = \tfrac{1}{3}\ln(z_1 z_2 z_3) - \tfrac{1}{2}\int_{-b}^{b} R(\alpha)\ln g^2(\alpha)\,\mathrm{d}\alpha \tag{442}$$

(using (426) and (422)).

4. *Solution of the Integral Equation*

Eliminating k between (427) and (437), we find that

$$\frac{\mathrm{d}g}{\mathrm{d}\alpha} = \frac{1}{2L}\{4 - g^2(3S - g^2)^2\}^{1/2}. \tag{443}$$

This equation can be integrated using elliptic functions (Sections 3.147.2 and 8.11–8.15 of Gradshteyn and Ryzhik, 1965). Let u, v, w be the three values of x which satisfy the cubic equation

$$x(3S - x)^2 - 4 = 0. \tag{444}$$

Since $S \geqslant 1$, these roots are real and positive. Choosing them so that

$$u > v \geqslant w \tag{445}$$

and letting

$$L = \tfrac{1}{2}\{(u-w)v\}^{\frac{1}{2}}, \tag{446}$$

we find that

$$g^2(\alpha) = \frac{uw\,\mathrm{sn}^2(\alpha)}{u - w + w\,\mathrm{sn}^2(\alpha)}, \tag{447}$$

where $\mathrm{sn}(\alpha)$ is the usual elliptic sn function (Gradshteyn and Ryzhik, 1965), with

$$\kappa = \left\{\frac{(u-v)\,w}{(u-w)\,v}\right\}^{\frac{1}{2}}. \tag{448}$$

Fourier analyzing, we find that

$$\xi(\alpha) = \frac{\pi}{\mathbf{K}} \sum_{m=-\infty}^{\infty} \frac{\exp(i\pi m\alpha/\mathbf{K})}{r^m + 1 + r^{-m}}, \tag{449}$$

where $\mathbf{K}$ is the complete elliptic integral of modulus κ, $\mathbf{K}'$ is the complete elliptic integral of conjugate modulus $\kappa' = (1-\kappa^2)^{1/2}$, and

$$r = \exp(-2\pi\mathbf{K}'/3\mathbf{K}). \tag{450}$$

Clearly $\xi(\alpha)$ is periodic with period $2\mathbf{K}$. Hence when $b = \mathbf{K}$ and $Q = \pi/3$ the integral equation (439) can be solved by Fourier series, giving

$$R(\alpha) = \frac{\pi}{\mathbf{K}} \sum_{m=-\infty}^{\infty} \frac{\exp(i\pi m\alpha/\mathbf{K})}{r^m + r^{-m}}. \tag{451}$$

Substituting this result into the condition (441), we find that

$$n = N/2 \text{ or } y = 0, \tag{452}$$

i.e. there are as many down arrows as up arrows in each row of the lattice. As with the ice model, we expect this value of n to correspond to the maximum eigenvalue of the transfer matrix.

We now evaluate the partition function by first Fourier analyzing $\ln\{g^2(\alpha)\}$, giving

$$\ln\{g^2(\alpha)\} = -\frac{4\pi\mathbf{K}'}{9\mathbf{K}} - 2\sum_{m=1}^{\infty} \frac{(1-r^{2m})\cos(\pi m\alpha/\mathbf{K})}{m(r^{2m} + r^m + 1)}. \tag{453}$$

Substituting (451) and (453) into (442) and performing the integration, it follows that

$$z(0) = \tfrac{1}{3}\ln(z_1 z_2 z_3) + \frac{\pi \mathbf{K}'}{9\mathbf{K}}$$

$$+ \sum_{m=1}^{\infty} \frac{r^m - r^{3m}}{m(1 + r^{2m})(1 + r^m + r^{2m})}, \tag{454}$$

This series can be summed to give

$$W = \lim_{\substack{M\to\infty \\ N\to\infty}} Z^{1/MN}, \tag{455}$$

where

$$W = \mathrm{e}^{z(0)} = (z_1 z_2 z_3)^{1/3} \frac{4uvw^{\frac{1}{2}}}{[(u-w)^3 u]^{\frac{1}{2}} - [(v-w)^3 v]^{\frac{1}{2}}}. \tag{456}$$

To summarize: the parameter S is defined by (428); u, v, w by (444) and (445); and the partition function by (455, 456). Thus W is an algebraic function of the activities z_1, z_2, z_3. We can verify that it is analytic for all real positive values of z_1, z_2, z_3 except when $z_1 = z_2 = z_3$.

This non-analytic case is equivalent to the ice-model. In particular, if $z_1 = z_2 = z_3 = 1$, we find that $S = 1$, $u = 4$, $v = w = 1$ and

$$W = (\tfrac{4}{3})^{3/2}, \tag{457}$$

which is the ice model result (4).

5. *Hard Squares Model*

If we regard colour 1 as particles and colours 2 and 3 as forming a background, then we have a model which is similar to hard-square lattice gas (Gaunt and Fisher, 1965). Letting z be the activity of the "particles", we set

$$z_1 = z, \quad z_2 = z_3 = 1. \tag{458}$$

The density of particles is then

$$\rho = z \frac{\mathrm{d}\ln W}{\mathrm{d}z}, \tag{459}$$

and cannot exceed the close-packed value of $\frac{1}{2}$.

Substituting the expressions (458) for the activities into the above equations, we find that the two smaller roots of (444) cross over as z passes the

value unity. Thus W is a different algebraic function of z according to whether $z < 1$ or $z > 1$. At $z = 1$ the system undergoes a phase transition from a fluid to a solid state, the corresponding density being $\rho = 1/3$.

Consider W as a function of ρ. When $0 \leqslant \rho \leqslant 1/3$, W is the positive real root of the equation

$$W^4 - \sigma^2(4 + 8\sigma - 27\sigma^4)W^2 - 16\sigma^6 = 0 \tag{460}$$

where

$$\sigma = 1 - \rho; \tag{461}$$

when $\frac{1}{3} \leqslant \rho < \frac{1}{2}$, W is given very simply by

$$W^2 = \frac{4(1-\rho)^4}{1-2\rho}. \tag{462}$$

Both these expressions for W are analytic functions of ρ throughout the entire permissible range $0 \leqslant \rho < \frac{1}{2}$. However, it is apparent that one is not the analytic continuation of the other. Taylor expanding each expression about the transition density $\rho = 1/3$ gives

$$\ln W = \tfrac{3}{2}\ln\tfrac{4}{3} \pm \tfrac{3}{4}(3\rho - 1)^2 + O\{(3\rho - 1)^3\}, \tag{463}$$

the plus sign applying for $\rho > 1/3$, the minus sign for $\rho < 1/3$. Thus $dW/d\rho$ is zero at the transition point and the compressibility is infinite.

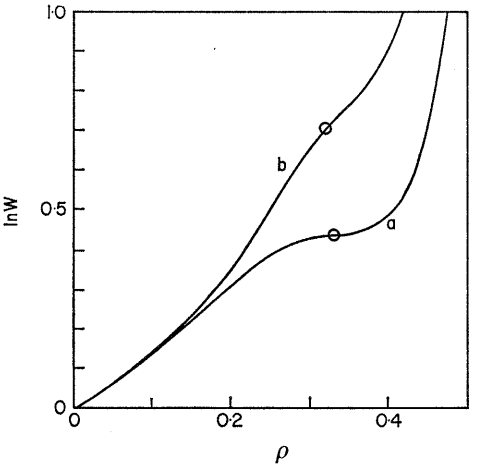

FIG. 46. Equation of state of: (a) Baxter's hard-square model; (b) the true hard-square lattice gas (Gaunt and Fisher, 1965). The circles indicate critical points. (From Baxter, 1970c.)

The grand-potential $\ln W$ is plotted in Fig. 46, together with the corresponding function for the true hard-square lattice gas. The two models agree well at low densities, but there are considerable differences in the transition region and above.

B. The F model on a triangular lattice

One can formulate ferroelectric-type models on any lattice of even coordination number, the analogue of the ice condition being that the number of arrows into and out of each vertex should be equal (see discussions in Section II.A).

Consider in particular the plane triangular lattice (coordination number 6) and place arrows on the bonds of the lattice so that there are three entering and leaving each vertex (Baxter, 1969). There are then 20 possible configurations of arrows at a vertex. If configurations which differ only by rotation or reflection are treated alike, they can be classified as follows: (i) 6 configurations in which the incoming arrows are adjacent, (ii) 2 configurations in which the incoming and outgoing arrows alternate round the vertex, (iii) 12 configurations containing two incoming arrows directly opposite one another. Examples of these are shown in Fig. 47.

If we assign interaction energies ε_1, ε_2, ε_3, respectively, to these three types of vertex configurations, then we have the triangular lattice analogue of the F model. When all three energies are zero, this in turn reduces to a triangular lattice "ice-model".

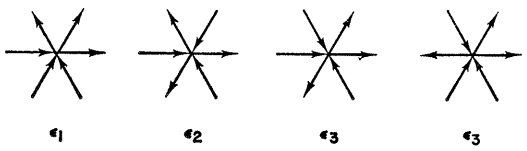

FIG. 47. Examples of the three types of allowed vertex configurations with corresponding vertex energies for the triangular lattice F model.

1. *Transfer Matrix Equation*

Consider a triangular lattice of M rows, each with $N/2$ vertices (N even), wound on a torus. Then there are N vertical (i.e. non-horizontal) bonds between two rows, which we label as in Fig. 48. As with the square lattice, we can see that if there are n down arrows in any row of vertical bonds, then there are n in every row. Again the partition function is given by (75) and (76), but the transfer matrix equation is more complicated. For the sake of clarity we write it down only for the case $n = 2$ and later state appropriate generalizations for arbitrary n.

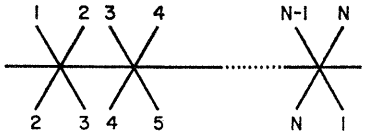

FIG. 48. Labelling of the bonds of the triangular lattice.

When $n = 2$ the transfer matrix equation is

$$\begin{aligned} \Lambda f(x_1, x_2) = &\sum_{y_1=1}^{x_1'} \sum_{y_2=x_1'-1}^{x_2'} D_R(\mathbf{X}, \mathbf{Y}) f(y_1, y_2) \\ &+ \sum_{y_1=x_1'-1}^{x_2'} \sum_{y_2=x_2'-1}^{N} D_L(\mathbf{X}, \mathbf{Y}) f(y_1, y_2) \\ &- u^{N-2} \sum_{j=1}^{2} \{c_e(x_j) f(x_j' - 1, x_j' - 1) \\ &+ uw f(x_j', x_j' - 1) + (vw - w^2) f(x_j' - 1, x_j') \\ &+ c_0(x_j) f(x_j', x_j')\}, \end{aligned} \tag{464}$$

where

$$\begin{aligned} x_j' &= x_j + 2 \quad \text{if } x_j \text{ is odd}, \\ &= x_j + 1 \quad \text{if } x_j \text{ is even}, \end{aligned} \tag{465}$$

$$u = \exp(-\beta\varepsilon_1), \quad v = \exp(-\beta\varepsilon_2), \quad w = \exp(-\beta\varepsilon_3), \tag{466}$$

$$\begin{aligned} &c_e(x) = w^2 \text{ and } c_0(x) = uv \quad \text{if } x \text{ is odd}, \\ &c_e(x) = uv \text{ and } c_0(x) = w^2 \quad \text{if } x \text{ is even}, \end{aligned} \tag{467}$$

$$D_R(\mathbf{X}, \mathbf{Y}) = u^{N-4}\, \mathrm{d}_R(x_1, y_1)[\mathrm{d}_R(x_2, y_2) + \mathrm{d}_L(x_1, y_2)]$$

$$D_L(\mathbf{X}, \mathbf{Y}) = u^{N-4}[\mathrm{d}_R(x_2, y_1) + \mathrm{d}_L(x_1, y_1)][w^2 + \mathrm{d}_L(x_2, y_2)], \tag{468}$$

and $\mathrm{d}_R(x, y)$, $\mathrm{d}_L(x, y)$ have the values given in the following table (defining x' in terms of x according to (465)):

		$y < x' - 1$	$y = x' - 1$	$y = x'$	$y > x'$
$\mathrm{d}_R(x, y)$:	x odd	w^2	uw	u^2	
	x even	w^2	uv	uw	
$\mathrm{d}_L(x, y)$:	x odd		$uw - w^2$	$uv - w^2$	0
	x even		$u^2 - w^2$	$uw - w^2$	0

The first two terms on the right-hand side of (464) are clearly analogous to those occurring in the square-lattice models. The others are correction terms which subtract off the contributions from the cases when $y_2 \leqslant y_1$ and ensure the correct weight when $y_1 = x_j' - 1$ and $y_2 = x_j'$. [Note that we are not using the * convention of eqn (89).]

Equation (464) is valid in the domain $1 \leqslant x_1, x_1' < x_2', x_2 \leqslant N$, provided that on the right-hand side we adopt the convention that

$$f(y, N+1) = f(1, y). \tag{469}$$

The only other cases are when both down arrows in the upper row point into the same vertex, so that $x_1' = x_2'$. Using the above definitions of D_L and D_R, we find that (464) is also valid for these cases, provided

$$v = (u^2 - uw + w^2)/u \tag{470}$$

and the values of $f(x, x-1)$ and $f(x, x)$ we use in (464) are such that

$$uw[f(x'-1, x'-1) + f(x', x')] + u^2 f(x', x'-1) - (u^2 + uw - w^2) f(x'-1, x') = 0 \tag{471}$$

for all odd integers x'.

Clearly (470) is a restriction on the allowed values of the vertex weights u, v, w. It turns out that we can solve the F model on a triangular lattice only when this condition is satisfied. Note that this includes the triangular "ice-model", when u, v, w are equal.

2. *Bethe Ansatz*

We now make a guess at the form of the eigenvector f and substitute it into the transfer matrix equation (464). The generalization of the resulting equations to arbitrary n is straightforward, so we consider the general case.

Some inspection of (464) suggests that the appropriate analogue of Bethe ansatz for this system is

$$f(\mathbf{X}) = \sum_P \mathfrak{A}(P) \prod_{j=1}^{n} \phi_{Pj}(x_j), \tag{472}$$

where the summation is over all $n!$ permutations P, as in (420). Due to the difference between odd and even vertical bonds, we cannot expect the single-particle functions $\phi_1(x), \ldots, \phi_n(x)$ to be simple plane waves (as in the

square lattice F model). Rather we expect them to be plane waves modulo 2, i.e. there exist wave numbers $k_1, \ldots, k_n$ such that

$$\phi_j(x+2) = \phi_j(x) \exp(2ik_j). \tag{473}$$

Substituting this form for f into (464), the wanted terms on both sides are found to be equal provided

$$\Lambda = u^{\frac{1}{2}N-2n}\{\gamma_1^- \ldots \gamma_n^- + \gamma_1^+ \ldots \gamma_n^+\}, \tag{474}$$

γ_j^- and γ_j^+ being parameters such that

$$\gamma_j^- \phi_j(x) = \sum_{y=1}^{x'} \mathrm{d}_R(x, y)\phi_j(y) + C_j,$$

$$\gamma_j^+ \phi_j(x) = \sum_{y=1}^{x'} \mathrm{d}_L(x, y)\phi_j(y) - C_j \tag{475}$$

for all integers x, the domain of $\mathrm{d}_L(x, y)$ being extended by defining

$$\mathrm{d}_L(x, y) = -w^2 \quad \text{if } y < x' - 1. \tag{476}$$

The constants C_j are to be chosen so as to satisfy (473). Together with this condition, both the equations (475) form quadratic eigenvalue equations with eigenvector $\phi_j(x)$. It turns out that when the vertex weights satisfy the restriction (470) these equations can be simultaneously diagonalized, giving

$$\phi_j(x) = \exp\{i[k_j x - \tfrac{1}{2}(-1)^j g_j]\}, \tag{477}$$

where $g_j = g(k_j)$ and the function $g(k)$ is defined by

$$u \sin k = w \sin[g(k)]. \tag{478}$$

The eigenvalues $\gamma_j^{\pm}$ are then given by

$$\gamma_j^{\pm} = \frac{u^2 \mathrm{e}^{ik_j}}{2 \sin^2 g_j}\{[\sin(k_j + g_j)][2 \sin g_j - \sin k_j] \pm i[\sin k_j][1 + \cos(k_j + g_j)]\}. \tag{479}$$

Both the requirement that the unwanted internal terms in the transfer matrix equation cancel, and the condition (471), lead to equations of the

form (429). As with the three colouring problem it appears at first sight that we obtain three such sets of equations, but it turns out that they are in fact identical. We find that

$$B(p,q) = -\frac{1 + T(p)T(q) + \omega^{-1}T(q) + (\omega - 1 - \omega^{-1})T(p)}{1 + T(q)T(p) + \omega^{-1}T(p) + (\omega - 1 - \omega^{-1})T(q)} \tag{480}$$

where

$$\omega = w/u \tag{481}$$

and

$$T(p) = \exp\{i[p + g(p)]\}. \tag{482}$$

Again we find that the vanishing of the unwanted boundary terms leads to the equations

$$\exp(ik_jN) = \prod_{\substack{i=1 \\ \neq j}}^{n} B(k_j, k_i) \tag{483}$$

for $j = 1, \ldots, n$, as in (147) and (432). These also ensure that the condition (469) is satisfied.

The equations (483) determine the k's. The eigenvalues $\gamma_j^{\pm}$ and Λ are then given by the previous equations.

The relations between k_j, g_j, $\gamma_j^{\pm}$ can be simplified by expressing them in terms of $T_j = T(k_j)$. We find that

$$\exp(2ik_j) = T_j \frac{u + wT_j}{w + uT_j}, \tag{484}$$

$$\gamma_j^{-} = \frac{(u + wT_j)(uT_j + w - u)}{T_j - 1}, \tag{485}$$

$$\gamma_j^{+} = \frac{(u + wT_j)[(u - w)T_j - u]}{T_j - 1}. \tag{486}$$

3. *The Limit $N \to \infty$*

Once more we assume that in the limit of N large the k's fill some interval $-Q \leqslant k \leqslant Q$, with a density function $\rho(k)$. In this way we regain (433–435), while (436) is replaced by

$$z(y) = \lim_{\substack{M\to\infty \\ N\to\infty}} \frac{2}{MN} \ln Z = \lim_{N\to\infty} \frac{2}{N} \ln \Lambda(y)$$

$$= (2y - 1)\ln u + 2\int_{-Q}^{Q} \rho(k)\{\ln \gamma^{-}(k)\}\, dk, \tag{487}$$

where $y = 1 - 2n/N$ and $-kTz(y)$ is the free energy per vertex. $\gamma^-(k)$ is defined so that $\gamma_j^- = \gamma^-(k_j)$, and we have used the fact that the k's must occur in pairs $k, -k$, so that $\gamma_1^- \ldots \gamma_n^- = \gamma_1^+ \ldots \gamma_n^+$.

We now look for a transformation from k to a new variable α so as to reduce (434) to an integral equation with a difference kernel. We find that it is

$$T(k) = \frac{e^{i\mu} - e^{\alpha}}{e^{i\mu+\alpha} - 1} \quad \text{for } \omega < 3, \tag{488}$$

$$= \frac{e^{\lambda} - e^{-i\alpha}}{e^{\lambda-i\alpha} - 1} \quad \text{for } \omega > 3,$$

where μ and λ are defined by

$$\omega = 1 + 2\cos\mu, \qquad \omega < 3,$$

$$= 1 + 2\cosh\lambda, \qquad \omega > 3. \tag{489}$$

For definiteness we require that $0 < \mu < 2\pi/3$ and $\lambda > 0$.

Introducing a density function $R(\alpha)$ in the new variable, so that $R(\alpha)\,d\alpha = 2\pi\rho(k)\,dk$, the free energy per vertex, $-kTz(y)$, is given by

$$z(y) = \ln u + \frac{1}{2\pi}\int_{-b}^{b} R(\alpha)C(\alpha)\,d\alpha, \tag{490}$$

where

$$C(\alpha) = \ln\left\{\frac{(\cosh\alpha - \cos 3\mu)(\cosh\alpha - \cos 2\mu)}{(\cosh\alpha - \cos\mu)(\cosh\alpha - 1)}\right\}, \qquad \omega < 3,$$

$$= \ln\left\{\frac{(\cosh 3\lambda - \cos\alpha)(\cosh 2\lambda - \cos\alpha)}{(\cosh\lambda - \cos\alpha)(1 - \cos\alpha)}\right\}, \qquad \omega > 3. \tag{491}$$

The function $R(\alpha)$ and the limit b are determined by the integral equation

$$R(\alpha) = \xi(\alpha) - \int_{-b}^{b} K(\alpha - \beta)\,R(\beta)\,d\beta \tag{492}$$

and the condition

$$\pi(1 - y) = \int_{-b}^{b} R(\alpha)\,d\alpha, \tag{493}$$

where

$$\xi(\alpha) = \tfrac{1}{2}\left\{\frac{\sin\mu}{\cosh\alpha - \cos\mu} + \frac{\sin 2\mu}{\cosh\alpha - \cos 2\mu}\right\}, \quad \omega < 3,$$

$$= \tfrac{1}{2}\left\{\frac{\sinh\lambda}{\cosh\lambda - \cos\alpha} + \frac{\sinh 2\lambda}{\cosh 2\lambda - \cos\alpha}\right\}, \quad \omega > 3, \tag{494}$$

$$K(\alpha) = \frac{1}{2\pi}\frac{\sin 3\mu}{\cosh\alpha - \cos 3\mu}, \quad \omega < 3,$$

$$= \frac{1}{2\pi}\frac{\sinh 3\lambda}{\cosh 3\lambda - \cos\alpha}, \quad \omega > 3. \tag{495}$$

The integral equation (492) can be solved by Fourier transforms when $b = \infty$ and $\omega < 3$, or when $b = \pi$ and $\omega > 3$. We find that

$$R_0(\alpha) = \tfrac{1}{2}\int_{-\infty}^{\infty} \frac{e^{ik\alpha}}{2\cosh(k\mu) - 1}\,dk, \quad \omega < 3,$$

$$= \tfrac{1}{2}\sum_{n=-\infty}^{\infty} \frac{e^{in\alpha}}{2\cosh(n\lambda) - 1}, \quad \omega > 3. \tag{496}$$

Substituting these expressions into (493), these values of b are found to correspond to $n = \frac{1}{2}N$. Thus there are as many up arrows as down arrows in each row of the lattice. As with the square lattice F model, we expect this to correspond to the largest Λ of the transfer matrix.

The free energy can now be found by substituting (496) into (490). Performing the integration with respect to α then gives

$$z(0) = \ln u + P\int_{-\infty}^{\infty} \frac{(1 + e^{-k\mu})(1 - e^{-2k\mu})}{k(e^{k\mu} - 1 + e^{-k\mu})(1 - e^{-2k\pi})}\,dk, \quad \omega < 3,$$

$$= \ln u + 2\lambda + \sum_{n=1}^{\infty} \frac{(1 + e^{-n\lambda})(1 - e^{-2n\lambda})}{n(e^{n\lambda} - 1 + e^{-n\lambda})}. \quad \omega > 3. \tag{497}$$

Clearly $z(0)$ has a different form above and below $\omega = 3$, so that at this value the system undergoes a non-analytic phase transition. However, z can be formally expanded in powers of $(\omega - 3)$, and the expansions are the same above and below $\omega = 3$. Thus the transition is of infinite order, as in the square lattice F model.

One special case of particular interest is the triangular "ice model", in which $u = v = w = 1$, and hence $\mu = \pi/2$. The integral (497) can then be

evaluated, giving

$$W = \frac{3\sqrt{3}}{2} = 2{\cdot}598\ldots, \tag{498}$$

where

$$W = \mathrm{e}^{z(0)} = \lim_{\substack{M\to\infty \\ N\to\infty}} Z^{2/MN}. \tag{499}$$

For $\omega > 3$ the expression (497) can be cast into a rather interesting form by expanding the summand in powers of $\exp(-n\lambda)$ and summing term by term. This gives

$$W = \frac{u}{t^2(1-t)(1-t^2)^2} \prod_{n=1}^{\infty} \left\{ \frac{(1-t^{6n-1})(1-t^{6n-2})}{(1-t^{6n+1})(1-t^{6n+2})} \right\}^3, \tag{500}$$

where

$$t = \exp(-\lambda). \tag{501}$$

C. Three colourings of the edges of the hexagonal lattice

Let Z be the number of ways of colouring the bonds of the hexagonal lattice with three colours A, B, C, so that no two bonds at a vertex have the same colour. This problem can be thought of as a kind of dimer problem, in which two of the colours are two types of dimers, and we require that there be one and only one dimer of each type at every vertex (Baxter, 1970a).

Alternatively, one can show (by an argument similar to that relating the ice problem on a square lattice to a three colouring problem) that $4Z$ is the number of ways of colouring the faces of the hexagonal lattice with four colours so that no two adjacent faces have the same colour.

Returning to the original formulation of the problem as a colouring of bonds, draw the lattice as in Fig. 49 and suppose it to be wound on a torus. Then one can verify that the number of vertical bonds of a given colour must be the same in each row of the lattice. The transfer matrix for this pro-

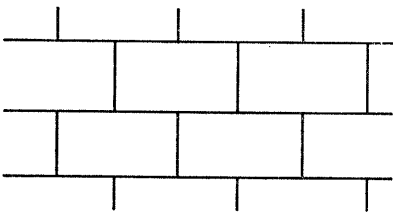

FIG. 49. The hexagonal lattice.

blem therefore breaks up into diagonal blocks, and one can specify the state ϕ of a row by giving the locations $x_1, x_2, \ldots$ of the $B-$ and C-coloured bonds, and be specifying which are coloured C.

In this way one can set up transfer matrix equations similar to the ferroelectric models, but complicated by the fact that there are two types of "down arrows" to consider. It turns out that the equations can be solved by an ansatz similar to that used in the short-range, one-band model for electron correlations (Lieb and Wu, 1968), and to that used in a two-component one-dimensional system of fermions with delta-function interaction (Gaudin, 1967a, b and C. N. Yang, 1967).

While in principle straightforward, the necessary extensions of the Bethe ansatz take us well beyond that needed for the ferroelectric problems, so we content ourselves with stating the result (Baxter, 1970a), namely

$$Z^{2/N} \sim \prod_{n=1}^{\infty} \frac{(3n-1)^2}{3n(3n-2)} = 1{\cdot}46099\ldots, \tag{502}$$

where N is the total number of sites in the lattice (N large).

D. Ice rule ferroelectric models with non-constant weights

As a final example of lattice models in satistical mechanics that can be solved by the transfer matrix—Bethe ansatz technique, we return to the square lattice and consider ferroelectric problems in which the Boltzmann factors $\omega_j = \exp(-\beta e_j)$ are allowed to vary from vertex to vertex (Baxter, 1971a).

Such a generalization includes any alternating square-lattice model, some of which are known to be soluble by an appropriate Bethe-type ansatz, while others appear intractable. It is therefore interesting to consider the most general problem and seek the conditions under which a solution can be obtained.

1. *Transfer Matrix*

As with the regular ferroelectric problems, consider a lattice of M rows and N columns, wound on a tours. Let $\omega_j(I, J)$, where $j = 1, \ldots, 6$, be the six possible Boltzmann factors of the vertex in row I and column J. Since these vary from row to row we must define a transfer matrix $T^{(I)}$ for each row and the analogue of the equation (75) for the partition function Z is

$$Z = \text{Trace}\,\{T^{(1)}T^{(2)}\ldots T^{(M)}\} = \sum \lambda_1 \ldots \lambda_M, \tag{503}$$

where $\lambda_1, \ldots, \lambda_M$ and a set of 2^N-dimensional vectors $\Psi^{(1)}, \ldots, \Psi^{(M)}$ are defined by

$$\lambda_I \Psi^{(I+1)} = T^{(I)}\Psi^{(I)} \tag{504}$$

for $I = 1, \ldots, M$, and $\Psi^{(M+1)} \equiv \Psi^{(1)}$. The summation in (503) is over all the 2^N independent solutions of (504).

The number n of down arrows in each row is of course still conserved, and just as (77) becomes (90), so does (504) become

$$\lambda_I f_{I+1}(x_1, \ldots, x_n) = \sum_R D_I{}^R(\mathbf{X}, \mathbf{Y}) f_I(y_1, \ldots, y_n) + \sum_L D_I{}^L(\mathbf{X}, \mathbf{Y}) f_I(y, \ldots, y_n), \quad (505)$$

the summations $\sum_R$, $\sum_L$ having the meaning given in Section IV.B. Defining

$$\xi_I = \prod_{J=1}^{N} \omega_1(I, J), \quad (506)$$

$$\eta_I = \prod_{J=1}^{N} \omega_4(I, J), \quad (507)$$

$$g_I(J) = \frac{\omega_6(I, J)}{\omega_1(I, J)} \prod_{K=1}^{J-1} \frac{\omega_4(I, K)}{\omega_1(I, K)}, \quad (508)$$

$$h_I(J) = \frac{\omega_5(I, J)}{\omega_4(I, J)} \prod_{K=1}^{J-1} \frac{\omega_1(I, K)}{\omega_4(I, K)}, \quad (509)$$

$$u_{I,J} = \frac{\omega_1(I, J)\, \omega_2(I, J)}{\omega_5(I, J)\, \omega_6(I, J)}, \quad (510)$$

$$v_{I,J} = \frac{\omega_3(I, J)\, \omega_4(I, J)}{\omega_5(I, J)\, \omega_6(I, J)}, \quad (511)$$

$$U_I(J, J') = 1 + (u_{I,J} - 1)\delta(J - J'), \quad (512)$$

$$V_I(J, J') = 1 + (v_{I,J} - 1)\delta(J - J'), \quad (513)$$

we find that the coefficients in (505) are

$$D_I{}^R(\mathbf{X}, \mathbf{Y}) = \xi_I \prod_{r=1}^{n} \{g_I(x_r) h_I(y_r) U_I(x_{r-1}, y_r) V_I(x_r, y_r)\}$$

$$D_I{}^L(\mathbf{X}, \mathbf{Y}) = \eta_I \prod_{r=1}^{n} \{g_I(x_r) h_I(y_r) U_I(x_r, y_r) V_I(x_{r+1}, y_r)\} \quad (514)$$

(choosing $x_0 < 1$, $x_{n+1} > N$).

2. *Bethe-Type Ansatz*

We now make the ansatz

$$f_I(x_1, \ldots, x_n) = \sum_P \mathfrak{A}_I(P) \prod_{j=1}^{n} \phi_{Pj}(I, x_j), \tag{515}$$

the summation having the same meaning as in (140), (420) and (472). We find that this can be made to satisfy (505) provided:

(i)
$$\frac{(u_{I,J} + v_{I,J} - 1)^2}{u_{I,J} v_{I,J}} = 4\Delta^2, \tag{516}$$

where Δ is some constant, independent of I and J. Setting

$$2\Delta = -t - t^{-1}, \tag{517}$$

we can then find parameters $p_{I,J}$, $\kappa_{I,J}$, $\alpha_{I,J}$, $\beta_{I,J}$, $\gamma_{I,J}$ such that

$$\begin{aligned}
\omega_1(I, J) &= \kappa_{I,J}(1 - tp_{I,J})\alpha_{I,J}\beta_{I,J} \\
\omega_2(I, J) &= \kappa_{I,J}(1 - tp_{I,J})/\{\alpha_{I,J}\beta_{I,J}\} \\
\omega_3(I, J) &= \kappa_{I,J}(p_{I,J} - t)\alpha_{I,J}/\beta_{I,J} \\
\omega_4(I, J) &= \kappa_{I,J}(p_{I,J} - t)\beta_{I,J}/\alpha_{I,J} \\
\omega_5(I, J) &= \kappa_{I,J}(t^{-1} - t)p_{I,J}\gamma_{I,J} \\
\omega_6(I, J) &= \kappa_{I,J}(1 - t^2)/\gamma_{I,J}.
\end{aligned} \tag{518}$$

If $\Delta = 0$ the partition function Z can be evaluated by Pfaffians (Baxter, 1970b). Failing this, we further require that:

(ii) There exist quantities ρ_I, σ_J such that

$$p_{I,J} = \rho_I \sigma_J, \tag{519}$$

(iii)
$$\frac{\gamma_{I,J+1}\gamma_{I+1,J}\alpha_{I,J}\alpha_{I,J+1}\beta_{I,J+1}\beta_{I+1,J+1}}{\gamma_{I,J}\gamma_{I+1,J+1}\alpha_{I+1,J}\alpha_{I+1,J+1}\beta_{I,J}\beta_{I+1,J}} = 1, \tag{520}$$

for all values of I and J.

Substituting (515) into (505) and using the above three conditions on the vertex weights, we find that the wanted terms on both sides of the transfer matrix equation cancel provided there exist parameters $z_1, \ldots, z_n$ such that

$$\begin{aligned}
\lambda_I = \beta_{I,1}{}^{-2n} \Bigg\{ &\xi_I \prod_{j=1}^{n} \frac{t - t^{-1}\rho_I z_j}{\rho_I z_j - 1} \\
&+ \eta_I \prod_{j=1}^{n} \frac{t^{-1} - t\rho_I z_j}{\rho_I z_j - 1} \Bigg\},
\end{aligned} \tag{521}$$

and

$$\phi_j(I, J) = \varepsilon_{I,J}\psi_j(J), \tag{522}$$

where

$$\varepsilon_{I,J} = \frac{\alpha_{I,1}\gamma_{I,1}\alpha_{I,J}\beta_{I,J}}{\beta_{I,1}\gamma_{I,J}} \prod_{K=1}^{J} \alpha_{I,K}{}^{-2}, \tag{523}$$

$$\psi_j(J) = \frac{1}{t\sigma_J - z_j} \prod_{K=1}^{J-1} \frac{tz_j - \sigma_K}{t\sigma_K - z_j}. \tag{524}$$

Since the single-particle functions $\phi_j(I, x)$ are no longer plane waves, the wave numbers $k_1, \ldots, k_n$ of the regular ferroelectric models no longer occur naturally. If we wish, we can introduce them by regarding the toroidal boundary conditions as equivalent to a periodicity every N lattice columns and requiring that

$$\phi_j(I, x + N) = \phi_j(I, x) \exp(iNk_j). \tag{525}$$

Using (522)–(524), we then find that k_j and z_j are related by

$$e^{iNk_j} = H^{-2} \prod_{K=1}^{N} \frac{tz_j - \sigma_K}{t\sigma_K - z_j}, \tag{526}$$

where

$$H = \prod_{J=1}^{N} \alpha_{I,J}. \tag{527}$$

At first sight H appears to depend on I, but it can be shown from (520) that this is not so. Similarly, the quantity

$$V = \prod_{I=1}^{M} \beta_{I,J} \tag{528}$$

is independent of J. H and V can be thought of as Boltzmann factors arising from applying horizontal and vertical electric fields, respectively, to the lattice.

With the normalizations implied by (521) and (522), the coefficients $\mathfrak{A}_I(P)$ are independent of I. Dropping the suffix I, the unwanted internal terms in the transfer matrix equation are found to vanish provided

$$\mathfrak{A}(P) = \mathfrak{A}(Q)B(z_l, z_m), \tag{529}$$

where P and Q are permutations related as in (429), and

$$B(z, z') = -\frac{t^{-1}z' - tz}{t^{-1}z - tz'}. \tag{530}$$

Finally, the unwanted boundary terms vanish provided

$$e^{iNk_j} = \prod_{\substack{i=1 \\ \neq j}}^{n} B(z_j, z_i), \tag{531}$$

or, more explicitly,

$$H^{-2} \prod_{K=1}^{N} \frac{tz_j - \sigma_K}{t\sigma_K - z_j} = (-1)^{n-1} \prod_{i=1}^{n} \frac{t^{-1}z_i - tz_j}{t^{-1}z_j - tz_i} \tag{532}$$

for $j = 1, \ldots, n$.

Using (521) and the relations between the various Boltzmann factors, we see that

$$\lambda_1 \ldots \lambda_M = V^{N-2n} Z_0 \prod_{I=1}^{M} \left\{ H \left\{ \prod_{J=1}^{N} (1 - t\rho_I \sigma_J) \right\} \left\{ \prod_{j=1}^{n} \frac{t - t^{-1}\rho_I z_j}{\rho_I z_j - 1} \right\} + H^{-1} \left\{ \prod_{J=1}^{N} (\rho_I \sigma_J - t) \right\} \left\{ \prod_{j=1}^{n} \frac{t^{-1} - t\rho_I z_j}{\rho_I z_j - 1} \right\} \right\}, \tag{533}$$

where

$$Z_0 = \prod_{I=1}^{M} \prod_{J=1}^{N} \kappa_{I,J}. \tag{534}$$

The equations (532) determine $z_1, \ldots, z_n$. Substituting these values into (533) gives $\lambda_1 \ldots \lambda_M$. The partition function Z is then obtained by summing $\lambda_1 \ldots \lambda_M$ over all independent solutions of (532) and all values of n from 0 to N.

Note that the field weights $\alpha_{I,J}$, $\beta_{I,J}$, $\gamma_{I,J}$ enter the final equations only via H and V. Thus the partition function is independent of local variations in the fields, so long as the condition (520) is satisfied.

3. *Equations as Polynomial Identities*

It is illuminating to introduce two polynomials, of degree N and n, respectively:

$$S(z) = \prod_{J=1}^{N} (z - \sigma_J) \tag{535}$$

$$Q(z) = \prod_{j=1}^{n} (z - z_j). \tag{536}$$

The equations (532) can then be written as

$$\Gamma(z_j) = 0 \quad \text{for } j = 1, \ldots, n, \tag{537}$$

where

$$\Gamma(z) \equiv (-t)^{N-2n} H S(t^{-1}z) Q(t^2 z) + H^{-1} S(tz) Q(t^{-2}z). \tag{538}$$

Clearly $\Gamma(z)$ is a polynomial of degree $N + n$. Further, n of its zeros coincide with those of $Q(z)$. Thus $Q(z)$ must be a factor of $\Gamma(z)$, and there exists an Nth degree polynomial $R(z)$ such that

$$\Gamma(z) = R(z) Q(z). \tag{539}$$

Using the definitions (535) and (536), we can write (533) as

$$\lambda_1 \dots \lambda_M = V^{N-2n} Z_0 \prod_{I=1}^{M} \frac{(-t)^n \rho_I{}^N \Gamma(\rho_I{}^{-1})}{Q(\rho_I{}^{-1})}, \tag{540}$$

so from (538) it follows that

$$\lambda_1 \dots \lambda_M = V^{N-2n} Z_0 \prod_{I=1}^{M} \{(-t)^n \rho_I{}^N R(\rho_I{}^{-1})\}. \tag{541}$$

Thus (538) and (539) can be regarded as identities defining the polynomials $Q(z)$ and $R(z)$. Once these are known, $\lambda_1 \dots \lambda_M$ is given by (541).

4. *Ordered F Model State*

With such a general system a great variety of thermodynamic states are possible. We do not attempt to consider all of these, but focus attention on one—the ordered F model state. In this case we can obtain the partition function Z for an infinite lattice by a simple trick.

As a first step, suppose all the weights $\omega_5(I, J), \omega_6(I, J)$ are much greater than all $\omega_1(I, J), \dots, \omega_4(I, J)$. Then the system will tend to assume one of two ordered states, in which either all vertices on the sublattice with $I + J$ even are in configuration 5 and all vertices with $I + J$ odd are in configuration 6, or vice versa. These are the ordered states that occur in the F model.

If this is so then it follows from (516) that Δ is large, so we can choose $|t| \ll 1$. Assuming that H and $\sigma_1, \dots, \sigma_N$ are of order unity, we see that when $N = 2n$, (532) has solutions such that $z_1, \dots, z_n$ are distinct and of order unity, the equation becoming

$$z_j{}^n + (-1)^n H^{-2} \frac{\sigma_1 \dots \sigma_N}{z_1 \dots z_n} \simeq 0 \tag{542}$$

for $j = 1, \dots, n$. Regarding this as an nth degree polynomial equation with roots $z_1, \dots, z_n$, we see that

$$z_1 \dots z_n \simeq H^{-2} \frac{\sigma_1 \dots \sigma_N}{z_1 \dots z_n}, \tag{543}$$

and hence

$$z_1 \dots z_n \simeq \pm H^{-1}(\sigma_1 \dots \sigma_N)^{\frac{1}{2}}. \tag{544}$$

Thus there are two such solutions of (532), corresponding to which sign we choose in (544). This reflects the fact that there are two possible ordered states for the lattice. For a large lattice (with V of order unity) these two solutions dominate the summation in (503), and it is unnecessary to consider any others.

Now do perturbation theory on either solution. Using the definitions of $Q(z)$ and $S(z)$, we can write (542) as

$$\frac{S(t^{-1}z)}{Q(t^{-2}z)} + H^{-2}\frac{S(tz)}{Q(t^2z)} = 0 \tag{545}$$

when $z = z_j$, $j = 1, \dots, n$. Supposing $|z| \sim 1$ and expanding in increasing powers of t, we find that to order t^{n-1} or less, the left-hand side of this equation is a polynomial of degree n, with leading coefficient unity. Further, its zeros are those of $Q(z)$, so that when $|z| \sim 1$,

$$Q(z) \simeq \frac{S(t^{-1}z)}{Q(t^{-2}z)} + H^{-2}\frac{S(tz)}{Q(t^2z)}. \tag{546}$$

Thus from (538),

$$\Gamma(z) \simeq HQ(z)Q(t^{-2}z)Q(t^2z), \tag{547}$$

and hence from (540)

$$\lambda_1 \dots \lambda_M \simeq Z_0 \prod_{I=1}^{M}\left[(-t)^n \rho_I{}^N H Q\left\{\frac{t^{-2}}{\rho_I}\right\} Q\left\{\frac{t^2}{\rho_I}\right\}\right]. \tag{548}$$

We can regard (546) as an approximate polynomial identity, true for all z, provided we replace the first (second) term on the right-hand side by the first n terms of its expansion in decreasing (increasing) powers of z. When $|z| \lesssim t^{-2}$ only the contributions to this polynomial from the first term are significant, so that

$$Q(z) \simeq \frac{S(t^{-1}z)}{Q(t^{-2}z)}. \tag{549}$$

When $|z| \lesssim t^2$, the contributions from the second term dominate, giving

$$Q(z) \simeq H^{-2}\frac{S(tz)}{Q(t^2z)}. \tag{550}$$

Letting $z = 0$ in (550), we regain (543). Thus (543) and (544) are in fact accurate to order t^{n-1}.

Replacing z by $t^{-2}z$, $t^{-4}z$, $t^{-6}z$, etc. in (549), we obtain a sequence of recursion relations between $Q(z)$, $Q(t^{-2}z)$, $Q(t^{-4}z)$, etc. Using the known large z behaviour of $Q(z)$ and $S(z)$, we can solve these relations to obtain

$$Q(t^{-2}z) \simeq t^{-2n} z^n \prod_{J=1}^{N} F(\sigma_J/z) \tag{551}$$

when $|z| \geqslant 1$, where

$$F(z) = \prod_{m=1}^{\infty} \frac{1 - t^{4m-1}z}{1 - t^{4m+1}z}. \tag{552}$$

Similarly, replacing z by t^2z, t^4z, etc. in (550), we obtain

$$Q(t^2z) \simeq (-1)^n z_1 \ldots z_n \prod_{J=1}^{N} F(z/\sigma_J) \tag{553}$$

when $|z| \leqslant 1$.

Substituting these results into (548), we therefore have

$$\lambda_1 \ldots \lambda_M \simeq Z_0 \prod_{I=1}^{M} \left\{ Hz_1 \ldots z_n \left(\frac{\rho_I}{t} \right)^n \prod_{J=1}^{N} F(\rho_I \sigma_J) F\left[\frac{1}{\rho_I \sigma_J} \right] \right\}. \tag{554}$$

Providing M is even, we see that it does not matter which sign we choose for $z_1 \ldots z_n$ in (544). Thus the two ordered states are degenerate and, using (518),

$$Z \simeq 2 \prod_{I=1}^{M} \prod_{J=1}^{N} \frac{[\omega_5(I, J)\omega_6(I, J)]^{\frac{1}{2}}}{1 - t^2} F(\rho_I \sigma_J) F\left(\frac{1}{\rho_I \sigma_J} \right). \tag{555}$$

When M is large this result is accurate to order t^{n-1}. Taking the thermodynamic limit when N and n become infinitely large, we expect it to be exact provided t is less than some critical value (and H, V, $\rho_1, \ldots, \rho_M$, $\sigma_1, \ldots, \sigma_N$ are of order unity). For the regular F model we can verify that (555) is in fact correct provided $\Delta < -1$ and $t < 1$.

Note that in this state Z is independent of H and V. Thus there is no polarization unless sufficiently strong electric fields are applied.

In a sense it is unfortunate that the two ordered F-model states are degenerate. This means that it is impossible to put on a staggered electric field so as to resolve this degeneracy and still satisfy the conditions (516), (519) and (520). If it could be obtained, the solution of the staggered field problem would give considerable information concerning the nature of the F model phase transition and related problems (Nagle, 1969b).

VIII. Unsolved Problems

The following is a partial list of problems for further research. Some of them are "loose ends" of the analysis in the text, while others require breakthrough in technique.

1. The conjecture in Section V.B, p. 390 following equation (194), that the free energy is analytic in K_1 at $K_1 = 0$.

2. The conjecture in Section V.H, p. 447 that the transfer matrix is normal for the ice rule models.

3. The solution of the two-dimensional ferrielectric model in a horizontal field (Section V. H).

4. In Section V. I we give the correlation function between vertical arrows when $\Delta = 0$. One problem is to evaluate the correlation between vertical and horizontal arrows. A more difficult problem is to extend the calculation to $\Delta \neq 0$. One can also try to calculate the correlation between vertex types at different vertices.

5. Establish the equivalence of free and periodic boundary conditions for the ice rule models (Section III).

6. Answer the four questions on the "canonical ensemble" posed in Section III. C, p. 361.

7. Find a non-trivial linear Hamiltonian that commutes with the transfer matrix for the sixteen vertex problem (goal 2 of Section IV. D, p. 367). Do same the for the Baxter models of Section VII.

8. Evaluate the F model free energy in a staggered field for $\Delta \neq 0$ (cf. Sections IV. E and V. H). Generally, the solution of any model with variable vertex weights (beyond that given in Section VII. D) would be useful.

9. Solve the triangular lattice F model for all temperatures, i.e. without the restriction on the weights given by (470).

10. Solve the ice rule models for other lattices, e.g. the Kagome lattice. In particular, what is the value of W for the Kagome lattice?

11. It has been conjectured by Wu (1969a) that, for the general ferroelectric model, the transition temperature cannot decrease if any vertex energy other than the lowest one is increased. It would be useful to establish this conjecture.

12. Is there an analogue of the Griffiths–Kelly–Sherman inequalities for the ferroelectric models?

13. If the above problems are solved, there are still the general eight and sixteen vertex models. The former would yield, among other things, the solution to the crossed bond Ising model and the latter would contain the solution of the Ising model in a non-zero magnetic field.

Glossary of Principal Symbols

α_0, defined by (177)
β, $= 1/kT$
C, specific heat per vertex
χ, polarizability
χ_0, polarizability at $T = T_0$
Δ, defined by (138)
e_ξ, vertex energy
$\varepsilon_1, \varepsilon_2$, energy parameters, cf. (93) and Table I
$\bar{\varepsilon}$, $= \max(0, \varepsilon_1) - \varepsilon_2$, cf. (94)
η, $= \exp|K_1|$
$\mathscr{F}$, free energy per vertex
$G_y(\mathbf{r})$, correlation function at a fixed y, cf. Section V. I
H, $= \beta h$
H, magnetic field (in (38–42) only)
H, Hamiltonian (in (28) and (34) and Section IV.D only)
h, horizontal electric field
k, Boltzmann constant
K, $= \beta\varepsilon$
K_1, $= \beta\varepsilon_1$
K_2, $= \beta\varepsilon_2$
λ, defined by $\Delta = -\cosh\lambda$, cf. Table II, line 1
λ_j, eigenvalues of the transfer matrix, cf. (75)
Λ, the largest eigenvalue of the transfer matrix, cf. (76)
Λ, a lattice domain (in Section III only)
μ, defined by $\Delta = -\cos\mu$, cf. Table II, line 1
M, number of rows in a square lattice
N, number of columns in a square lattice
n, number of down arrows in a row
ω_ξ, vertex weight
ϕ_0, defined by (175)
$\Xi(\phi)$, defined by (307)
s, staggered field
S, entropy
T, temperature
T_0, critical temperature in the absence of external fields
T_c critical temperature when external fields are present
θ_0, defined by (176)
U, internal energy
V, $= \beta v$
v, vertical electric field
W, defined by (3)

x, horizontal polarization per horizontal bond
y, vertical polarization per vertical bond
Z, partition function
Z_0, partition function at $T = \infty$; also as defined by (534), (Section VII.D only).
Z_D, dimer generating function
$z(\Lambda)$, $-\beta\mathscr{F}$ defined by (43)
$z(y)$, defined by (148)

References

Abraham, D., Glasser, M. L., and Lieb, E. (1972). The analyticity properties of two-dimensional ferroelectric models. *J. Maths. Phys.* **12**. To be published.

Abraham, D., Lieb, E., Oguchi, T., and Yamamoto, T. (1970). Residual entropy of sodium trihydrogen selenite. *Prog. Theor. Physics (Kyoto).* **44,** 114–115.

Abraham, D., and Lieb, E. H. (1971). The residual entropy of sodium trihydrogen selenite: an associated combinatorial problem. *J. Chem. Phys.* **54,** 1446–1450.

Bacon, G. E. and Pease, R. S. (1953). A neutron diffraction study of KH_2PO_4 by Fourier synthesis. *Proc. Roy. Soc.* **A220,** 397–421.

Barouch, E. (1971). Long range order of Wu's modified F model. *Phys. Letters* **34A,** 347–348.

Baxter, R. J. (1969). F model on a triangular lattice. *J. Math. Phys.* **10,** 1211–1216.

Baxter, R. J. (1970a). Colouring of a hexagonal lattice. *J. Math. Phys.* **11,** 784–789.

Baxter, R. J. (1970b). Exact isotherm for the F model in direct and staggered electric fields. *Phys. Rev.* **B1,** 2199–2202.

Baxter, R. J. (1970c). Three-colourings of the square lattice: a hard square model. *J. Math. Phys.* **11,** 3116–3124.

Baxter, R. J. (1971a). Generalized ferroelectric model on the square lattice. *Stud. Appl. Math.* **50,** 51–69.

Baxter, R. J. (1971b). Eight-vertex model in lattice statistics. *Phys. Rev. Lett.* **26,** 832–833.

Baxter, R. J. (1972). Partition function of the eight-vertex lattice model. *Ann. Phys. (N.Y.)* **70,** 193–228.

Bernal, J. D. and Fowler, R. H. (1933). A Theory of water and ionic solution, with particular reference to hydrogen and hydroxyl ions. *J. Chem. Phys.* **1,** 515–548.

Brauer, A. (1964). "On the Characteristic Roots of Non-Negative Matrices," *In* "Recent Advances in Matrix Theory", (H. Schneider, ed.), pp. 3–38. University of Wisconsin Press, Madison. (In particular see Theorem 29.)

Dalton, N. W., and Wood, D. W. (1969). Critical point behaviour of the Ising model with a higher-neighbour interactions present. *J. Math. Phys.* **10,** 1271–1302.

Domb, C. (1960). On the theory of cooperative phenomena in crystals. *Adv. Phys.* **9,** 149–361.

Fan, C. and Wu, F. Y. (1969). Ising model with second-neighbour interaction. I. Some exact results and an approximate solution. *Phys. Rev.* **179,** 560–570.

Fan, C. and Wu, F. Y. (1970). General lattice statistical model of phase transitions. *Phys. Rev.* **B2,** 723–733.

Fisher, M. E. (1960). Lattice statistics in a magnetic field I. A two-dimensional super-exchange antiferromagnet. *Proc. Roy. Soc.* **A254,** 66–85.

Gaudin, M. (1967a). Un système à une dimension de fermions en interactions. *Phys. Letters* **24A**, 55–56.
Gaudin, M. (1967b). Thesis, University of Paris (unpublished).
Gaunt, D. G. and Fisher, M. E. (1965). Hard square lattice gases. I. Plane-square lattice. *J. Chem. Phys.*. **43**, 2840–2863.
Giauque, W. F. and Stout, J. W. (1963). The entropy of water and the third law of rhermodynamics. *J. Am. Chem Soc.* **58.** 1144–1151.
Glasser, M. L. (1969). Evaluation of the partition function for some two-dimensional ferroelectric models. *Phys. Rev.* **184,** 539–542.
Gradshteyn, I. S. and Ryzhik, I. M. (1965). "Table of Integrals, Series, and Products". Academic Press, New York.
Haynsworth, E. V. and Goldberg, K. (1964). "Bernoulli and Euler Polynomials, Riemann Zeta Function", *In* "Handbook of Mathematical Functions", (M. Abramowitz and I. A. Stegun, eds.) National Bureau of Standards.
Hulthén, L. (1938). *Arkiv. Mat. Astron. Fysik.* **26A,** 1.
Hurst, C. A. (1966). New Approach to the Ising problem, *J. Math. Phys.* **7,** 305–310.
Hurst, C. A. and Green, H. S. (1960). New solution of the Ising problem for a rectangular lattice. *J. Chem. Phys.* **33,** 1059–1062.
Hurst, C. A. and Green, H. S. (1964). "Order-Disorder Phenomena", Wiley-Interscience, Inc., New York.
Jona, F. and Shirane, G. (1962). "Ferroelectric Crystals". MacMillan, New York.
Kac, M. and Ward, J. C. (1952). A combinatorial solution of the two-dimensional ising model. *Phys. Rev.* **88,** 1332–1336.
Kasteleyn, P. W. (1963). Dimer statistics and phase transitions, *J. Math. Phys.* **4,** 287–293.
Katsura, S., Abe, Y. and Ohkohchi, K (1970). Distribution of zeros of the partition function for the Slater model of ferroelectricity. *J. Phys. Soc. Japan* **29,** 845–850.
Kramers, H. A. and Wannier, G. H. (1941). Statistics of the 2–dimensional ferromagnetic I. *Phys. Rev.* **60,** 252–262.
Lebowitz, J. L. (1968). Statistical mechanics—a review of selected rigorous results. *Ann. Rev. Phys. Chem.* **19,** 389–418.
Levine, S. and Perram, J. W. (1968). "A Statistical Mechanical Treatment of Hydrogen-Bonding in Water" *In* "Hydrogen-Bonded Solvent Systems", (A. K. Covington and P. Jones, eds.) pp. 115–129. Taylor and Francis, London.
Lieb, E. H. (1967a). Eaxct solution of the problem of the entropy of two-dimensional ice. *Pyhs. Rev. Letters* **18,** 692–694.
Lieb. E. H. (1967b). Residual entropy of square ice. *Phys. Rev.* **162,** 162–171.
Lieb, E. H. (1967c). Exact solution of the F model of an antiferroelectric. *Phys. Rev. Letters* **18,** 1046–1048.
Lieb, E. H. (1967d). Exact solution of the two-dimensional Slater KDP model of a ferroelectric. *Phys. Rev. Letters* **19,** 108–110.
Lieb, E. H. and Wu, F. Y. (1968). Absence of Mott transition in an exact solution of the short-range, one-band model in one dimension. *Phys. Rev. Letters* **20,** 1445–1448.
Lieb, E. H. (1969a). Two-dimensional ferroelectric models. *J. Phys. Soc. Japan* **26,** Supplement, pp. 94–95.
Lieb, E. H. (1969b). "Two Dimensional Ice and Ferroelectric Models", *In* "Lectures in Theoretical Physics", Vol. XI (K. T. Mahantappa and W. E. Brittin, eds.), pp. 329–354. Gordon and Breach, New York. A more up to date version is in the 1970 "Proceedings of Ecole d'été de Physique Théorique" (1971) (Les Houches), Gordon and Breach, New York.

Lieb, E. H. (1970). "Ice, Ferro and Antiferroelectrics" in "Methods and Problems of Theoretical Physics in Honour of R. E. Peierls" (J. E. Bowcock, ed.), pp. 21–28 North Holland Publishing Co., Amsterdam.
Magnus, W. and Oberhettinger, F. (1948). "Formeln und Sätze für die Speziellen Funktionen der Mathematischen Physik". Springer Verlag, Berlin.
Majumdar, C. K. (1966). Analytic properties of the Onsager solution of the Ising model. *Phys. Rev.* **145**, 158–163.
Makita, Y. and Miki, M. (1970). Anomalous specific heat and configurational entropy change in sodium trihydrogen selenite. *J. Phys. Soc. Japan* **28**, 1221–1227.
McCoy, B. and Wu, T. T. (1968). Hydrogen-bonded crystals and the anisotropic Heisenberg chain. *Nuovo Cimento* **LVI B**, 311–314.
Meijering, J. L. (1957). Residual entropy of ice, and related combinatorial problems. *Philips Res. Rep.* **12**, 333–350.
Milne-Thomson, L. M. (1964). "Chap. 16 Jacobian Elliptic and Theta Functions and Chap. 17, Elliptic Integrals", *In* "Handbook of Mathematical Functions", (M. Abramowitz and I. A. Stegun, eds.), National Bureau of Standards.
Nagle, J. F. (1965). "Lattice Statistics of Hydrogen Bonded Crystals". Ph.D. Dissertation. Yale University.
Nagle, J. F. (1966a). Lattice statistics of hydrogen bonded crystals. I. The residual entropy of ice. *J. Math. Phys.* **7**, 1484–1491.
Nagle, J. F. (1966b). Lattice statistics of hydrogen bonded crystals. II. The Slater KDP model and the Rys F model. *J. Math. Phys.* **7**, 1492–1496.
Nagle, J. F. (1968). The one-dimensional KDP model in statistical mechanics. *Am. J. Phys.* **36**, 1114–1117.
Nagle, J. F. (1969a). Proof of the first order phase transition in the Slater KDP model. *Commun. Math. Phys.* **13**, 62–67.
Nagle, J. F. (1969b). Study of the F model using low-temperature series. *J. Chem. Phys.* **50**, 2813–2818.
Newell, G. F. and Montroll, E. W. (1953). On the theory of the Ising model of ferromagnetism. *Rev. Mod. Phys.* **25**, 353–389.
Oberhettinger, F. (1966). "Tabellen zur Fourier Transformation", Springer Verlag, Berlin.
Onsager, L. (1939). Discussion at Conference on Dielectrics. New York Academy of Sciences.
Onsager, L. and Dupuis, M. (1960). Rendiconti S.I.F., X Corso, 294.
Pauling, L. (1935). The structure and entropy of ice and of other crystals with some randomness of atomic arrangement. *J. Am. Chem. Soc.* **57**, 2680–2684.
Percus, J. K. (1969). "Combinatorial Methods", Lecture Notes of the Courant Institute, New York University.
Peterson, S. W. and Levy, H. A. (1953). Neutron diffraction study of tetragonal potassium dihydrogen phosphate. *J. Chem. Phys.* **21**, 2084–2085.
Reese, W. (1969). Studies of phase transitions in order-disorder ferroelectrics. III. *Phys. Rev.* **181**, 905-919.
Ruelle, D. (1969). "Statistical Mechanics", W. A. Benjamin, New York.
Rys, F. (1963). Über ein zweidimensionales klassisches konfigurations-modell. *Helv. Phys. Acat.* **36**, 537–559.
Slater, J. C. (1941). Theory of the transition in KH_2PO_4. *J. Chem. Phys.* **9**, 16–33.
Stephenson, J. (1969). Close-packed anisotropic antiferromagnetic Ising lattices. *Can. J. Phys.* **47**, 2621–2631.
Stephenson, J. (1970). Ising-model spin correlations on the triangular lattice. IV. *J. Math. Phys.* **11**, 420–431.

Sutherland, B. (1967). Exact solution of a two-dimensional model for hydrogen-bonded crystals. *Phys. Rev. Letters* **19,** 103–104.
Sutherland, B. (1968). Correlation functions for two-dimensional ferroelectrics. *Phys. Letters* **26A,** 532–533.
Sutherland, B., Yang, C. N., and Yang, C. P. (1967). Exact solution of a model of two-dimensional ferroelectrics in an arbitrary external electric field. *Phys. Rev. Letters* **19,** 588–591.
Sutherland, B. (1970). Two-dimensional hydrogen bonded crystals without the ice rule. *J. Math. Phys.* **11,** 3183–3186.
Suzuki, M. and Fisher, M. E. (1970). Zeros of the partition function for the Heisenberg, ferroelectric and general Ising models. *J. Math. Phys.* **12,** 235–246.
Takagi, Y. (1948). Theory of the transition in KH_2PO_4, II. *J. Phys. Soc. Japan* **3,** 273–275.
Takahashi, H. (1941). Zur Slaterschen theorie der umwandlung von KH_2PO_4 (Teil I.). *Proc. Phys. Math. Soc. Japan* **23,** 1069–1079.
van der Waerden, B. L. (1941). Die lange Reichweite der regelmassigen atomanordnung in mischkristallen. *Z. Physik* **118,** 473–488.
Walker, L. R. (1959). Antiferromagnetic linear chain. *Phys. Rev.* **116,** 1089–1090.
Wannier, G. H. (1945). The statistical problem in cooperative phenomena. *Rev. Mod. Phys.* **17,** 50–60.
West, J. (1930). A quantitative X-ray analysis of the structure of KH_2PO_4. *Z. Krist* **74,** 306–332.
Wu, F. Y. (1967). Exactly soluble model of ferroelectric phase transition in two dimensions. *Phys. Rev. Letters* **18,** 605–607.
Wu, F. Y. (1968). Remarks on the modified KDP model of a ferroelectric. *Phys. Rev.* **168,** 539–543.
Wu, F. Y. (1969a). Critical behaviour of two-dimensional hydrogen-bonded antiferroelectrics. *Phys. Rev. Letters* **22,** 1174–1176.
Wu, F. Y. (1969b). Exact solution of a model of an antiferroelectric transition. *Phys. Rev.* **183,** 604–607.
Wu, F. Y. (1970). Critical behaviour of two-dimensional hydrogen-bonded ferroelectrics. *Phys. Rev. Letters* **24,** 1476–1478.
Wu, F. Y. (1971a). Modified KDP model in a staggered field. *Phys. Rev.* **B3,** 3895–3900.
Wu, F. Y. (1971b). Ising model with four-spin interactions. *Phys. Rev.* **B4,** 2312–2314.
Wu, F. Y. (1972). Exact results on a general lattice statistical model. *Solid Stat. Comm.* **10,** 115–117.
Yang, C. N. (1967). Some exact results for the many-body problem in one-dimension with repulsive delta-function interaction. *Phys. Rev. Letters* **19,** 1312–1315.
Yang, C. N. and Yang, C. P. (1966a). One-dimensional chain of anisotropic spin-spin interactions. I. Proof of Bethe's hypothesis for ground state in a finite system. *Phys. Rev.* **150,** 321–327.
Yang, C. N. and Yang, C. P. (1966b). One-dimensional chain of anisotropic spin-spin interactions. II. Properties of the ground-state energy per lattice site for an infinite system. *Phys. Rev.* **150,** 327–339.
Yang, C. N. and Yang, C. P. (1966c). One-dimensional chain of anisotropic spin-spin interactions. III. Applications. *Phys.* **151,** 258–264.
Yang, C. P. (1967). Exact solution of a model of two-dimensional ferroelectrics in an arbitrary external field. *Phys. Rev.* **19,** 586–588.